UNIVERSITY OF CALIFORNIA, SAN DIEGO

Layered Transmissions over Decode-and-Forward Wireless Relay Networks

A dissertation submitted in partial satisfaction of the
requirements for the degree

Doctor of Philosophy

in

Electrical Engineering
(Communication Theory and Systems)

by

Tu Viet Nguyen

Committee in charge:

Professor Pamela C. Cosman, Co-Chair
Professor Laurence B. Milstein, Co-Chair
Professor Patrick J. Fitzsimmons
Professor William S. Hodgkiss
Professor Bhaskar D. Rao

2013

The dissertation of **Tu Viet Nguyen** is approved, and it is acceptable in quality and form for publication on microfilm and electronically:

_____

_____

_____

_____
Co-Chair

_____
Co-Chair

University of California, San Diego

2013

DEDICATION

To my beloved family

TABLE OF CONTENTS

LIST OF FIGURES

ACKNOWLEDGEMENTS

I would like to express my gratitude to all those who supported me during my Ph.D. study at UC San Diego for the last five years.

First of all, I am deeply indebted to my advisors, Professor Laurence Milstein and Professor Pamela Cosman, whose knowledge, experience, guidance, and encouragement have helped me to the completion of this dissertation. Professor Milstein has been advising me from the early year of my graduate study. I have learned a lot from his broad and depth knowledge in wireless communications. His kindness also helped me overcome the difficulties over the years. Professor Cosman has guided me in the field of image processing and communications. Without her supervision and support, the dissertation would not have been possible.

I would like to thank my dissertation committee members, Professor Patrick Fitzsimmons, Professor William Hodgkiss, and Professor Bhaskar Rao for their time and invaluable feedbacks. Their suggestions have strengthened the dissertation.

I also indebted to many other Professors in the ECE, CSE, and Mathematics departments for their teachings, which set a foundation to make this dissertation possible. Also, I would like to thank Professor Young-Han Kim for being my academic advisor during my first year, and Professor Elias Masry for his advice in the field of Statistics and Mathematics.

I also thank my friends in the lab, Dr. Laura Tony, Dr. Hyun Kwangmin, Mr. Madushanka Soysa, and Mr. Brian Lewis for their positive interactions. The

discussions with them were very helpful, especially in communications theory and image processing.

I am deeply indebted to my parents, Luan Viet Nguyen and Lan Thi-Bich Nguyen, for their unconditional love, supports and encouragements. They encouraged me to pursue higher education, regardless of difficulties faced. I also would like to thank my brothers, Quoc Viet Nguyen, Tuan Viet Nguyen, and Huong Viet Nguyen, and my relatives for their supports and encouragements. My thanks also go to my friends in the United State and in Viet Nam, especially, Ms. Thuy Tran and Mr. San Nguyen for their sharing over the years.

Chapter II of this dissertation is, in full, a reprint of the material as it appears in Tu V. Nguyen and Laurence B. Milstein, "Layered Transmission over Decode-and-Forward Wireless Relay Networks using Superposition Coding," submitted to *IEEE Transactions on Communications,* 2013 and in Tu V. Nguyen and Laurence B. Milstein, "Optimal Linear-Combining Receiver for Layered Transmission for Decode-and-Forward Relays with Superposition Coding," *submitted to IEEE Asilomar Conference on Signals, Systems and Computers*, 2013. I was the primary author of all these publications and the co-author Professor Milstein directed and supervised the research which forms the basis for Chapters II.

Chapter III of this dissertation is, in full, a reprint of the material as it appears in Tu V. Nguyen, Pamela C. Cosman, and Lauence B. Milstein, "Layered Video Transmission over Decode-and-Forward Wireless Relay Networks using Hierarchical Modulation," submitted to *IEEE Transactions on Image Processing,*

2013, and in Tu V. Nguyen and Laurence B. Milstein, "Layered Transmission over Decode-and-Forward Wireless Relay Networks using Superposition Coding," *submitted to IEEE Transactions on Communications*, 2013. I was the primary author of all these publications. The co-authors Professor Cosman and Professor Milstein directed and supervised the research which forms the basis for Chapters III.

VITA

2004	B.Sc., Electrical Engineering, Posts and Telecommunications Institute of Technology, Ha Noi
2005 – 2005	Network Administrator, LG Electronic Vietnam, Ha Noi
2005 – 2007	Lecturer, Posts and Telecommunications Institute of Technology, Ha Noi
2007 – 2013	Graduate Research Assistant, Department of Electrical and Computer Engineering, University of California, San Diego, San Diego
2009	M.Sc., Electrical Engineering (Communications Theory and System), University of California, San Diego
Summer 2010	Research Intern, VA San Diego Medical Center, San Diego
Summer 2012	Research Intern, System engineering, Nextivity Inc, San Diego
2013	Ph.D., Electrical Engineering (Communications Theory and System), University of California, San Diego

PUBLICATIONS

Tu V. Nguyen, Pamela C. Cosman, Laurence B. Milstein, "Layered Video Transmission over Decode-and-Forward Wireless Relay Networks using Hierarchical Modulation," *submitted to IEEE Transactions on Image Processing*, 2013.

Tu V. Nguyen and Laurence B. Milstein, "Layered Transmission over Decode-and-Forward Wireless Relay Networks using Superposition Coding," *submitted to IEEE Transactions on Communications*, 2013.

Tu V. Nguyen, Pamela C. Cosman, Laurence B. Milstein, "Optimized Receiver Design for Layered Transmission for Decode-and-Forward Relays using Hierarchical Modulation," *submitted to IEEE Asilomar Conference on Signals, Systems and Computers*, 2013.

Tu V. Nguyen and Laurence B. Milstein, "Optimal Linear-Combining Receiver for Layered Transmission for Decode-and-Forward Relays with Superposition Coding," *submitted to IEEE Asilomar Conference on Signals, Systems and Computers*, 2013.

Tu V. Nguyen, Elias Masry, and Laurence B. Milstein, "Channel Model and Performance Analysis of QAM Multiple Antenna Systems at 60-GHz in the Presence of Human Activity," *IEEE, Globecom Conference*, Texas Houston, Dec. 2011.

ABSTRACT OF THE DISSERTATION

Layered Transmissions over Decode-and-Forward Wireless Relay Networks

by

Tu Viet Nguyen

Doctor of Philosophy in Electrical Engineering
(Communication Theory and Systems)

University of California, San Diego, 2013

Professor Pamela C. Cosman, Co-Chair
Professor Laurence B. Milstein, Co-Chair

In this dissertation, we consider a wireless relay network with a single source, a single destination, and multiple relays. The relays are half-duplex and use the decode-and-forward protocol. In the first part, we consider the layered transmission using an information-theoretic approach, where a successively refinable Gaussian source is transmitted using superposition coding. In the second part, we consider the layered transmission using a communication-theoretic approach,

where a layered video-encoded bitstream is transmitted using hierarchical modulation. In both cases, we assume the transmitted source can be partitioned into a base layer (BL) and an enhancement layer (EL). The BL is more important than the EL, and the source cannot be reconstructed without the BL.

It takes two time slots for each transmission. In the first time slot, the source broadcasts a message that consists of a BL and an EL to all the relays and the destination. The relays detect the transmitted message individually. Each relay detects the BL first, and, if successful, then it detects the EL. Unlike other cooperation techniques, we assume the relays are not able to communicate with each other, and that there is no feedback channel from the destination to the relays, or from the relays to the source. Hence, a given relay does not know if any other relay successfully decodes a specific layer. Rather, we assume that, in the second time slot, each relay will forward all its successfully decoded layers to the destination. That is, a relay can transmit either only the BL or both the BL and the EL to the destination (or not transmit at all).

Chapter 1

Introduction

1.1 Overview

Multimedia transmission has many challenges, such as the need for large bandwidth and low latency, and the fact that transmitted signals over wireless networks can experience large fading fluctuations. Many techniques have been studied for reliable multimedia delivery over wireless links, such as multiple-input-multiple-output (MIMO), cooperation, and unequal error protection (UEP). MIMO has been extensively studied in recent years, and widely used to achieve spatial diversity and/or multiplexing gain for data transmissions by employing multiple antennas at both transmitter and receiver [1–3]. However, in many scenarios, multiple antennas cannot be deployed, due to the size limitation of the end-user devices. In cooperation schemes, single antenna terminals can achieve spatial diversity by sharing their antennas with each other to create a virtual MIMO system [4–12].

Cooperation diversity can improve the system performance and increase the coverage [10–12]. A simple and efficient cooperation scheme, namely, choosing the best relay, was analyzed in [13], and shown to achieve full diversity gain while maintaining high spectral efficiency. In this scheme, and other cooperation schemes, in general, slow fading and feedback channels are generally assumed for relay selection/cooperation purposes. Therefore, these schemes cannot be efficiently applied in high mobility environments, or when a feedback channel does not exist.

For layered or embedded sources, some components of the source are more important than others in terms of source distortion. Hence, these components generally require different levels of protection against transmission errors. To provide unequal error protection, different layers are allocated different amounts of the available resources, such as power and bandwidth, according to their levels of importance. There are several methods of providing UEP for embedded sources, for example, superposition coding [14, 15], rate-compatible punctured convolutional/turbo coding [16, 17], and hierarchical modulation [18, 19]. Hierarchical modulation has been used in commercial standards such as Digital Video Broadcasting [20] and MediaFlo [21] to provide multiple levels of quality of service (QoS).

In [22–25], several UEP methods were proposed for multimedia data over MIMO systems. For example, in [22], closed-loop MIMO with UEP using a scalable video encoder was considered. In [23], channel coding and spatial diversity were exploited to achieve UEP. In [26, 27], the authors proposed layered video coding and two-hop relaying to deliver video to two groups of users with different QoS,

depending on the weakest instantaneous channel SNR in each group. In [28–30], source-channel rate optimization for block fading channel was considered.

1.2 General system model and problem description

In this dissertation, we consider a wireless relay network with a single source, a single destination, and multiple relays, as shown in Fig. 1.1. The source transmits a layered source to the destination using the help of the relays. The relays are half-duplex and use the decode-and-forward protocol.

Unlike other cooperation techniques in the literature, we assume there is no feedback channel from the destination to the relays or from the relays to the source. Also, the relays are not able to communicate with each other. Lastly, automatic repeat request is not considered. These constraints are aimed at minimizing the transmission latency for multimedia applications and reducing the system complexity.

In the following, we present the general transmission protocol, which will be used throughout the dissertation. More detailed protocol description will be presented later. Due to the relays' half-duplex, it takes two time slots for each transmission. In the first time slot, the source broadcasts a message consisting of a base layer (BL) and an enhancement layer (EL) to all the relays and the destination. The relays separately decode the message. A relay decodes the BL first, and, if successful, decodes the EL. Depending on the channel status, a relay

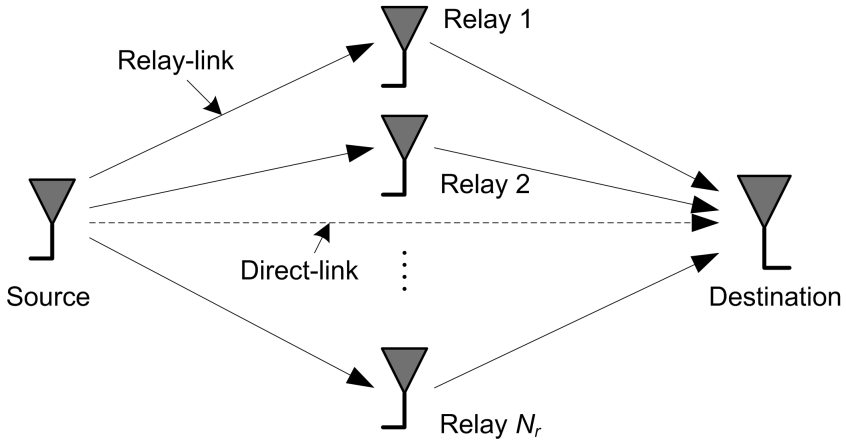

Figure 1.1: Relay network: a single source, a single destination, and multiple relays.

can successfully decode both the BL and the EL, only the BL, or nothing. Note that, since the relays cannot communicate with each other, a relay does not know if any other relay successfully decoded a given layer. In the second time slot, each relay will forward all its successfully decoded layers to the destination using orthogonal channels. Depending on the number of layers transmitted, a relay may use different coding or modulation schemes to communicate with the destination.

With the above protocol, the destination can receive multiple signals, which can include different numbers of layers. Therefore, in general, a conventional maximal-ratio-combining receiver cannot be straightforwardly applied (or it is not optimal). In [31] and [32], the authors used two different suboptimal combining techniques. In this dissertation, we use both information-theoretic and communication-theoretic approaches to design and analyze the layered transmission over decode-and-forward wireless relay networks. For each approach, we focus

on deriving the optimal linear-combining receiver. The system performance in terms of the system throughput and/or the source distortion are then analyzed, and key system parameters, such as power and rates, are optimized to improve the end-to-end system performance.

1.3 Information-theoretic approach

In the information-theoretic approach, we assume the transmitted source is a successively refinable Gaussian source, which can be partitioned into two layers: a base layer and an enhancement layer. A block fading channel model is assumed, and superposition coding is used for multiplexing.

Superposition coding was first applied to a relay network to improve the transmission rate in [15], where one relay was considered and the channel gains were deterministic. The relay decoded and forwarded only the enhancement layer to the destination in order to enhance the direct link. Superposition coding has also been studied in [32, 33] for relay networks to improve the system throughput over single layer transmission, although a suboptimal combining technique was used at the destination.

In this dissertation, we propose a novel linear combining technique to combine the received signals at the destination to first detect the BL, and then the EL, using a two step combining method. We show that this combining technique is optimal in terms of maximizing the received signal-to-interference-plus-noise ratio

(SINR); thus, it also maximizes the mutual information from the source to the destination for this relay network with the considered protocol. The optimal weights and the maximum combined SINRs for both the BL and the EL (the BL/EL) have a closed form, from which we can obtain the distribution of the maximum combined SINR in a simple form. We note here that the combining technique is also optimal for a single relay selection protocol [13], because the destination receives the BL/EL from the direct link, and either the BL/EL or only the BL from the selected relay.

Using the optimal combining method at the destination, we analyze the system performance in terms of the average throughput and the expected distortion. Numerical results showed that the proposed two-layer scheme outperforms a conventional one-layer scheme by several dB in channel SNR.

1.4 Communication-theoretic approach

In the communication-theoretic approach, the transmitted source is a layered video-encoded bitstream, which can also be partitioned into a BL and an EL. For layered transmission, hierarchical QAM modulation scheme is used. Note that, for hierarchical QAM modulation with Gray-coded bit mapping, generally, the most significant bits (MSBs) are more protected than the least significant bits (LSBs) against transmission errors. Hence, the BL is mapped to the MSBs, and the EL is mapped to the LSBs for layered transmission. The relays, however,

adaptively use different modulation schemes, depending on number of successfully decoded layers. In particular, if a relay successfully decodes both the BL and the EL, it will transmit both layers to the destination using hierarchical 16-QAM. If only the BL is successfully decoded, a relay will transmit only the BL to the destination using QPSK. Because of different modulation schemes used at the relays, conventional maximal-ratio-combining (MRC) receiver cannot straightforwardly be applied at the destination.

In this dissertation, we derive the optimal linear combining receivers for the BL and the EL by a two-step combining method, which minimizes the uncoded bit-error-rate (BER). In the first step, we optimize over the weight vector's direction, in which the optimal solution has a closed form. In the second step, we optimize over the weight vector's length. For the BL, convex optimization programming [34] can be used to efficiently solve for the optimal weight vector length. For the EL, such convex optimization programming does not lead to a global optimum (thus, only a local optimum can be guaranteed by convex optimization programming, or a global search method needs to be used). We also present a suboptimal solution for the BL by minimizing an upper-bound for the BER of the BL, which has a closed-form solution and performs very close to optimal. Both the optimal and suboptimal methods for the BL significantly outperform the combining methods in [31, 32]. A simple combining method for the EL in the second step is also presented, which performs well compared to the optimal.

Numerical results show that the proposed layered scheme using hierarchi-

cal modulation significantly outperform a classical single-layer scheme using the conventional modulation.

1.5 Dissertation outline

In Chapter II, we present the details of the information-theoretic approach for layered transmission using superposition coding, based upon a block fading channel model. The optimal linear combining receiver is derived, and closed-form expressions for weight vectors and the combined SINR are obtained. The system performances in terms of the average throughput and expected distortion are analyzed. We present a lower bound for the average throughput and an upper bound for the expected distortion, both of which have a closed form. The system parameters such as the power and rate allocations are found by optimizing the closed form bounds. The exact system performances corresponding to these parameters are evaluated numerically.

In Chapter III, we present the details of the communication-theoretic approach, where hierarchical QAM modulation is used to provide UEP for a layered video bitstream, which is encoded with a H.264/AVC encoder [35–38]. The video-encoded bitstream is partitioned into a BL and an EL. The optimal linear combining receiver at the destination is derived based on a two-step combining method which minimizes the uncoded BER. We also present a derivation that yields a closed-form expression for a suboptimal set of combining weights, for both the BL

and the EL. The proposed scheme is then used for transmitting a layered video bitstream over the wireless relay network. The performance of layered transmission scheme is evaluated and compared to the conventional transmission scheme. Numerical results show that the former scheme significantly outperforms the latter scheme.

In Chapter IV, we summarize the contributions of this dissertation and discuss potential future work.

Chapter 2

Layered Transmission over Wireless Relay Networks using Superposition Coding

2.1 Introduction

In this chapter, we consider a relay network with a single source, a single destination, and multiple relays. A block fading channel model is assumed. The relays are half-duplex and use the decode-and-forward protocol. The transmitted source is a successively refinable Gaussian source, which can be partitioned into two layers: a base layer (BL) and an enhancement layer (EL). The BL is more important than the EL, and the source cannot be reconstructed without the BL. In the first time slot, the source broadcasts a message consisting of both the BL and the EL (the BL/EL) to all the relays and the destination. The relays decode the message individually. A relay might successfully decode the BL/EL, successfully

decode only the BL, or decode nothing. Instead of using relay selection-based protocols, which generally require feedback channels from the destination to the relays and thus introduce more latency, we assume all the relays forward all their successfully decoded layers to the destination using orthogonal channels. The destination can thus receive multiple signals, each of which contains either the BL/EL or only the BL. Since the received signals at the destination can include a different number of signal layers, a conventional maximal-ratio combining (MRC) receiver cannot be applied straightforwardly (or, if it is applied, it is not optimal).

To the best of our knowledge, MRC for uncorrelated branches was first presented in [39]. In [40], the authors show that the MRC solution is also optimal if the branches' signals are correlated, as long as the branches' noise processes are independent. In [41], maximal-ratio eigen-combining was proposed for smart antenna arrays, where it was assumed that the signals can be correlated but the noise terms are independent. We will see later that these results are not applicable to our problem, because in our case the interference terms, which we treat as noise, are correlated. Another approach for MRC uses the eigenfilter method, which can be applied for both correlated signals and correlated noise [42]; however, this method, in general (and in our case), results in neither a closed-form solution for each individual branch weight nor the optimum signal-to-interference-and-noise ratio (SINR), because it depends on the inverse of the noise covariance matrix.

A suboptimal-combining method was proposed in [32] for linear combining the received signals at the destination to decode the BL (and then the EL); how-

ever, this method is suboptimal because not all the received signals are used for combining. Another combining method uses a conventional MRC-like solution [31], which is only optimal if all the received signals at the destination have the same number of layers.

In this chapter, we derive the optimal linear solution to combine the received signals at the destination using a two-step combining method. The optimality is in terms of maximizing the received SINR. We note that the optimal weight vector has a closed form, and the corresponding combined SINRs for the BL and the EL also have closed forms. Using the optimal-combining method at the destination, we derive the average throughput and the expected distortion. Since these quantities are not expressed in closed form, we derive a closed-form lower bound to the average throughput and a closed-form upper bound to the expected distortion. We find suboptimal system parameters, such as the power allocation parameter for superposition coding and transmission rate for each layer, based on the closed-form bounds. We then obtain the actual average throughput and the actual expected distortion numerically corresponding to the suboptimal system parameters. Numerical results show that the proposed two-layer scheme using superposition coding can gain up to several dBs in channel SNR, compared to a conventional one-layer counterpart.

The rest of this chapter is organized as follows. In Section 2.2, we present the system model. The optimal linear-combining receiver is presented in Section 2.3, and the system performance analysis is presented in Section 2.4. Section 2.5

is for numerical results, and finally, Section 2.6 concludes the chapter.

2.2 System model

2.2.1 General description

In Fig. 1.1, we demonstrate a wireless relay network with a single source (s), a single destination (d), and N relays (r_n, for $n = 1, 2, \ldots, N$). We assume a block fading channel model. The transmitted source is successively refinable Gaussian, which is partitioned into a BL and an EL [14, 32]. The relays are half-duplex and use the decode-and-forward protocol. In the first time slot, the source broadcasts a message with two layers using superposition coding to all the relays and the destination. We assume the relays are not able to communicate with each other; hence, they do not know if any other relay successfully decodes a layer. Rather, we assume in the second time slot that if a relay does not successfully decode any layer, it will keep silent; if it successfully decodes only the BL, it will transmit only the BL to the destination; and finally, if it successfully decodes both layers, it will transmit the BL/EL using superposition coding [32, 33]. We assume the total available bandwidth, which is equally divided into N sub-bands, each of bandwidth W, is allocated to the relay-destination links. The broadcast channel from the source to the relays and destination can use any one of the sub-bands (see Fig. 2.1), since it transmits in different time slot. With this protocol, the destination receives multiple signals, each of which can include either the BL/EL or only the BL.

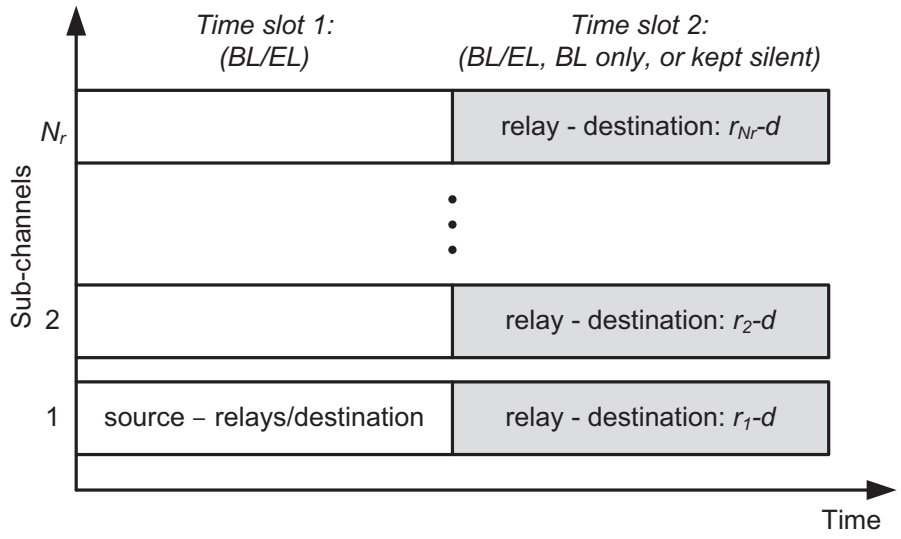

Figure 2.1: Relay protocol description: the transmission bandwidth is equally divided into N sub-bands, and the relays use the half-duplex protocol.

2.2.2 Channel and signal models

We assume the channels of the links $s-d$, $s-r_n$ and r_n-d experience Rayleigh flat-fading, with the real-valued gains, respectively, denoted by α_{sd}, $\alpha_{sr}^{(n)}$ and $\alpha_{rd}^{(n)}$. Due to the spatial separation, we assume these fading gains are independent. Also, the second moments are denoted by

$$\Omega_{sd} \triangleq E[\alpha_{sd}^2], \quad \Omega_{sr}^{(n)} \triangleq E[(\alpha_{sr}^{(n)})^2], \quad \Omega_{rd}^{(n)} \triangleq E[(\alpha_{rd}^{(n)})^2] \tag{2.1}$$

We assume the maximum transmit powers at the source and at the relays are limited by P_s and P_r, respectively. In the following, we consider the received signals at the relays and the destination.

- In the first time slot, the received signal at the n-th relay (at the output of

a coherent matched filter) can be written as follows [43]:

$$y_r^{(n)} = \alpha_{sr}^{(n)} \sqrt{P_s} \big(\sqrt{\rho} x_{bl} + \sqrt{\bar{\rho}} x_{el} \big) + z_r^{(n)}, \tag{2.2}$$

where x_{bl} and x_{el} denote the BL and EL signals, respectively, and are independent and Gaussian with zero mean and unit variance. The parameter $\rho \in (0, 1]$ is the transmit power allocation at the source. That is, ρP_s is the transmit power allocated to the BL, and $\bar{\rho} P_s$, where $\bar{\rho} \triangleq 1 - \rho$, is the transmit power allocated to the EL [32]. The $\{z_r^{(n)}\}$ represent the additive Gaussian noise, which are assumed to be i.i.d. with zero mean and variance σ_0^2. Similarly, the received signal at the destination is given by

$$y_d^{(0)} = \alpha_{sd} \sqrt{P_s} \big(\sqrt{\rho} x_{bl} + \sqrt{\bar{\rho}} x_{el} \big) + z_d^{(0)}, \tag{2.3}$$

We note that after receiving the signal $y_d^{(0)}$, the destination does not decode the message immediately, but saves it in the memory and waits for the signals in the second time slot.

- In the second time slot, the received signal at the destination from the n-th relay is given by

$$y_d^{(n)} = \alpha_{rd}^{(n)} \sqrt{P_r} \big(\sqrt{\rho} x_{bl} + \sqrt{\bar{\rho}} x_{el} \big) + z_d^{(n)} \tag{2.4}$$

if both layers have been successfully decoded, where ρ is the power allocation parameter at the n-th relay. If only the BL has been successfully decoded, we allocate all the power to the BL (i.e., $\rho = 1$), and thus the received signal

is given by

$$y_d^{(n)} = \alpha_{rd}^{(n)} \sqrt{P_r} x_{bl} + z_d^{(n)} \tag{2.5}$$

We also assume $\{z_d^{(n)}\}$ for $n = 0, 1, \ldots, N$ are i.i.d. and Gaussian with zero mean and variance σ_0^2, where $n = 0$ denotes the direct link $s - d$ (in the first time slot).

For notational convenience, we consider the source itself as a virtual relay, referred to as relay 0, which always sends the BL/EL to the destination, where the received signal at the destination is given in (2.3). To express (2.3) in the form of (2.4), the received signal from an actual relay, we denote the 'effective' fading gain from the source (i.e., relay 0) to the destination as follows:

$$\alpha_{rd}^{(0)} \triangleq \sqrt{P_s/P_r}\alpha_{sd}, \tag{2.6}$$

such that Equation (2.3) can be expressed as

$$\begin{aligned} y_d^{(0)} &= \alpha_{sd}\sqrt{P_s}\big(\sqrt{\rho}x_{bl} + \sqrt{\bar{\rho}}x_{el}\big) + z_d^{(0)}, \\ &= \alpha_{rd}^{(0)}\sqrt{P_r}\big(\sqrt{\rho}x_{bl} + \sqrt{\bar{\rho}}x_{el}\big) + z_d^{(0)} \end{aligned} \tag{2.7}$$

that is, Equation (2.4) with $n = 0$. We also denote $\Omega_{rd}^{(0)} = (P_s/P_r)\Omega_{sd}$.

We define the received SNR at the output of the n-th relay's receiver as

$$\Gamma_r^{(n)} \triangleq P_s\Omega_{sr}^{(n)}/\sigma_0^2, \quad \text{for } n = 1, 2, \ldots, N \tag{2.8}$$

and similarly the received SNR of the n-th received signal at the destination as

$$\Gamma_d^{(n)} \triangleq P_r\Omega_{rd}^{(n)}/\sigma_0^2, \quad \text{for } n = 0, 1, 2, \ldots, N \tag{2.9}$$

where we note that $\Gamma_d^{(0)} \triangleq P_r\Omega_{rd}^{(0)}/\sigma_0^2 = P_s\Omega_{sd}/\sigma_0^2$ for the direct link. Note that because each relay transmits the signal to the destination using its dedicated sub-band, there is no interference among the received signals from the relays. At the destination, the received signals as shown in (2.4) and (2.5) will be combined to first decode the BL, and then the EL. For combining and detection at the destination, in practice, each relay needs to send a signalling message (of two bits) to inform the destination which type of signal it will send. For simplicity, we assume the signalling message is received at the destination error-free, and ignore the signalling overhead.

2.3 Combining methods for the received signals at the destination

Let (Θ_k, Ψ_k), for $k = 1, 2, \ldots$, be all possible pairs of subsets of relays (excluding the virtual relay 0), which successfully decode only the BL, and the BL/EL, respectively, where $\Theta_k \cap \Psi_k = \emptyset$ and $\Theta_k \cup \Psi_k \subset \{1, 2, \ldots, N\}$. Also, if the direct link is used, we denote

$$\Psi_k^+ \;=\; \{0, \Psi_k\}, \tag{2.10}$$

otherwise, we denote $\Psi_k^+ = \Psi_k$. That is, Ψ_k^+ is the set of all relays, including the virtual relay 0 (if the direct link is used).

Let w_n be the combining weight for the received signal $y_d^{(n)}$ for $n \in \Theta_k \cup \Psi_k^+$. Since the channel gains are real-valued, we can assume the $\{w_n\}$ are real-valued.

The general linear combining signal is given by

$$\hat{y}_{d,bl} = \sum_{n\in\Theta_k} w_n y_d^{(n)} + \sum_{n\in\Psi_k^+} w_n y_d^{(n)} \tag{2.11}$$

$$= \sum_{n\in\Theta_k} w_n \big(\sqrt{P_r}\alpha_{rd}^{(n)} x_{bl} + z_d^{(n)}\big) + \sum_{n\in\Psi_k^+} w_n \big(\alpha_{rd}^{(n)}\sqrt{P_r}(\sqrt{\rho}x_{bl} + \sqrt{\bar{\rho}}x_{el}) + z_d^{(n)}\big) \tag{2.12}$$

where we substituted $\{y_d^{(n)}\}$ from (2.4) and (2.5) for $n \in \Theta_k$ and $n \in \Psi_k^+$, respectively.

For notational simplicity, we define

$$\begin{aligned} C_{\Theta_k}(\mathbf{w}_{\Theta_k}) &\triangleq \sum_{n\in\Theta_k} w_n \alpha_{n,l}^{rd} = \mathbf{w}_{\Theta_k}^T \boldsymbol{\alpha}_{\Theta_k}, \\ C_{\Psi_k^+}(\mathbf{w}_{\Psi_k^+}) &\triangleq \sum_{n\in\Psi_k^+} w_n \alpha_{n,l}^{rd} = \mathbf{w}_{\Psi_k^+}^T \boldsymbol{\alpha}_{\Psi_k^+} \end{aligned} \tag{2.13}$$

$$\begin{aligned} N_{\Theta_k}(\mathbf{w}_{\Theta_k}) &\triangleq \sum_{n\in\Theta_k} w_n z_{n,l}^{(d)} = \mathbf{w}_{\Theta_k}^T \mathbf{z}_{\Theta_k}, \\ N_{\Psi_k^+}(\mathbf{w}_{\Psi_k^+}) &\triangleq \sum_{n\in\Psi_k^+} w_n z_{n,l}^{(d)} = \mathbf{w}_{\Psi_k^+}^T \mathbf{z}_{\Psi_k^+} \end{aligned} \tag{2.14}$$

where $\mathbf{w}_{\Theta_k}$ and $\mathbf{w}_{\Psi_k^+}$ denote the vectors whose elements are w_n for $n \in \Theta_k$ and $n \in \Psi_k^+$, respectively, and similarly for $\boldsymbol{\alpha}_{\Theta_k}, \boldsymbol{\alpha}_{\Psi_k^+}, \mathbf{z}_{\Theta_k}$, and $\mathbf{z}_{\Psi_k^+}$. The superscript T denotes transpose. From (3.10), we note that $N_{\Theta_k}(\mathbf{w}_{\Theta_k}) \sim \mathcal{CN}(0, \|\mathbf{w}_{\Theta_k}\|^2\sigma_0^2)$ and $N_{\Psi_k^+}(\mathbf{w}_{\Psi_k^+}) \sim \mathcal{CN}(0, \|\mathbf{w}_{\Psi_k^+}\|^2\sigma_0^2)$, where we use $\|\mathbf{x}\| \triangleq \sqrt{\mathbf{x}^T\mathbf{x}}$ to denote the Euclidean norm of a vector $\mathbf{x}$. Since $\Theta_k \cap \Psi_k^+ = \emptyset$, N_{Θ_k} and $N_{\Psi_k^+}$ are independent. In the following, we will drop the dependence on $\mathbf{w}_{\Theta_k}$ and $\mathbf{w}_{\Psi_k^+}$, wherever there is no confusion.

Using the definitions (2.13) and (2.14) in (2.11), after reorganizing, we have

$$\hat{Y}_{d,bl} = \left(\sqrt{P_r}C_{\Theta_k} + \sqrt{\rho}\sqrt{P_r}C_{\Psi_k^+}\right)x_{bl} + \sqrt{\bar{\rho}}C_{\Psi_k^+}\sqrt{P_r}x_{el} + N_{\Theta_k} + N_{\Psi_k^+} \tag{2.15}$$

Considering the EL as interference, the SINR of the BL is given as follows

$$SINR_{BL}(\mathbf{w}_{\Theta_k}, \mathbf{w}_{\Psi_k^+}) = \frac{P_r\left(C_{\Theta_k}(\mathbf{w}_{\Theta_k}) + \sqrt{\rho}C_{\Psi_k^+}(\mathbf{w}_{\Psi_k^+})\right)^2}{\bar{\rho}P_r[C_{\Psi_k^+}(\mathbf{w}_{\Psi_k^+})]^2 + (\|\mathbf{w}_{\Theta_k}\|^2 + \|\mathbf{w}_{\Psi_k^+}\|^2)\sigma_0^2} \tag{2.16}$$

We need to find $\mathbf{w}_{\Theta_k}$ and $\mathbf{w}_{\Psi_k^+}$ to maximize the SINR of the BL

$$SINR_{BL}^* = \underset{\mathbf{w}_{\Theta_k}, \mathbf{w}_{\Psi_k^+}}{\text{maximize}}\ SINR_{BL}(\mathbf{w}_{\Theta_k}, \mathbf{w}_{\Psi_k^+}) \tag{2.17}$$

In the following, we consider both the suboptimal and optimal combining methods for detecting the BL.

2.3.1 Simple method

It was proposed in [32] to use the received signals which include only the BL to decode the BL, as shown in (2.5), if at least one is available, i.e., $\Theta_k \neq \emptyset$. Otherwise, all the received signals which include the BL/EL will be combined to decode the BL/EL. By this method, in both cases, the conventional MRC receiver can be used [32]. That is, the suboptimal combining weight vectors for the BL are given by

$$\mathbf{w}_{\Theta_k} = \boldsymbol{\alpha}_{\Theta_k},\ \mathbf{w}_{\Psi_k^+} = \mathbf{0}, \qquad \text{if } \Theta_k \neq \emptyset \tag{2.18}$$

$$\mathbf{w}_{\Theta_k} = \mathbf{0}, \qquad \mathbf{w}_{\Psi_k^+} = \boldsymbol{\alpha}_{\Psi_k^+}, \quad \text{if } \Theta_k = \emptyset\ (\Psi_k^+ \neq \emptyset) \tag{2.19}$$

The corresponding SINR for the BL are given by

$$SINR_{d,bl}(\Theta_k, \Psi_k^+) = \frac{P_r \|\boldsymbol{\alpha}_{\Theta_k}\|^2}{\sigma_0^2}, \qquad \text{if } \Theta_k \neq \emptyset \tag{2.20}$$

$$SINR_{d,bl}(\Theta_k, \Psi_k^+) = \frac{\rho P_r \|\boldsymbol{\alpha}_{\Psi_k^+}\|^2}{\sigma_0^2 + \bar{\rho} P_r \|\boldsymbol{\alpha}_{\Psi_k^+}\|^2}, \text{ if } \Theta_k = \emptyset \ (\Psi_k^+ \neq \emptyset) \tag{2.21}$$

2.3.2 MRC-like method

In this method, the combined weight vectors are given by

$$\mathbf{w}_{\Theta_k} = \boldsymbol{\alpha}_{\Theta_k}, \text{ and } \mathbf{w}_{\Psi_k^+} = \boldsymbol{\alpha}_{\Psi_k^+} \tag{2.22}$$

which is equivalent to an MRC receiver if all the received signals have the same number of layers. This method has been used in [31]. Substituting (2.22) in (2.16), the SINR for the BL is given by

$$SINR_{d,bl}(\Theta_k, \Psi_k^+) = \frac{P_r\big(\|\boldsymbol{\alpha}_{\Theta_k}\|^2 + \sqrt{\rho}\|\boldsymbol{\alpha}_{\Psi_k^+}\|^2\big)^2}{\bar{\rho} P_r \|\boldsymbol{\alpha}_{\Psi_k^+}\|^4 + \big(\|\boldsymbol{\alpha}_{\Theta_k}\|^2 + \|\boldsymbol{\alpha}_{\Psi_k^+}\|^2\big)\sigma_0^2} \tag{2.23}$$

2.3.3 Optimal method

In this subsection, we consider the optimal linear-combining solution, which maximizes the output SINR. The optimal linear-combining procedure can be divided into two steps, as shown in Fig. 2.2. In the first step, we apply an MRC receiver to the signals which include only the BL, and use the same technique for the signals which include the BL/EL, separately. In the second step, we apply an MRC receiver to the two resulting signals.

In Appendix A.1, we show that the optimal combining weight vectors are

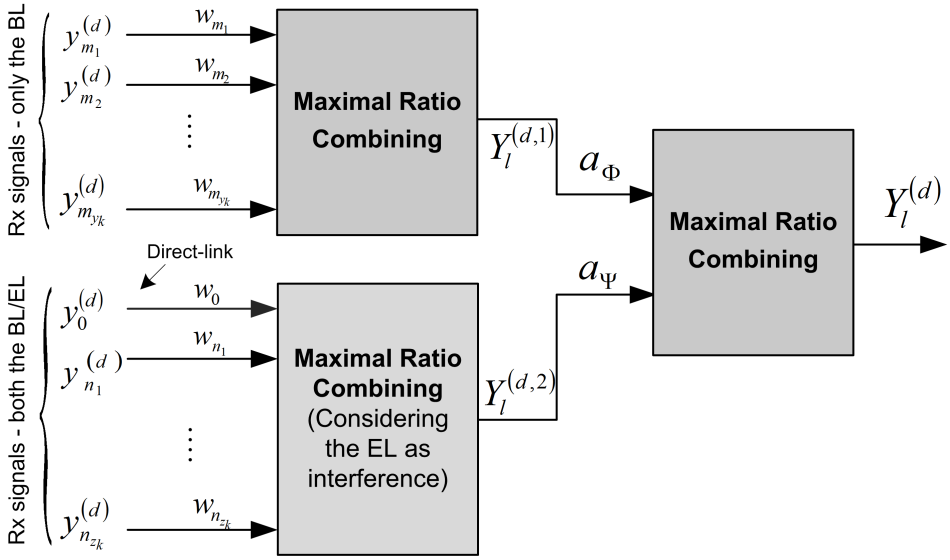

Figure 2.2: Optimal linear-combining receiver: Two-step combining procedure.

given by

$$\mathbf{w}_{\Theta_k} = \frac{\boldsymbol{\alpha}_{\Theta_k}}{\sigma_0^2}, \quad \text{and } \mathbf{w}_{\Psi_k^+} = \frac{\sqrt{\rho}\boldsymbol{\alpha}_{\Psi_k^+}}{\bar{\rho}P_r\|\boldsymbol{\alpha}_{\Psi_k^+}\|^2 + \sigma_0^2} \tag{2.24}$$

which depend on not only the channel gains but also the power allocation parameter and the channel SNR. The optimal weights in the first and second steps are, respectively, given in (A.11), (A.15) and (A.18). The maximum SINR for the BL is given by

$$SINR_{d,bl}(\Theta_k, \Psi_k^+) = \frac{P_r\|\boldsymbol{\alpha}_{\Theta_k}\|^2}{\sigma_0^2} + \frac{\rho P_r\|\boldsymbol{\alpha}_{\Psi_k^+}\|^2}{\bar{\rho}P_r\|\boldsymbol{\alpha}_{\Psi_k^+}\|^2 + \sigma_0^2} \tag{2.25}$$

We note that if the suboptimal combining method in [32] was used, the combined SINR would be only the first term in (2.25) for Θ_k being an non-empty set, and only the second term in (2.25) for Θ_k being an empty set. Also, we can show that the suboptimal SINR, as shown in (2.23), is strictly less that the optimum, as

shown in (2.25), for $0 < \rho < 1$ (and both $\|\boldsymbol{\alpha}_{\Theta_k}\|, \|\boldsymbol{\alpha}_{\Psi_k^+}\| > 0$, which happens with probability one).

2.3.4 Combining method for the EL

Provided the BL is decoded successfully (regardless the method used), it is subtracted from the received signals in the set Ψ_k^+, which include the BL/EL, as shown in (2.4). The resulting signals are given by

$$y_{d,el}^{(n)} = \alpha_{rd}^{(n)}\sqrt{\bar{\rho}}\sqrt{P_r}x_{el} + z_d^{(n)}, \qquad \text{for } n \in \Psi_k^+. \tag{2.26}$$

The signals $\{y_{d,el}^{(n)}\}$ are then combined by using a classical MRC receiver. The combined conditional SINR for the EL at the destination, given that the BL was successfully decoded, is given by

$$SINR_{d,el}(\Theta_k, \Psi_k^+) = \frac{\bar{\rho}P_r\|\boldsymbol{\alpha}_{\Psi_k^+}\|^2}{\sigma_0^2} \tag{2.27}$$

2.4 System performance

2.4.1 The outage probability of the $s - r_n$ links.

The instantaneous mutual information (MI), normalized by the subband bandwidth W, for the BL from the source to the n-th relay (for $n = 1, 2, \ldots, N$) is given by [14, 32]

$$MI_{r,bl}^{(n)} = \log_2\left(1 + \frac{\rho P_s|\alpha_{sr}^{(n)}|^2}{\sigma_0^2 + \bar{\rho}P_s|\alpha_{sr}^{(n)}|^2}\right) \quad [bps/Hz] \tag{2.28}$$

where we consider the EL as interference. Similar to [32], the outage probability for the BL at rate R_{bl}[bps/Hz] from the source to the n-th relay is computed as follows:

$$\begin{aligned}\pi_{r,bl}^{(n)}(R_{bl}) &\triangleq \Pr\big(\text{BL is not decoded}\big) \triangleq \Pr\big(MI_{r,bl}^{(n)} < R_{bl}\big) \\ &= \Pr\Big(\frac{\rho P_s|\alpha_{sr}^{(n)}|^2}{\sigma_0^2 + \bar{\rho}P_s|\alpha_{sr}^{(n)}|^2} < 2^{R_{bl}} - 1\Big) \\ &= \Pr\Big(\frac{P_s}{\sigma_0^2}|\alpha_{sr}^{(n)}|^2(\rho - \bar{\rho}(2^{R_{bl}} - 1)) < 2^{R_{bl}} - 1\Big) \end{aligned} \tag{2.29}$$

We note that if $\rho - \bar{\rho}(2^{R_{bl}} - 1) \leq 0$, then the outage probability of the BL is $\pi_{r,bl}^{(n)}(R_{bl}) = 1$, for all n, regardless of the channel SNR. In this case, nothing is successfully received at any relay, so are the destination. Hence, in the following, we assume that ρ and R_{bl} satisfy

$$\rho - \bar{\rho}(2^{R_{bl}} - 1) > 0 \tag{2.30}$$

With the constraint in (2.30), we can write (2.29) as follows:

$$\begin{aligned}\pi_{r,bl}^{(n)}(R_{bl}) &= \Pr\Big(\frac{(\alpha_{sr}^{(n)})^2}{\Omega_{sr}^{(n)}} < \frac{2^{R_{bl}} - 1}{(\rho - \bar{\rho}(2^{R_{bl}} - 1))P_s\Omega_{sr}^{(n)}/\sigma_0^2}\Big) \\ &= \gamma_{inc}\Big(\frac{2^{R_{bl}} - 1}{(\rho - \bar{\rho}(2^{R_{bl}} - 1))\Gamma_r^{(n)}}, 1\Big) \triangleq \gamma_{inc}\big(x_1, 1\big) \end{aligned} \tag{2.31}$$

where we use (2.8), and define

$$x_1 \triangleq \frac{2^{R_{bl}} - 1}{(\rho - \bar{\rho}(2^{R_{bl}} - 1))\Gamma_r^{(n)}}, \tag{2.32}$$

and

$$\gamma_{inc}(t, k) \triangleq \frac{1}{\Gamma(k)}\int_0^t e^{-u}u^{k-1}du, \tag{2.33}$$

where $\gamma_{inc}(t,k)$ is the incomplete Gamma function [44] with $\Gamma(k) \triangleq \int_0^\infty e^{-u}u^{k-1}du$.

When the BL is decoded successfully, it is subtracted from the receiver signal to decode the EL. Thus, the conditional MI of the EL, conditioned on the event that the BL is successfully decoded, is given by

$$MI^{(n)}_{r,el|bl} = \log_2\left(1+\frac{\bar{\rho}P_s(\alpha^{(n)}_{sr})^2}{\sigma_0^2}\right) \quad [bps/Hz] \tag{2.34}$$

The joint probability that the BL is successfully decoded and the EL is unsuccessfully decoded is calculated as follows:

$$\begin{aligned}
\pi^{(n)}_{r,bl^*,el}(R_{bl},R_{el}) &\triangleq \Pr\big(\text{BL decoded, EL not decoded}\big)\\
&= \Pr\left(MI^{(n)}_{r,bl} \geq R_{bl}, MI^{(n)}_{r,el|bl} < R_{el}\right)\\
&= \Pr\left(\frac{\rho P_s(\alpha^{(n)}_{sr})^2}{\sigma_0^2+\bar{\rho}P_s(\alpha^{(n)}_{sr})^2} \geq 2^{R_{bl}}-1, \frac{\bar{\rho}P_s(\alpha^{(n)}_{sr})^2}{\sigma_0^2} < 2^{R_{el}}-1\right)\\
&= \Pr\left(\frac{2^{R_{bl}}-1}{(\rho-\bar{\rho}(2^{R_{bl}}-1))P_s/\sigma_0^2} \leq (\alpha^{(n)}_{sr})^2 < \frac{2^{R_{el}}-1}{\bar{\rho}P_s/\sigma_0^2}\right)
\end{aligned}$$

Using the notation in (2.8) and (2.32), we have

$$\begin{aligned}
\pi^{(n)}_{r,bl^*,el}(R_{bl},R_{el}) &= \Pr\left(x_1 \leq \frac{(\alpha^{(n)}_{sr})^2}{\Omega^{(n)}_{sr}} < \frac{2^{R_{el}}-1}{\bar{\rho}\Gamma^{(n)}_r}\right)\\
&= \gamma_{inc}(x_2,1)-\gamma_{inc}(x_1,1)
\end{aligned} \tag{2.35}$$

where we denote

$$x_2 \triangleq \max\left\{x_1, \frac{2^{R_{el}}-1}{\bar{\rho}\Gamma^{(n)}_r}\right\} \tag{2.36}$$

The joint probability that both the BL and the EL are successfully decoded

is thus given by

$$\begin{aligned}
\pi^{(n)}_{r,bl^*,el^*}(R_{bl},R_{el}) &\triangleq \Pr\big(\text{BL decoded, EL decoded}\big) \\
&= 1-\Pr\big(\text{BL not decoded}\big) \\
&\quad -\Pr\big(\text{BL decoded, EL not decoded}\big) \\
&= 1-\pi^{(n)}_{r,bl}(R_{bl})-\pi^{(n)}_{r,bl^*,el}(R_{bl},R_{el}) \\
&= 1-\gamma_{inc}(x_2,1) \qquad (2.37)
\end{aligned}$$

2.4.2 Joint probability of the layers successfully decoded at the relays

In the following, we consider the joint probability that a subset of relays successfully decodes the BL/EL, another subset of relays successfully decodes only the BL but not the EL, and the remaining relays do not successfully decode the BL (and thus, not the EL). It can be shown that the joint probability of (Θ_k,Ψ_k^+) is given by

$$\Pr(\Theta_k,\Psi_k^+)=\prod_{n\in\Theta_k}\pi^{(n)}_{r,bl^*,el}(R_{bl},R_{el})\times\prod_{m\in\Psi_k^+}\pi^{(m)}_{r,bl^*,el^*}(R_{bl},R_{el})\times\prod_{l\notin\Theta_k\cup\Psi_k^+}\pi^{(l)}_{r,bl}(R_{bl}) \qquad (2.38)$$

where the first product term is the probability that the set Θ_k successfully decodes only the BL but not the EL, the second product term is the probability that the set Ψ_k^+ successfully decodes the BL/EL, and the third product term is the probability that the remaining relays do not successfully decode the BL.

If all the relays' channel gains have the same statistics, the outage proba-

bility of the BL and the EL in (2.38) are the same for all relays, and thus (2.38) reduces to[1]

$$\Pr(\Theta_k, \Psi_k^+) = \left[\pi_{r,bl^*,el}(R_{bl}, R_{el})\right]^{y_k} \times \left[\pi_{r,bl^*,el^*}(R_{bl}, R_{el})\right]^{z_k} \times \left[\pi_{r,bl}(R_{bl})\right]^{N-y_k-z_k} \tag{2.39}$$

where y_k and z_k are the number of elements in the set Θ_k and Ψ_k^+, respectively.

Note that the probability in (2.39) is corresponding to one particular pair of sets (Θ_k, Ψ_k^+). The number of pairs of sets which have the number of elements y_k and z_k (for $y_k + z_k \leq N$), are $C_N^{y_k} C_{N-y_k}^{z_k} = \frac{N!}{y_k! z_k! (N-y_k-z_k)!}$. Thus, in this case (i.e., the i.i.d. channels), the probability of having y_k relays successfully decode only the BL but not the EL, and z_k relays successfully decode the BL/EL is given by

$$\bar{P}_N(y_k, z_k) = \frac{N!}{y_k! z_k! (N-y_k-z_k)!} \left[\pi_{r,bl^*,el}(R_{bl}, R_{el})\right]^{y_k} \times \left[\pi_{r,bl^*,el^*}(R_{bl}, R_{el})\right]^{z_k} \times \left[\pi_{r,bl}(R_{bl})\right]^{N-y_k-z_k} \tag{2.40}$$

2.4.3 System throughput and distortion

From (2.25), the conditional MI for the BL at the destination is given by

$$MI_{d,bl}(\Theta_k, \Psi_k^+) = \log_2\left(1 + SINR_{d,bl}(\Theta_k, \Psi_k^+)\right) \quad [bps/Hz] \tag{2.41}$$

[1]We drop the relays' indices for simplicity of notation.

and the outage probability for the BL is given by

$$\begin{aligned}\pi_{d,bl}(R_{bl},\Theta_k,\Psi_k^+) &= \Pr\left(MI_{d,bl}(\Theta_k,\Psi_k^+)<R_{bl}\right)\\ &= \Pr\left(SINR_{d,bl}(\Theta_k,\Psi_k^+)<2^{R_{bl}}-1\right)\\ &\triangleq F_{SINR_{d,bl}}(2^{R_{bl}}-1),\end{aligned} \tag{2.42}$$

where $F_{SINR_{d,bl}}(.)$ denotes the CDF of $SINR_{d,bl}(\Theta_k,\Psi_k^+)$. where $F_{SINR_{d,bl}}(.)$ denotes the CDF of $SINR_{d,bl}(\Theta_k,\Psi_k^+)$. If the channel gains from the relays to the destination are independently Rayleigh fading with second moment $\Omega_{rd}^{(n)} = E[(\alpha_{rd}^{(n)})^2] \triangleq \Omega_0$, then the SNR $\Gamma_d^{(n)} = \Gamma_d = P_r\Omega_0/\sigma_0^2$, for all $n \in \Psi_k^+$ (i.e., including $n=0$).[2] and the CDF of the maximum SINR of the BL given in (2.25) is derived in Appendix A.2, with the final result given as follows:

$$\begin{aligned}F_{SINR_{d,bl}}(x) &\triangleq \Pr(SINR_{d,bl}(\Theta_k,\Psi_k^+)\le x)\\ &= \int_0^x \frac{(u/\Gamma_d)^{y_k-1}e^{-u/\Gamma_d}}{(y_k!)\Gamma_d}F_{V_{z_k}}(x-u)du\end{aligned} \tag{2.43}$$

where $F_{V_{z_k}}(.)$ is given in (A.24).

Similarly, from (2.27), the conditional MI for the EL at the destination, given that the BL is decoded successfully, is given by

$$MI_{d,el|bl}(\Theta_k,\Psi_k^+) = \log_2\left(1+SINR_{d,el}(\Theta_k,\Psi_k^+)\right) \tag{2.44}$$

The conditional joint probability, conditioned on the pair of sets (Θ_k,Ψ_k^+), that the BL is successfully decoded and the EL is *not* successfully decoded at the

[2]Note that the assumption implies $E[|\alpha_{rd}^{(0)}|^2] = (P_s/P_r)E[|\alpha_{sd}|^2] = (P_s/P_r)\Omega_{sd} = \Omega_{rd}^{(n)} = \Omega_0$, for all n, see (2.6).

destination, is given by

$$\begin{aligned}
&\pi^{(n)}_{d,bl^*,el}(R_{bl}, R_{el}, \Theta_k, \Psi_k^+) \triangleq \Pr\big(\text{BL decoded, EL not decoded}\big) \\
&\quad \triangleq \Pr\left(MI_{d,bl}(\Theta_k, \Psi_k^+) \geq R_{bl}, MI_{d,el|bl}(\Theta_k, \Psi_k^+) < R_{el}\right) \\
&\quad = \Pr\left(SINR_{d,bl}(\Theta_k, \Psi_k^+) \geq 2^{R_{bl}} - 1, \frac{\bar{\rho} P_r \|\boldsymbol{\alpha}_{\Psi_k^+}\|^2}{\sigma_0^2} < 2^{R_{el}} - 1\right) \qquad (2.45)
\end{aligned}$$

where we substituted (2.41), (2.44), and (2.27). Because of the non-linear form of $SINR_{d,bl}(\Theta_k, \Psi_k^+)$, as shown in (2.25), we cannot find a closed-form solution of (2.45). In the following, we find an upper bound.

We note that for $0 \leq A < B$, we have $\frac{A}{1+A} < \frac{B}{1+B}$. Thus, given that $(\bar{\rho} P_r/\sigma_0^2)\|\boldsymbol{\alpha}_{\Psi_k^+}\|^2 < 2^{R_{el}} - 1$, i.e., the second inequality in (2.35) holds, we have

$$\frac{\bar{\rho} P_r \|\boldsymbol{\alpha}_{\Psi_k^+}\|^2}{\sigma_0^2 + \bar{\rho} P_r \|\boldsymbol{\alpha}_{\Psi_k^+}\|^2} = \frac{(\bar{\rho} P_r/\sigma_0^2)\|\boldsymbol{\alpha}_{\Psi_k^+}\|^2}{1 + (\bar{\rho} P_r/\sigma_0^2)\|\boldsymbol{\alpha}_{\Psi_k^+}\|^2} < \frac{2^{R_{el}} - 1}{2^{R_{el}}} \qquad (2.46)$$

Hence, from (2.25), we have

$$\begin{aligned}
SINR_{d,bl}(\Theta_k, \Psi_k^+) &= \frac{P_r \|\boldsymbol{\alpha}_{\Theta_k}\|^2}{\sigma_0^2} + \frac{\rho P_r \|\boldsymbol{\alpha}_{\Psi_k^+}\|^2}{\sigma_0^2 + \bar{\rho} P_r \|\boldsymbol{\alpha}_{\Psi_k^+}\|^2} \\
&< \frac{P_r \|\boldsymbol{\alpha}_{\Theta_k}\|^2}{\sigma_0^2} + \frac{\rho}{\bar{\rho}} \frac{2^{R_{el}} - 1}{2^{R_{el}}} \qquad (2.47)
\end{aligned}$$

By denoting $K_\rho(R_{el}) \triangleq \frac{\rho}{\bar{\rho}} \frac{2^{R_{el}} - 1}{2^{R_{el}}}$, from (2.45), we have

$$\begin{aligned}
&\pi_{d,bl^*,el}(R_{bl}, R_{el}, \Theta_k, \Psi_k^+) \\
&\quad \leq \Pr\left(\frac{P_r}{\sigma_0^2}\|\boldsymbol{\alpha}_{\Theta_k}\|^2 + K_\rho(R_{el}) \geq 2^{R_{bl}} - 1, \frac{\bar{\rho} P_r \|\boldsymbol{\alpha}_{\Psi_k^+}\|^2}{\sigma_0^2} < 2^{R_{el}} - 1\right) \\
&\quad = \Pr\left(\|\boldsymbol{\alpha}_{\Theta_k}\|^2 \geq \frac{2^{R_{bl}} - 1 - K_\rho(R_{el})}{P_r/\sigma_0^2}\right) \Pr\left(\|\boldsymbol{\alpha}_{\Psi_k^+}\|^2 < \frac{2^{R_{el}} - 1}{\bar{\rho} P_r/\sigma_0^2}\right) \qquad (2.48)
\end{aligned}$$

For i.i.d. Rayleigh fading, we have

$$\pi_{d,bl^*,el}(R_{bl},R_{el},\Theta_k,\Psi_k^+) \le \left[1-\gamma_{inc}\left(\frac{2^{R_{bl}}-1-K_\rho(R_{el})}{\Gamma_d},y_k\right)\right]\gamma_{inc}\left(\frac{2^{R_{el}}-1}{\bar{\rho}\Gamma_d},z_k\right)$$
$$\triangleq \pi^{(ub)}_{d,bl^*,el}(R_{bl},R_{el},\Theta_k,\Psi_k^+) \tag{2.49}$$

where we defined $\pi^{(ub)}_{d,bl^*,el}(R_{bl},R_{el},\Theta_k,\Psi_k^+)$ to be a closed-form upper bound of $\pi_{d,bl^*,el}(R_{bl},R_{el},\Theta_k,\Psi_k^+)$.

The conditional joint probability, conditioned on (Θ_k,Ψ_k^+), that the BL/EL is successfully decoded at the destination is given by

$$\begin{aligned}\pi_{d,bl^*,el^*}(R_{bl},R_{el},\Theta_k,\Psi_k^+) &= 1-\Pr(\text{BL not decoded})\\ &\quad -\Pr(\text{BL decoded, EL not decoded})\\ &= 1-\pi_{d,bl}(R_{bl},\Theta_k,\Psi_k^+)-\pi_{d,bl^*,el}(R_{bl},R_{el},\Theta_k,\Psi_k^+)\end{aligned} \tag{2.50}$$

The average outage probability for the BL, the average joint probability that the BL is successfully decoded but not the EL, and the average joint probability that the BL/EL is successfully decoded, averaged over all possible sets (Θ_k,Ψ_k^+), are, respectively, given by

$$\begin{aligned}\pi_{d,bl}(R_{bl}) &= \sum_{(\Theta_k,\Psi_k^+)}\Pr(\Theta_k,\Psi_k^+)\pi_{d,bl}(R_{bl},\Theta_k,\Psi_k^+)\\ \pi_{d,bl^*,el}(R_{bl},R_{el}) &= \sum_{(\Theta_k,\Psi_k^+)}\Pr(\Theta_k,\Psi_k^+)\pi_{d,bl^*,el}(R_{bl},R_{el},\Theta_k,\Psi_k^+)\\ \pi_{d,bl^*,el^*}(R_{bl},R_{el}) &= 1-\pi_{d,bl}(R_{bl})-\pi_{d,bl^*,el}(R_{bl},R_{el})\end{aligned} \tag{2.51}$$

From (2.49), we note that

$$\begin{aligned}\pi_{d,bl^*,el}(R_{bl},R_{el}) &\leq \sum_{(\Theta_k,\Psi_k^+)} \Pr(\Theta_k,\Psi_k^+)\pi^{(ub)}_{d,bl^*,el}(R_{bl},R_{el},\Theta_k,\Psi_k^+) \\ &\triangleq \pi^{(ub)}_{d,bl^*,el}(R_{bl},R_{el}) \end{aligned} \tag{2.52}$$

We define a lower bound on the probability that the BL/EL decoded successfully as follows:

$$\begin{aligned}\pi^{(lb)}_{d,bl^*,el^*}(R_{bl},R_{el}) &\triangleq 1-\pi_{d,bl}(R_{bl})-\pi^{(ub)}_{d,bl^*,el}(R_{bl},R_{el}) \\ &\leq 1-\pi_{d,bl}(R_{bl})-\pi_{d,bl^*,el}(R_{bl},R_{el}) \\ &= \pi_{d,bl^*,el^*}(R_{bl},R_{el}) \end{aligned} \tag{2.53}$$

We note that it takes two time slots to transmit a single message from the source to the destination due to the half-duplex relays. Therefore, the average system throughput is given by [32]

$$\bar{T}(R_{bl},R_{el}) = \pi_{d,bl^*,el}(R_{bl},R_{el})0.5R_{bl} + \pi_{d,bl^*,el^*}(R_{bl},R_{el})0.5(R_{bl}+R_{el}) \text{ [bps/Hz]} \tag{2.54}$$

and the expected distortion is given by

$$\begin{aligned}\bar{D}(R_{bl},R_{el}) = 2^0.\pi_{d,bl}(R_{bl},R_{el}) &+ \pi_{d,bl^*,el}(R_{bl},R_{el})2^{-0.5R_{bl}} \\ &+ \pi_{d,bl^*,el^*}(R_{bl},R_{el})2^{-0.5(R_{bl}+R_{el})} \end{aligned} \tag{2.55}$$

where we assume the distortion of a Gaussian source to be 2^{-R}, and where R [bps/Hz] is the normalized transmission rate [14].

From (2.52), a lower bound on the average throughput is given as follows:

$$\begin{aligned}\bar{T}(R_{bl},R_{el}) &\geq (1-\pi_{d,bl}(R_{bl})0.5R_{bl}+\pi^{(lb)}_{d,bl^*,el^*}(R_{bl},R_{el})0.5R_{el} &(2.56)\\ &= \pi^{(ub)}_{d,bl^*,el}(R_{bl},R_{el})0.5R_{bl}+\pi^{(lb)}_{d,bl^*,el^*}(R_{bl},R_{el})0.5(R_{bl}+R_{el})\\ &\triangleq \bar{T}^{(lb)}(R_{bl},R_{el}) &(2.57)\end{aligned}$$

Similarly, from (2.53), we can show that an upper bound on the average distortion is given by

$$\begin{aligned}\bar{D}(R_{bl},R_{el}) &\leq 2^0.\pi_{d,bl}(R_{bl},R_{el})+\pi^{(ub)}_{d,bl^*,el}(R_{bl},R_{el})2^{-0.5R_{bl}}\\ &\quad+\pi^{(lb)}_{d,bl^*,el^*}(R_{bl},R_{el})2^{-0.5(R_{bl}+R_{el})}\\ &\triangleq \bar{D}^{(ub)}(R_{bl},R_{el}) &(2.58)\end{aligned}$$

We note that these bounds are closed form for i.i.d. Rayleigh fading channels. In the following, we will numerically find an suboptimal set of the system parameters, such as the power allocation parameter ρ and the rates R_{bl} and R_{el} by maximizing the lower bound on the throughput, or minimizing the upper bound on the distortion. For the resulting suboptimal system parameters, we will find the actual average throughput and the actual expected distortion numerically.

2.5 Numerical results

In the numerical results, we assume there are 1, 2, or 4 relays; however, the direct link is assumed to be too weak and will be ignored. We assume the distances from the relays to the source and to the destination are approximately

equal such that the second moments of the channel gains of all links are the same, so that $\Omega_{sr}^{(n)} = \Omega_{rd}^{(n)} = \Omega_0$, for all $n = 1, 2, \ldots, N$. That is, the channel gains of all links are assumed to be i.i.d. Rayleigh with the second moment Ω_0. We assume the transmit power at the relays is limited by $P_r = P_s/N$. We define the received signal-to-noise ratio at a relay as follows:

$$SNR = \Gamma_r = \frac{P_s \Omega_0}{\sigma_0^2}. \tag{2.59}$$

In the following, we first consider the average combined SNR for the BL at the destination using the different combining techniques. We then plot the system performance in terms of the throughput and distortion using the optimal-combining method. We also plot the performance for a conventional single-layer system, for comparison.

2.5.1 Average combined SNR for the BL

In this subsection, we compare the three combining techniques, presented in Subsections 2.3.1, 2.3.2, and 2.3.3, by plotting the average combined SNR of the BL at the destination. For simplicity, we assume there are two relays, $N = 2$. One is always transmitting only the BL, and the other is always transmitting the BL/EL using superposition coding.

In Fig. 2.3, we plot the average combined SNRs for the BL with the power allocation parameter $\rho = 0.9$. We observe about 1dB gain in the average output SNR by using the optimal combining technique. We note that in the low SNR

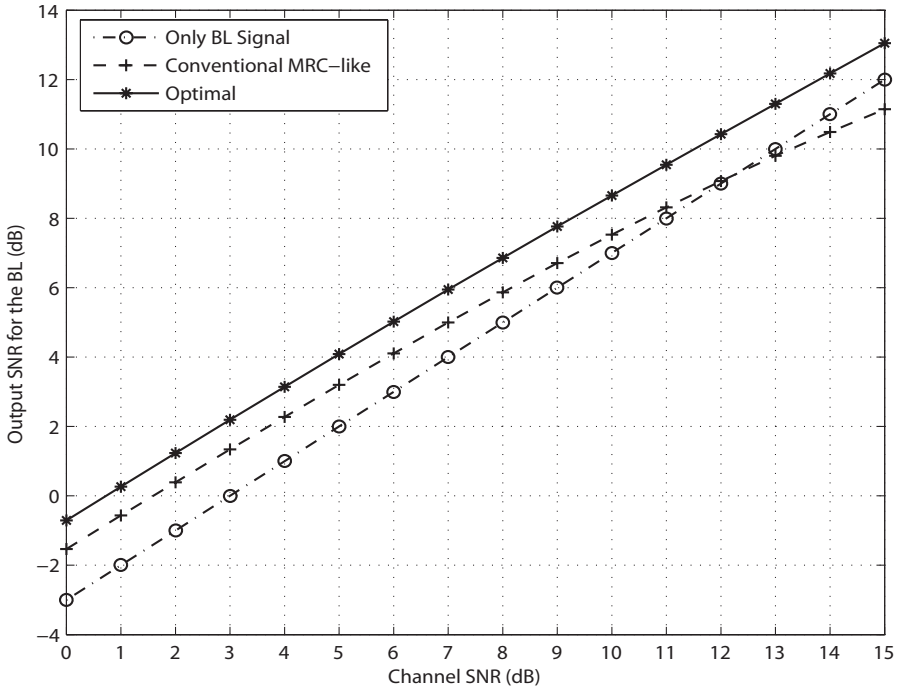

Figure 2.3: Average combined SNR for the BL at the destination: $\rho = 0.90$.

region, the conventional MRC-like combining method performs better than the method in [32] (i.e., using only the BL signals). This is because the former method exploits both the received signals, instead of using only one, and in the low SNR region, the output SINR is more dependent on the noise power than the interference caused by the EL. When channel SNR is high, however, the MRC-like method results in a lower SNR than the other methods, because the interference due to the EL becomes more pronounced. We note that if $\rho = 1$, the double-layer scheme reduces to a single-layer scheme. In this case, the MRC-like method becomes optimal. However, in Fig. 2.4, where we plot the average combined SNR for $\rho = 0.99$, which is close to 1, we can still observe about 0.8dB gain for the optimal

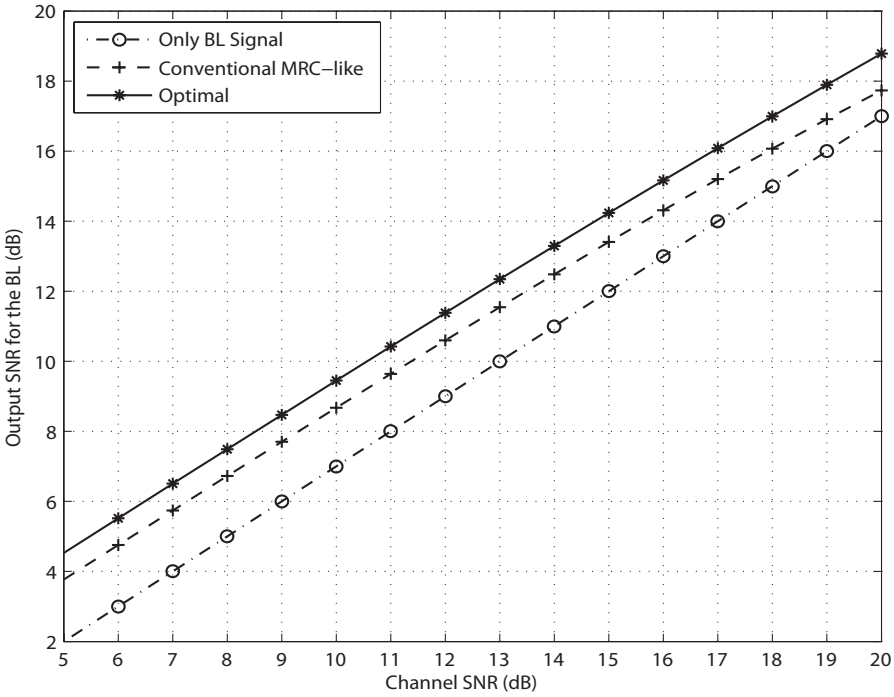

Figure 2.4: Average combined SNR for the BL at the destination: $\rho = 0.99$.

method, compared to the MRC-like method. Also, we note that the MRC-like method is significantly better than the simple method over the entire SNR range of the plot in this case, because the interference caused by the EL is small. In all cases, the optimal method is strictly better than other methods for $\rho \in (0, 1)$. Hence, in the following, we only use the optimal-combining method for the system throughput and distortion evaluation in comparison with the single-layer system.

2.5.2 Throughput and distortion

In this subsection, we consider the average throughput and the expected distortion of the system with various numbers of relays. In the following plots, we

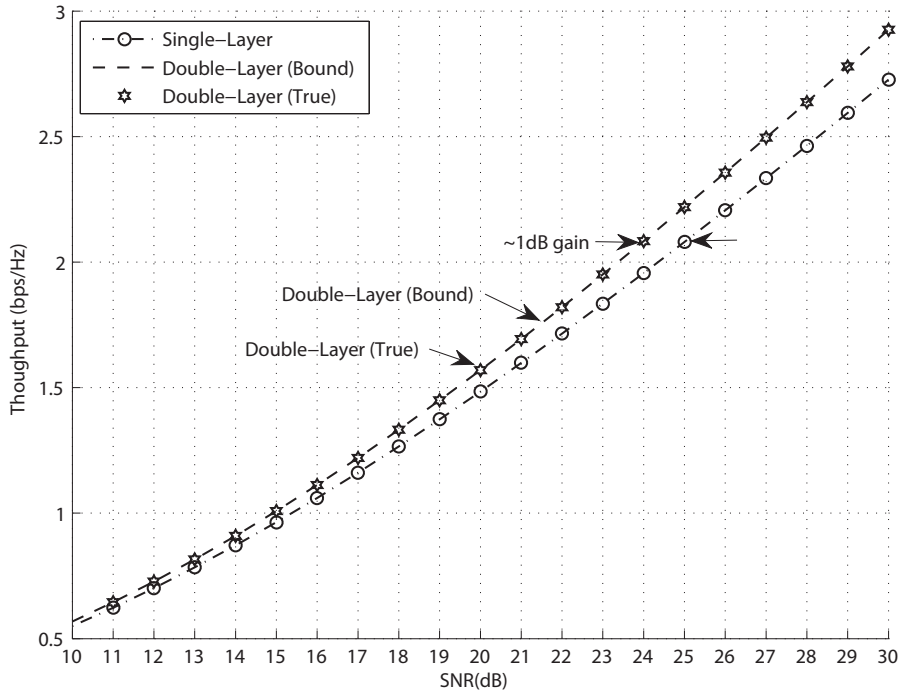

Figure 2.5: Throughput of the system with one relay.

assume the direct link is weak, and will not be used. For the double-layer system, besides the true values, we also plot the lower bound on the average throughput, as given in (2.56), and the upper bound on the expected distortion, as given in (2.58).

In Fig. 2.5, we plot the average throughput for the system with one relay for both the double-layer scheme and the single-layer scheme. Since there is only one relay and the direct link is not used, there is only one received signal at the destination. The lower bound and the true value are, in fact, identical, as shown in the plot. Compared to the single-layer system, we observe approximately 1dB gain in channel SNR when the SNR is about 25dB.

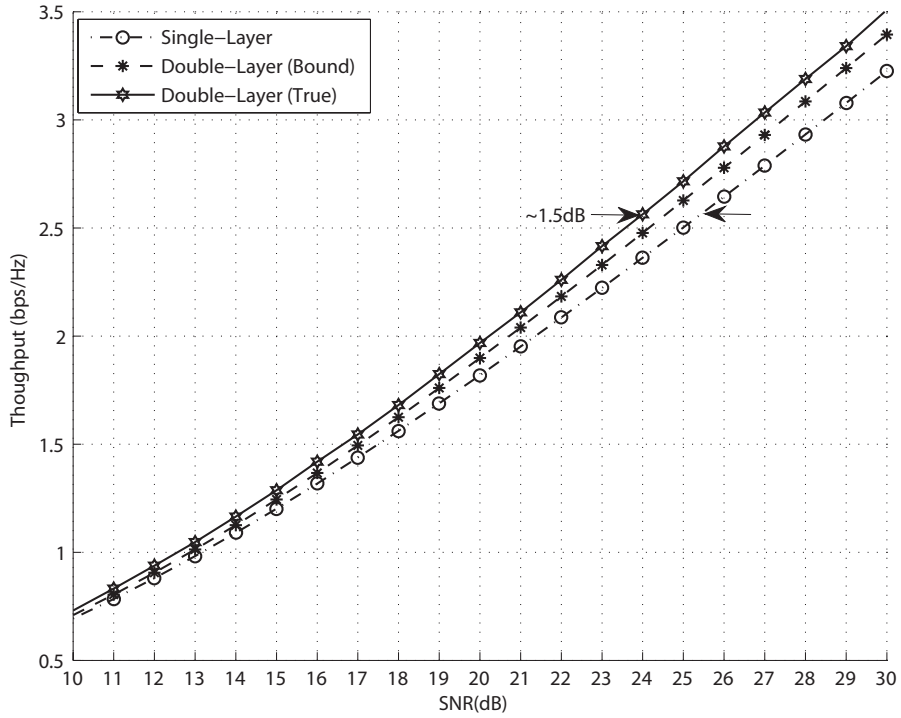

Figure 2.6: Throughput of the system with 2 relays.

In Fig. 2.6, we plot the average throughput for the system with two relays. Since there are possibly two kinds of received signals at the destination, the plot shows that the lower bound on the average throughput is strictly smaller than the true value. Compared to the single-layer system, we observe about 1.5 dB gain in channel SNR when the channel SNR is about 25 dB. Similarly, we observed about 1.5 dB gain in channel SNR for a system with 4 relays, although the curve is not shown here.

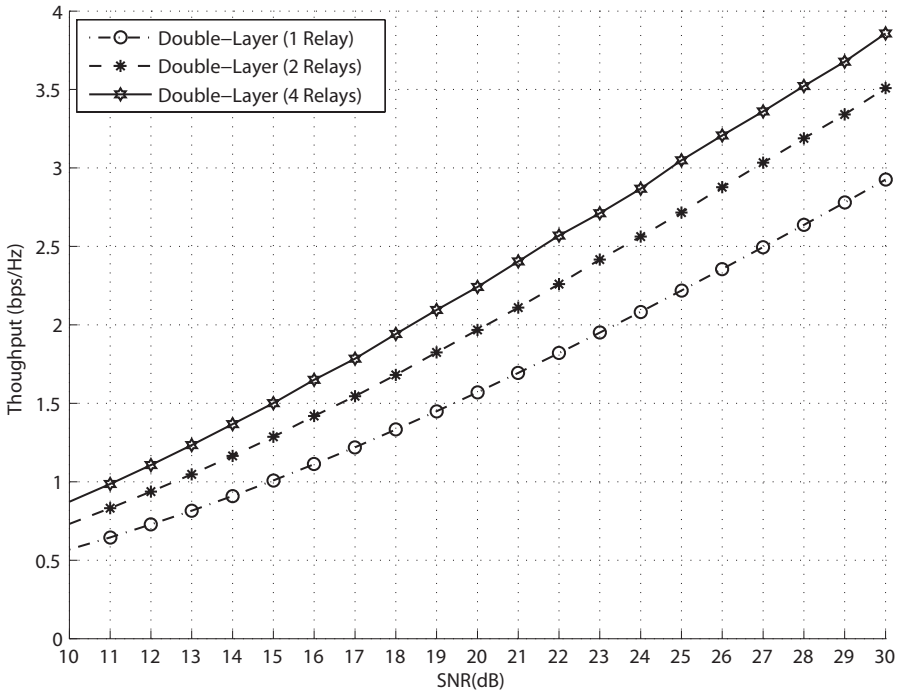

Figure 2.7: Throughput of the system with 1,2, or 4 relays.

In Fig. 2.7, we plot the average throughput for the system with 1, 2, or 4 relays for the double-layer scheme with the optimal-combining method. We can see significant improvement in the system throughput when the number of relays increases. We note here that, since we normalize the throughput by the sub-band bandwidth, when the number of relays increases, the total bandwidth used for the multiple access links from the relays to the destination linearly increases. That is, we trade off the bandwidth used for the multiple access channels for the system throughput. Note that the bandwidth of the broadcast channels (from the source) and the total transmitted power of the relays are fixed and do not depend on the number of relays.

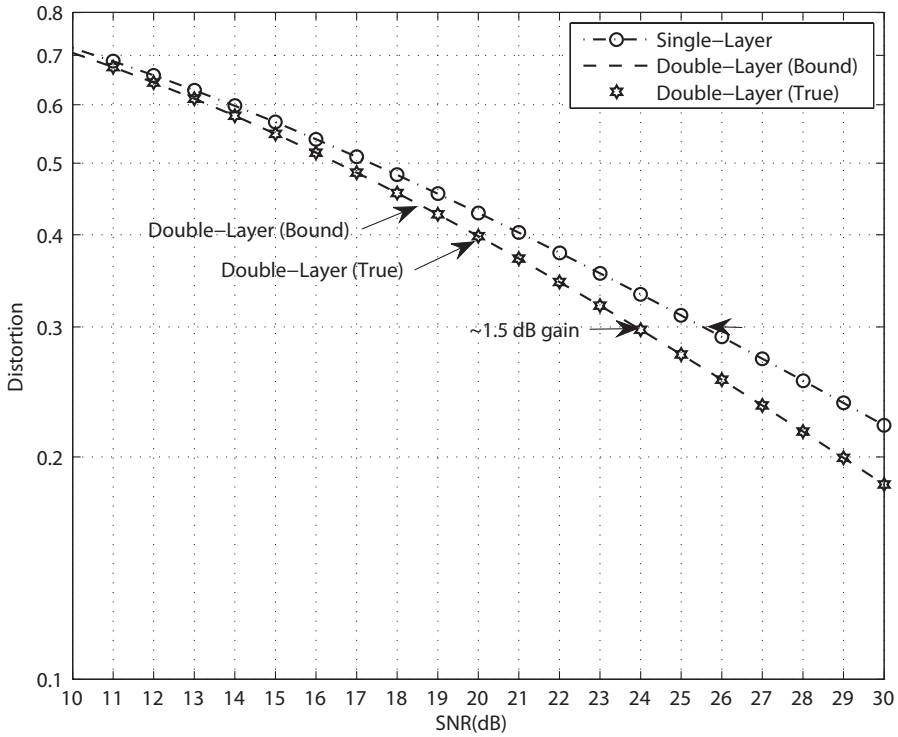

Figure 2.8: Distortion of the system with one relay.

In the following, we consider the system performance in terms of the expected distortion. In Fig. 2.8, we plot the expected distortion for the system with one relay for both the double-layer scheme and the single-layer scheme. Similar to the throughput case, both the lower bound and the true values are identical in this case, since there is only one received signal at the destination. Compared to the single-layer system, we observe about 1.5dB gain in channel SNR when the channel SNR is around 25 dB.

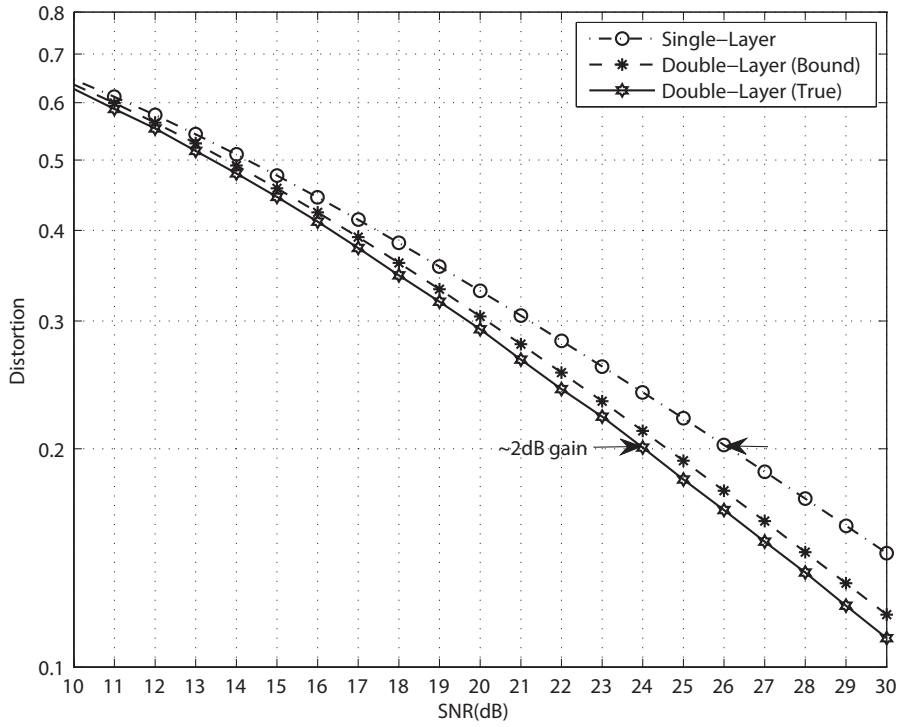

Figure 2.9: Distortion of the system with 2 relays.

In Fig. 2.9, we plot the expected distortion of the system with 2 relays. Compared to the single-layer system, we observe 2dB gain in channel SNR when the channel SNR is around 25 dB, which is also the case for a system with 4 relays (that curve is not shown).

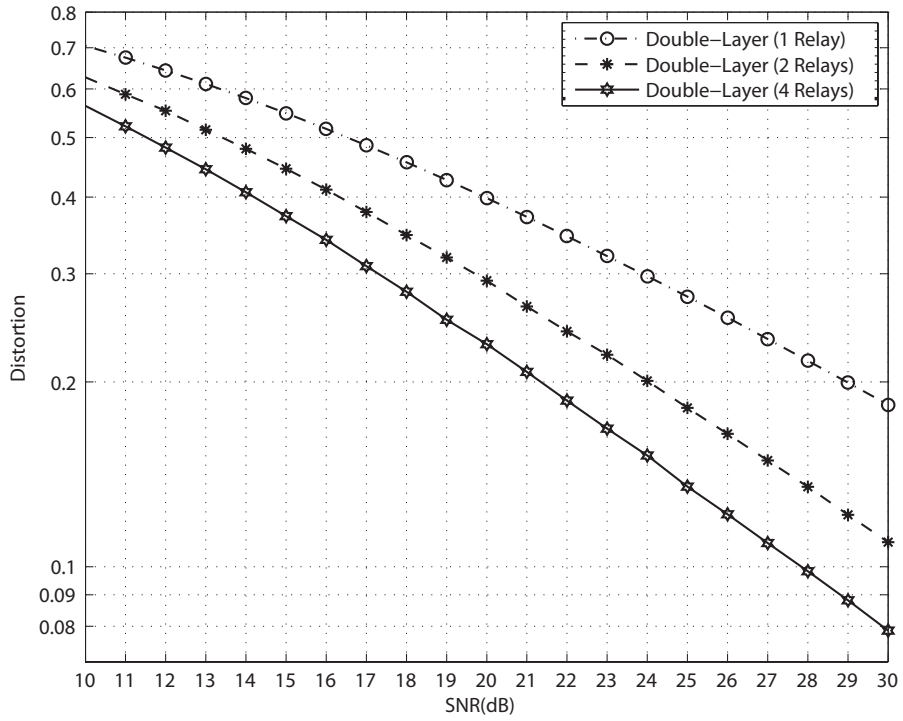

Figure 2.10: Distortion of the system with 4 relays.

Lastly, in Fig. 2.10, we plot the expected distortion for the systems with 1, 2, or 4 relays for the double-layer scheme with optimal combining. We observe a large improvement in the expected distortion as the number of relays increases. Again, we note that the trade off for the system improvement is the increase in the used for the multiple access channels, as the number of relays increases.

2.6 Conclusion

In this chapter, we considered a relay network with a single source, a single destination, and multiple relays. A successively refinable Gaussian source partitioned into two layers is transmitted using superposition coding. The relays forward all their successfully decoded layers to the destination using orthogonal channels. We derived the optimal linear-combining receiver at the destination, and showed that the optimal method gain about a dB compared to the suboptimal methods in terms of the output combined SINR. Using the optimal-combining method at the destination, we derived the average throughput and the expected distortion with the closed-form lower and upper bounds, respectively. We obtained suboptimal system parameters, based on the closed-form bounds, and obtained the actual average throughput and expected distortion numerically. Numerical results showed that the proposed two-layer scheme using superposition coding with the optimal linear combining method can gain up to 1-1.5 dB in channel SNR for the average throughput, or 1.5-2dB in channel SNR for the expected distortion, compared to the conventional one-layer counterpart.

2.7 Acknowledgements

Chapter II of this dissertation is, in full, a reprint of the material as it appears in Tu V. Nguyen and Laurence B. Milstein, "Layered Transmission over Decode-and-Forward Wireless Relay Networks using Superposition Coding," submitted to *IEEE Transactions on Communications,* 2013 and in Tu V. Nguyen and Laurence B. Milstein, "Optimal Linear-Combining Receiver for Layered Transmission for Decode-and-Forward Relays with Superposition Coding," *submitted to IEEE Asilomar Conference on Signals, Systems and Computers*, 2013. I was the primary author of all these publications and the co-author Professor Milstein directed and supervised the research which forms the basis for Chapters II.

Chapter 3

Layered Video Transmission over Wireless Relay Networks using Hierarchical Modulation

3.1 Introduction

In this chapter, we again consider wireless relay networks with a single source, a single destination, and multiple relays, all of which are equipped with a single antenna. Neither a feedback channel nor retransmission is allowed in order to reduce extra latency (and system design complexity). Also, the relays cannot communicate with each other for cooperation purpose. A layered video bitstream, encoded using the H.264/AVC reference encoder [35–38], is transmitted from the source to the destination using the help of the relays.

In our proposed scheme, hierarchical QAM modulation will be used to provide UEP for an embedded bitstream. We assume the embedded bitstream can be

partitioned into two layers with different levels of importance. The relays adaptively use different modulation schemes, depending on the number of successfully decoded layers. We will see later that, because of different modulation schemes used at the relays, classical maximal ratio combining (MRC) cannot straightforwardly be applied at the destination. The combining methods in [31] and [32] can be used; however, both of them are suboptimal.

In this chapter, we derive the optimal linear combining weight vectors for the BL and the EL by a two-step combining method, where the optimality is in terms of minimizing the uncoded BER. In the first step, we derive the optimal vectors' directions, which have closed-form optimal solutions for both the BL and the EL. In the second step, a weight, which represents the vector length, needs to be found. For the BL, convex optimization programming [34] can be used to solve for the optimal weight. For the EL, such convex optimization programming does not exist (thus only a local optimum can be guaranteed). We also present a suboptimal method to find the weight for the BL by minimizing an upper-bound BER, which has a closed-form solution and performs very close to the optimal. Both the optimal and suboptimal methods for the BL significantly outperform the combining methods in [31, 32]. A suboptimal combining method for the EL in the second step is also presented, which performs well compared to the optimal.

Numerical results show that our proposed double-layer scheme using hierarchical 16-QAM significantly outperforms a classical single-layer scheme using conventional modulation. For example, approximately 2-2.5dB gain in channel

SNR, or 5-7dB gain in the PSNR, can be observed.

The rest of this chapter is organized as follows. In Section 3.2, we present the system model. The novel combining technique and the system performance are presented in Section 3.3. The application to transmission of layered video bitstreams over the network is presented in Section 3.4, and Section 3.5 concludes the chapter.

3.2 System model

In this chapter we consider the same model as that in Chapter II. That is, we consider a relay network with a single source, a single destination, and N_r relays, all of which are equipped with a single antenna, as shown in Fig. 1.1. The relays are half-duplex, use the decode-and-forward protocol [7], and are not able to communicate with each other. Multiple access channels from the relays to the destination are orthogonal in the frequency domain, as shown in Fig. 2.1.

3.2.1 Channel model

We assume the channels from the source to the relays and from the relays to the destination experience flat Rayleigh fading, and we use the modified Jakes' model [45] to simulate different fading rates. Due to the spatial separation, we also assume that all the channels from the source to the relays and from the relays to the destination are independent. We assume that the channel gain is constant

for each symbol, and that it can be accurately estimated at the receiver. However, the channel gain is assumed to be unknown at the transmitter.

3.2.2 Source model

We consider the transmission of a layered video bitstream, encoded with the H.264/AVC encoder [35–38]. Similar to a refinable Gaussian source, the video-encoded bitstream can be partitioned into a BL and an EL, where the BL is more important than the EL in terms of the source distortion. The layer partition is not, however, a trivial problem, and will be presented in detail in Subsection 3.4.1. In this chapter, we adopt hierarchical QAM modulation [19,46] to provide unequal error protection.

3.2.3 Transmission schemes

A. Classical single-layer scheme - Baseline

For the classical single-layer scheme, we assume the system is unaware of the source's information; hence, it considers the source as an i.i.d. bitstream. Classical 16-QAM with Gray-coded bit-mapping is used, where all bits in a symbol are considered to be of the same importance. This is referred to as the equal error protection (EEP) scheme. In the first time slot, the source encodes and broadcasts a message to all the relays. The relays separately decode the message. If successful, they re-encode and forward it to the destination using the same modulation scheme. At the destination, since the received signals use the same modulation scheme, a

maximum-ratio-combining (MRC) receiver can be used to combine all the received signals to decode the message.

B. Proposed double-layer scheme

In the first time slot, the source encodes and broadcasts the message to all the relays and the destination. The first half of the message contains the BL and the second half of the message contains the EL. We use hierarchical 16-QAM as the modulation scheme,[1] where the BL is mapped into the most significant bits (MSBs) and the EL is mapped into the least significant bits (LSBs), as shown in Fig. 3.1. The relays separately decode the message. If the BL is decoded successfully, an attempt is made to decode the EL. Depending on the channel quality from the source to the relays, and the power allocation parameter for the hierarchical 16-QAM, a relay can successfully decode both the BL and the EL (the BL/EL), only the BL, or neither. In the second time slot, the relays re-encode and forward any successfully decoded layers to the destination. The hierarchical 16-QAM modulation scheme is used if both layers were successfully received. If, however, only the BL is successfully received at a relay, it will transmit only the BL to the destination using conventional QPSK. Lastly, the relay remains silent if no layer was successfully decoded. In this chapter, we propose combining methods to first detect the BL and then to detect the EL, which minimizes the uncoded BER.

[1]We note that the method proposed in this chapter can be generalized to higher order modulation schemes such as hierarchical 64-QAM or 256-QAM with 3 or 4 embedded source layers, respectively.

In both schemes, we use a cyclic redundancy check (CRC) to check whether or not a message is received correctly. Throughout this chapter, we assume the CRC is perfect in the sense that it can detect the error with probability one. Since the mathematical representation of the single-layer scheme with conventional 16-QAM is straightforward, in the following, we focus on the double-layer scheme with hierarchical 16-QAM modulation.

3.2.4 Signal model at the relays and the destination

We consider hierarchical 16-QAM modulation using Gray-coded bit mapping, as shown in Fig. 3.1. We can express a hierarchical 16-QAM symbol, denoted by A_l, as the weighted sum, or superposition, of two QPSK symbols as follows [15]:

$$A_l = \sqrt{\rho} b_l + \sqrt{\bar{\rho}} e_l \tag{3.1}$$

where b_l and e_l denote two QPSK-modulated symbols, which depend on the MSBs and the LSBs, respectively, of the hierarchical 16-QAM symbol. We use $\rho \in (0.5, 1]$ to denote the normalized power allocated to the MSB signal b_l, and $\bar{\rho} \triangleq 1 - \rho$ to denote the normalized power allocated to the LSB signal e_l.[2]

In the first time slot, the source broadcasts the embedded bitstream including both the BL/EL to all the relays using the hierarchical 16-QAM scheme using a fixed sub-band. The received signal sample at the n-th relay at the output of a

[2]Relative to the power allocation ratio in [19], we have $\alpha = d_M/d_L = (\sqrt{\rho} - \sqrt{\bar{\rho}})/\sqrt{\bar{\rho}}$ (where $\bar{\rho} = 1 - \rho$), that is, e.g., if $\rho = 0.70$ then $\alpha \approx 0.528$, if $\rho = 0.80$ then $\alpha = 1.0$ (i.e., conventional constellation), and if $\rho = 0.90$ then $\alpha = 2.0$.

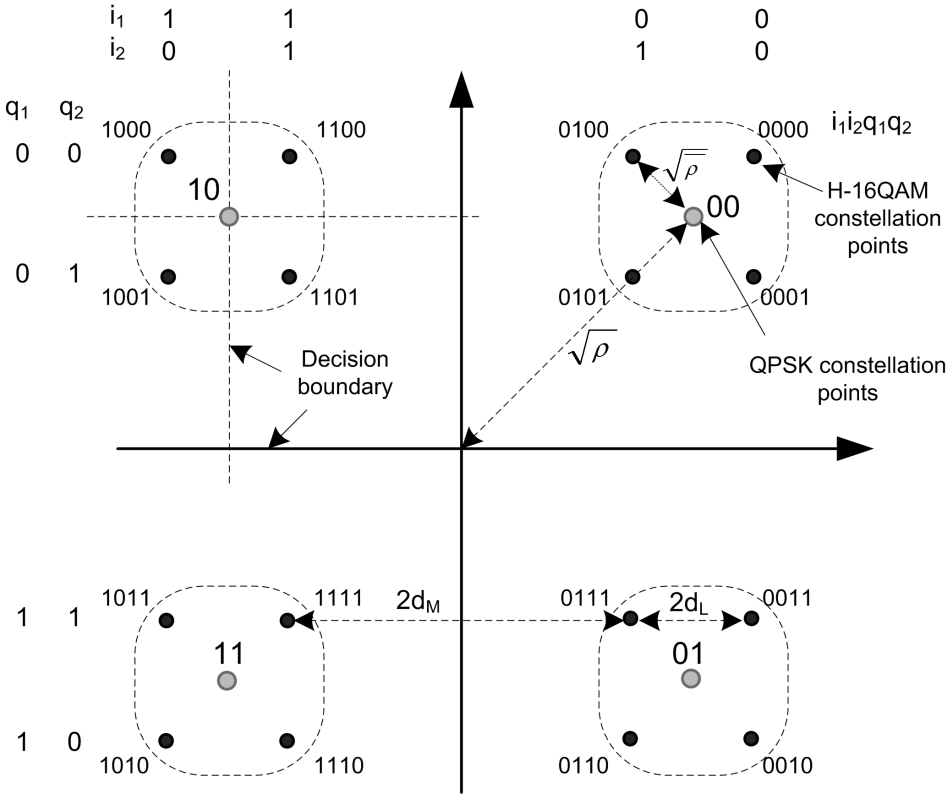

Figure 3.1: Hierarchical 16-QAM constellation as superposition mapping of two QPSK constellations.

matched filter can be written as

$$y_{n,l}^{(r)} = \alpha_{n,l}^{sr}\sqrt{2E_s}\big(\sqrt{\rho}b_l + \sqrt{\bar{\rho}}e_l\big) + z_{n,l}^{(r)}, \quad n = 1, 2, \ldots, N_r \tag{3.2}$$

where $\alpha_{n,l}^{sr}$ is the channel gain at the sampling time lT_s, which is assumed to be real-valued and non-negative (i.e., a coherent receiver is assumed), with T_s being the sampling period. In (3.2), E_s denotes the transmitted symbol energy at the source, b_l and e_l denote the BL and the EL modulated signals at time lT_s, respectively, each of which is a QPSK-modulated symbol with unity power, and ρ is the power allocation parameter (see Fig. 3.1). The terms $\{z_{n,l}^{(r)}\}$ are assumed to be independently and identically distributed (i.i.d.) and circularly symmetric complex

Gaussian noise $\mathcal{CN}(0, 2N_0)$. Similarly, the received signal at the destination in the first time slot is given by

$$y_{0,l}^{(d)} = \alpha_l^{sd}\sqrt{2E_s}\big(\sqrt{\rho}b_l + \sqrt{\bar{\rho}}e_l\big) + z_{0,l}^{(d)} \tag{3.3}$$

In the second time slot, depending on the number of successfully decoded layers at the relays, the destination can receive different signals in each sub-band. If the n-th relay transmitted both the BL/EL using hierarchical 16-QAM, the received signal in the n-th sub-band at the destination is given by

$$y_{n,l}^{(d)} = \alpha_{n,l}^{rd}\sqrt{2E_r}\big(\sqrt{\rho}b_l + \sqrt{\bar{\rho}}e_l\big) + z_{n,l}^{(d)}, \tag{3.4}$$

or, if only the BL is transmitted (using QPSK),

$$y_{n,l}^{(d)} = \alpha_{n,l}^{rd}\sqrt{2E_r}b_l + z_{n,l}^{(d)} \tag{3.5}$$

where E_r denotes the average transmit symbol energy at the relays. Note that all the power is allocated to the BL when QPSK is used (i.e., $\rho = 1$). In (3.4) and (3.5), similarly, we assume the $\{z_{n,l}^{(d)}\}$ are i.i.d. and complex Gaussian noise $\mathcal{CN}(0, 2N_0)$. For combining and detection at the destination, in practice, each relay needs to send a signalling message (of two bits) to inform the destination which type of signal it will send. For simplicity, we assume the signalling message is received at the destination error-free, and ignore the signalling overhead.

Due to the spatial separation, we assume the fading gains $\alpha_{n,l}^{sr}, \alpha_{n,l}^{rd}$, and α_l^{sd} are independent, with second moments $\Omega_n^{sr}, \Omega_n^{rd}$, and Ω^{sd}, respectively. For notational simplicity, we also consider the source itself as relay 0, and denote

$\alpha_{0,l}^{rd} = \sqrt{E_s/E_r}\alpha_l^{sd}$, and thus $\Omega_0^{rd} = \Omega^{sd}E_s/E_r$, such that the received signal at the destination in the first time slot, as shown in (3.3), can be written as

$$y_{0,l}^{(d)} = \alpha_{0,l}^{rd}\sqrt{2E_r}\left(\sqrt{\rho}b_l + \sqrt{\bar{\rho}}e_l\right) + z_{0,l}^{(d)} \tag{3.6}$$

which is (3.4) for $n = 0$.

Since the destination can receive two types of signals, one of which includes both the BL/EL using hierarchical 16-QAM and the other includes only the BL using QPSK, the classical MRC receiver cannot be applied straightforwardly. In [32], the received signals that include only the BL, if at least one is available, are combined to detect the BL. If no such signal is available, that is, all the received signals include both layers, then an MRC receiver is used to combine the received signals to detect the BL (and the EL). Clearly, this is a suboptimal receiver, because not all of the available received signals were exploited. In [31], another combining method was used which is equivalent to an MRC receiver when all the transmitted signals are identical, i.e., all are either hierarchical 16-QAM or QPSK. This is again a suboptimal method.

3.3 Proposed combining methods at the destination

Let Θ_k be the set of relay indices which have successfully decoded only the BL. Unlike Chapter II, let Ψ_k be the set of relay indices, including relay 0, i.e., the source, if the direct link is used, which have successfully decoded both the BL/EL.

We note that Θ_k and Ψ_k are subsets of the set of all relay indices, and $\Theta_k \cap \Psi_k = \emptyset$. The received signals at the destination from the relays in the set Θ_k and Ψ_k are given in (3.5) and (3.4), respectively.

In the following, we consider both the optimal and a suboptimal method to combine the received signals in the sets Θ_k and Ψ_k at the destination to decode the base layer signal. Optimality is defined in terms of minimizing the uncoded bit error rate. We note that if either Θ_k or Ψ_k is an empty set, i.e., only one kind of signal is received, the classical MRC receiver can be applied, and which is optimal. Thus, in the following, we consider the case that both sets are nonempty.

3.3.1 Combined signals and optimization problems

Given the received signals $y_{n,l}^{(d)}$ for $n \in \Theta_k$, as shown in (3.5), and $y_{n,l}^{(d)}$ for $n \in \Psi_k$, as shown in (3.4), we need to combine them to detect the BL and the EL. Generally, the optimal weights for detecting the BL and the EL are different. We first consider the combining for the BL (the combining for the EL is done in a similar manner). Let w_n be the weight corresponding to the received signal from the n-th relay. The combined signal for the BL at the destination is given by

$$Y_{l,bl}^{(d)} = \sum_{n \in \Theta_k \cup \Psi_k} w_n y_{n,l}^{(d)} = \sum_{n \in \Theta_k} w_n y_{n,l}^{(d)} + \sum_{n \in \Psi_k} w_n y_{n,l}^{(d)} \tag{3.7}$$

where, as noted above, $\Theta_k \cap \Psi_k = \emptyset$. Substituting $y_{n,l}^{(d)}$ from (3.5) and (3.4) for $n \in \Theta_k$ and $n \in \Psi_k$, respectively, we have

$$\begin{aligned} Y_{l,bl}^{(d)} &= \sqrt{2E_r} \sum_{n\in\Theta_k} w_n \alpha_{n,l}^{rd} b_l + \sum_{n\in\Theta_k} w_n z_{n,l}^{(d)} \\ &\quad + \sqrt{2E_r} \sum_{n\in\Psi_k} w_n \alpha_{n,l}^{rd} \big(\sqrt{\rho} b_l + \sqrt{\bar{\rho}} e_l\big) + \sum_{n\in\Psi_k} w_n z_{n,l}^{(d)} \end{aligned} \tag{3.8}$$

For notational simplicity, we consider the following definitions, as similar to (2.13) and (2.14) on page 18:

$$C_{\Theta_k}(\mathbf{w}_{\Theta_k}) \triangleq \sum_{n\in\Theta_k} w_n \alpha_{n,l}^{rd} = \mathbf{w}_{\Theta_k}^T \boldsymbol{\alpha}_{\Theta_k}, \quad C_{\Psi_k}(\mathbf{w}_{\Psi_k}) \triangleq \sum_{n\in\Psi_k} w_n \alpha_{n,l}^{rd} = \mathbf{w}_{\Psi_k}^T \boldsymbol{\alpha}_{\Psi_k} \tag{3.9}$$

$$N_{\Theta_k}(\mathbf{w}_{\Theta_k}) \triangleq \sum_{n\in\Theta_k} w_n z_{n,l}^{(d)} = \mathbf{w}_{\Theta_k}^T \mathbf{z}_{\Theta_k}, \quad N_{\Psi_k}(\mathbf{w}_{\Psi_k}) \triangleq \sum_{n\in\Psi_k} w_n z_{n,l}^{(d)} = \mathbf{w}_{\Psi_k}^T \mathbf{z}_{\Psi_k} \tag{3.10}$$

where we note that $\Theta_k \cap \Psi_k = \emptyset$, and thus N_{Θ_k} and N_{Ψ_k} are independent. Using the definitions (3.9) and (3.10) in (3.8), after re-organizing terms, we have

$$\begin{aligned} Y_{l,bl}^{(d)} &= \sqrt{2E_r}\big[C_{\Theta_k}(\mathbf{w}_{\Theta_k}) + C_{\Psi_k}(\mathbf{w}_{\Psi_k})\sqrt{\rho}\big] b_l + \sqrt{2E_r}\big[C_{\Psi_k}(\mathbf{w}_{\Psi_k})\sqrt{\bar{\rho}}\big] e_l \\ &\quad + N_{\Theta_k}(\mathbf{w}_{\Theta_k}) + N_{\Psi_k}(\mathbf{w}_{\Psi_k}) \end{aligned} \tag{3.11}$$

From (3.10), we note that if we change the sign of an element of the weight vector $\mathbf{w}_{\Theta_k}$ (or $\mathbf{w}_{\Psi_k}$), the statistics of the combining noise $N_{\Theta_k}(\mathbf{w}_{\Theta_k})$ (or $N_{\Psi_k}(\mathbf{w}_{\Psi_k})$) do not change. Since all the channel gains $\{\alpha_{n,l}^{rd}\}$ are non-negative, from (3.9), we observe that the optimal weights $\{w_n\}$ must be non-negative, otherwise we can change the signs of the negative weights to increase the signal component by increasing either $C_{\Theta_k}(\mathbf{w}_{\Theta_k})$ or $C_{\Psi_k}(\mathbf{w}_{\Psi_k})$, as shown in (3.11), while not changing the noise statistics. Hence, the optimal weight vectors $\mathbf{w}_{\Theta_k}$ and $\mathbf{w}_{\Psi_k}$ must have

all the elements being non-negative, which we denote by $\mathbf{w}_{\Theta_k} \succeq 0$ and $\mathbf{w}_{\Psi_k} \succeq 0$. As a result, both $C_{\Theta_k}(\mathbf{w}_{\Theta_k})$ and $C_{\Psi_k}(\mathbf{w}_{\Psi_k})$ are non-negative. Further, we note that if either $\mathbf{w}_{\Theta_k} = \mathbf{0}$ or $\mathbf{w}_{\Psi_k} = \mathbf{0}$, the combined weight vectors cannot be optimal because we do not use all the received signals for detection. Hence, in the following, we assume both $\mathbf{w}_{\Theta_k} \neq \mathbf{0}$ and $\mathbf{w}_{\Psi_k} \neq \mathbf{0}$ when solving for the optimal weight vectors.

Note that the combined signal in (3.11) is a noisy hierarchical 16-QAM symbol. The conditional BER expressions, conditioned on the channel gains, for the BL as follows [19, 46]:

$$\begin{aligned} BER_{BL}(\mathbf{w}_{\Theta_k}, \mathbf{w}_{\Psi_k}) = \frac{1}{2}Q\left(\frac{\sqrt{E_r}C_{\Theta_k}(\mathbf{w}_{\Theta_k}) + \sqrt{E_r}C_{\Psi_k}(\mathbf{w}_{\Psi_k})\big(\sqrt{\rho} - \sqrt{\bar{\rho}}\big)\big]}{\sqrt{(\|\mathbf{w}_{\Theta_k}\|^2 + \|\mathbf{w}_{\Psi_k}\|^2)N_0}}\right) \\ + \frac{1}{2}Q\left(\frac{\sqrt{E_r}C_{\Theta_k}(\mathbf{w}_{\Theta_k}) + \sqrt{E_r}C_{\Psi_k}(\mathbf{w}_{\Psi_k})\big(\sqrt{\rho} + \sqrt{\bar{\rho}}\big)\big]}{\sqrt{(\|\mathbf{w}_{\Theta_k}\|^2 + \|\mathbf{w}_{\Psi_k}\|^2)N_0}}\right) \end{aligned} \tag{3.12}$$

Similarly, the conditional BER expressions, conditioned on the channel gains, for the EL as follows:

$$\begin{aligned} BER_{EL}(\mathbf{v}_{\Theta_k}, \mathbf{v}_{\Psi_k}) = Q\left(\frac{\sqrt{E_r}C_{\Psi_k}(\mathbf{v}_{\Psi_k})\sqrt{\bar{\rho}}}{\sqrt{(\|\mathbf{v}_{\Theta_k}\|^2 + \|\mathbf{v}_{\Psi_k}\|^2)N_0}}\right) \\ + \frac{1}{2}Q\left(\frac{\sqrt{E_r}\big[2C_{\Theta_k}(\mathbf{v}_{\Theta_k}) + C_{\Psi_k}(\mathbf{v}_{\Psi_k})\big(2\sqrt{\rho} - \sqrt{\bar{\rho}}\big)\big]}{\sqrt{(\|\mathbf{v}_{\Theta_k}\|^2 + \|\mathbf{v}_{\Psi_k}\|^2)N_0}}\right) \\ - \frac{1}{2}Q\left(\frac{\sqrt{E_r}\big[2C_{\Theta_k}(\mathbf{v}_{\Theta_k}) + C_{\Psi_k}(\mathbf{v}_{\Psi_k})\big(2\sqrt{\rho} + \sqrt{\bar{\rho}}\big)\big]}{\sqrt{(\|\mathbf{v}_{\Theta_k}\|^2 + \|\mathbf{v}_{\Psi_k}\|^2)N_0}}\right) \end{aligned} \tag{3.13}$$

where $\mathbf{v}_{\Theta_k}$ and $\mathbf{v}_{\Psi_k}$ denote the combining vectors for the EL, whose elements are non-negative, as for the BL.

The optimization problem for minimizing the BER of the BL is formally

given by

$$BER_{BL}^{*} \triangleq \underset{\mathbf{w}_{\Theta_k},\mathbf{w}_{\Psi_k}\succeq 0}{\text{minimize}}\ BER_{BL}(\mathbf{w}_{\Theta_k},\mathbf{w}_{\Psi_k}) \tag{3.14}$$

and, similarly, for the EL

$$BER_{EL}^{*} \triangleq \underset{\mathbf{v}_{\Theta_k},\mathbf{v}_{\Psi_k}\succeq 0}{\text{minimize}}\ BER_{EL}(\mathbf{v}_{\Theta_k},\mathbf{v}_{\Psi_k}), \tag{3.15}$$

where the superscript $*$ denotes the optimal value for the corresponding quantity.

Due to the complexity of the BER expressions, as shown in (3.14) and (3.15), we will not solve the problem directly. Instead, we solve the problem in two steps. In the first step, we optimize over the vectors' directions. Then, in the second step, we optimize over the vectors' lengths. In the following, we present these steps precisely.

For $\mathbf{w}_{\Theta_k},\mathbf{w}_{\Psi_k},\mathbf{v}_{\Theta_k},\mathbf{v}_{\Psi_k}\succeq 0$, and which are not equal to the zero vector, we can write

$$\mathbf{w}_{\Theta_k}=a_{\Theta_k}\tilde{\mathbf{w}}_{\Theta_k},\quad \mathbf{w}_{\Psi_k}=a_{\Psi_k}\tilde{\mathbf{w}}_{\Psi_k} \tag{3.16}$$

for $a_{\Theta_k},a_{\Psi_k}>0$, $\tilde{\mathbf{w}}_{\Theta_k},\tilde{\mathbf{w}}_{\Psi_k}\succeq 0$, and $\|\tilde{\mathbf{w}}_{\Theta_k}\|=\|\tilde{\mathbf{w}}_{\Psi_k}\|=1$, and similarly

$$\mathbf{v}_{\Theta_k}=b_{\Theta_k}\tilde{\mathbf{v}}_{\Theta_k},\quad \mathbf{v}_{\Psi_k}=b_{\Psi_k}\tilde{\mathbf{v}}_{\Psi_k} \tag{3.17}$$

for $b_{\Theta_k},b_{\Psi_k}>0$, $\tilde{\mathbf{v}}_{\Theta_k},\tilde{\mathbf{v}}_{\Psi_k}\succeq 0$, and $\|\tilde{\mathbf{v}}_{\Theta_k}\|=\|\tilde{\mathbf{v}}_{\Psi_k}\|=1$.

Substituting (A.1) into (3.12), and (3.17) into (3.13), and noting from (3.9)

that $C_\Phi(\mathbf{x}) = C_\Phi(a\tilde{\mathbf{x}}) = aC_\Phi(\tilde{\mathbf{x}})$ for $\Phi \in \{\Theta_k, \Psi_k\}$, we have

$$\begin{aligned} &BER_{BL}(a_{\Theta_k}, a_{\Psi_k}, \tilde{\mathbf{w}}_{\Theta_k}, \tilde{\mathbf{w}}_{\Psi_k}) \triangleq BER_{BL}(a_{\Theta_k}\tilde{\mathbf{w}}_{\Theta_k}, a_{\Psi_k}\tilde{\mathbf{w}}_{\Psi_k}) \\ &= \frac{1}{2}Q\left(\frac{\sqrt{E_r}a_{\Theta_k}C_{\Theta_k}(\tilde{\mathbf{w}}_{\Theta_k}) + \sqrt{E_r}a_{\Psi_k}C_{\Psi_k}(\tilde{\mathbf{w}}_{\Psi_k})\big(\sqrt{\rho} - \sqrt{\bar{\rho}}\big)\big]}{\sqrt{(a_{\Theta_k}^2 + a_{\Psi_k}^2)N_0}}\right) \\ &+ \frac{1}{2}Q\left(\frac{\sqrt{E_r}a_{\Theta_k}C_{\Theta_k}(\tilde{\mathbf{w}}_{\Theta_k}) + \sqrt{E_r}a_{\Psi_k}C_{\Psi_k}(\tilde{\mathbf{w}}_{\Psi_k})\big(\sqrt{\rho} + \sqrt{\bar{\rho}}\big)\big]}{\sqrt{(a_{\Theta_k}^2 + a_{\Psi_k}^2)N_0}}\right) \end{aligned} \tag{3.18}$$

and

$$\begin{aligned} &BER_{EL}(b_{\Theta_k}, b_{\Psi_k}, \tilde{\mathbf{v}}_{\Theta_k}, \tilde{\mathbf{v}}_{\Psi_k}) \triangleq BER_{EL}(b_{\Theta_k}\tilde{\mathbf{v}}_{\Theta_k}, b_{\Psi_k}\tilde{\mathbf{v}}_{\Psi_k}) \\ &= Q\left(\frac{\sqrt{E_r}b_{\Psi_k}C_{\Psi_k}(\tilde{\mathbf{v}}_{\Psi_k})\sqrt{\bar{\rho}}}{\sqrt{(b_{\Theta_k}^2 + b_{\Psi_k}^2)N_0}}\right) \\ &+ \frac{1}{2}Q\left(\frac{\sqrt{E_r}\big[2b_{\Theta_k}C_{\Theta_k}(\tilde{\mathbf{v}}_{\Theta_k}) + b_{\Psi_k}C_{\Psi_k}(\tilde{\mathbf{v}}_{\Psi_k})\big(2\sqrt{\rho} - \sqrt{\bar{\rho}}\big)\big]}{\sqrt{(b_{\Theta_k}^2 + b_{\Psi_k}^2)N_0}}\right) \\ &- \frac{1}{2}Q\left(\frac{\sqrt{E_r}\big[2b_{\Theta_k}C_{\Theta_k}(\tilde{\mathbf{v}}_{\Theta_k}) + b_{\Psi_k}C_{\Psi_k}(\tilde{\mathbf{v}}_{\Psi_k})\big(2\sqrt{\rho} + \sqrt{\bar{\rho}}\big)\big]}{\sqrt{(b_{\Theta_k}^2 + b_{\Psi_k}^2)N_0}}\right) \end{aligned} \tag{3.19}$$

We note that the optimization problems, as shown in (3.14) and (3.15), are, respectively, equivalent to the following optimization problems:

$$BER_{BL}^* = \underset{\substack{a_{\Theta_k}, a_{\Psi_k} > 0, \tilde{\mathbf{w}}_{\Theta_k}, \tilde{\mathbf{w}}_{\Psi_k} \succeq 0 \\ \|\tilde{\mathbf{w}}_{\Theta_k}\| = \|\tilde{\mathbf{w}}_{\Psi_k}\| = 1}}{\text{minimize}} BER_{BL}(a_{\Theta_k}, a_{\Psi_k}, \tilde{\mathbf{w}}_{\Theta_k}, \tilde{\mathbf{w}}_{\Psi_k}) \tag{3.20}$$

and

$$BER_{EL}^* = \underset{\substack{b_{\Theta_k}, b_{\Psi_k} > 0, \tilde{\mathbf{v}}_{\Theta_k}, \tilde{\mathbf{v}}_{\Psi_k} \succeq 0 \\ \|\tilde{\mathbf{v}}_{\Theta_k}\| = \|\tilde{\mathbf{v}}_{\Psi_k}\| = 1}}{\text{minimize}} BER_{EL}(b_{\Theta_k}, b_{\Psi_k}, \tilde{\mathbf{v}}_{\Theta_k}, \tilde{\mathbf{v}}_{\Psi_k}) \tag{3.21}$$

Since the only constraints in (3.20) are that $a_{\Theta_k}, a_{\Psi_k} > 0$ and $\tilde{\mathbf{w}}_{\Theta_k}, \tilde{\mathbf{w}}_{\Psi_k} \succeq 0, \|\tilde{\mathbf{w}}_{\Theta_k}\|$ $= \|\tilde{\mathbf{w}}_{\Psi_k}\| = 1$, which are separate constraints, we can first optimize over $\tilde{\mathbf{w}}_{\Theta_k}, \tilde{\mathbf{w}}_{\Psi_k}$

and then over a_{Θ_k}, a_{Ψ_k} as follows:

$$BER^*_{BL} = \min_{a_{\Theta_k}, a_{\Psi_k} > 0} \min_{\substack{\tilde{\mathbf{w}}_{\Theta_k}, \tilde{\mathbf{w}}_{\Psi_k} \succeq 0 \\ \|\tilde{\mathbf{w}}_{\Theta_k}\| = \|\tilde{\mathbf{w}}_{\Psi_k}\| = 1}} BER_{BL}(a_{\Theta_k}, a_{\Psi_k}, \tilde{\mathbf{w}}_{\Theta_k}, \tilde{\mathbf{w}}_{\Psi_k}) \tag{3.22}$$

Similarly, from (3.21), we have

$$BER^*_{EL} = \min_{b_{\Theta_k}, b_{\Psi_k} > 0} \min_{\substack{\tilde{\mathbf{v}}_{\Theta_k}, \tilde{\mathbf{v}}_{\Psi_k} \succeq 0 \\ \|\tilde{\mathbf{v}}_{\Theta_k}\| = \|\tilde{\mathbf{v}}_{\Psi_k}\| = 1}} BER_{EL}(b_{\Theta_k}, b_{\Psi_k}, \tilde{\mathbf{v}}_{\Theta_k}, \tilde{\mathbf{v}}_{\Psi_k}) \tag{3.23}$$

These separations are illustrated in Fig. 3.2, where we first combine the received signals in the sets Θ_k and Ψ_k separately, and then combine the two resulting signals in the second step.

3.3.2 The first combining step: Optimal for both BL/EL

In Appendix B.1 on page 93, we show that

$$\min_{\substack{\tilde{\mathbf{w}}_{\Theta_k}, \tilde{\mathbf{w}}_{\Psi_k} \succeq 0 \\ \|\tilde{\mathbf{w}}_{\Theta_k}\| = \|\tilde{\mathbf{w}}_{\Psi_k}\| = 1}} BER_{BL}(a_{\Theta_k}, a_{\Psi_k}, \tilde{\mathbf{w}}_{\Theta_k}, \tilde{\mathbf{w}}_{\Psi_k}) = BER_{BL}(a_{\Theta_k}, a_{\Psi_k}, \tilde{\mathbf{w}}^*_{\Theta_k}, \tilde{\mathbf{w}}^*_{\Psi_k}) \tag{3.24}$$

where

$$(\tilde{\mathbf{w}}^*_{\Theta_k}, \tilde{\mathbf{w}}^*_{\Psi_k}) = (\tilde{\boldsymbol{\alpha}}_{\Theta_k}, \tilde{\boldsymbol{\alpha}}_{\Psi_k}) \triangleq (\boldsymbol{\alpha}_{\Theta_k}/\|\boldsymbol{\alpha}_{\Theta_k}\|, \boldsymbol{\alpha}_{\Psi_k}/\|\boldsymbol{\alpha}_{\Psi_k}\|) \tag{3.25}$$

Similarly, we have

$$\min_{\substack{\tilde{\mathbf{v}}_{\Theta_k}, \tilde{\mathbf{v}}_{\Psi_k} \succeq 0 \\ \|\tilde{\mathbf{w}}_{\Theta_k}\| = \|\tilde{\mathbf{w}}_{\Psi_k}\| = 1}} BER_{EL}(b_{\Theta_k}, b_{\Psi_k}, \tilde{\mathbf{v}}_{\Theta_k}, \tilde{\mathbf{v}}_{\Psi_k}) = BER_{EL}(b_{\Theta_k}, b_{\Psi_k}, \tilde{\mathbf{v}}^*_{\Theta_k}, \tilde{\mathbf{v}}^*_{\Psi_k}) \tag{3.26}$$

where

$$(\tilde{\mathbf{v}}^*_{\Theta_k}, \tilde{\mathbf{v}}^*_{\Psi_k}) = (\tilde{\boldsymbol{\alpha}}_{\Theta_k}, \tilde{\boldsymbol{\alpha}}_{\Psi_k}). \tag{3.27}$$

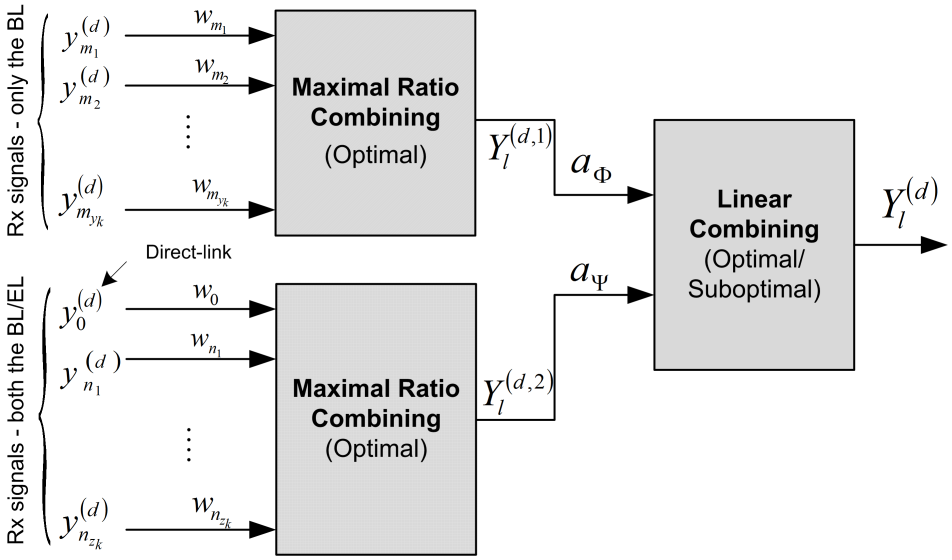

Figure 3.2: Two-step combining procedure for the base layer.

Both of the inner optimization problems, as shown in (3.22) and (3.23), have the same optimal solutions $(\tilde{\mathbf{w}}^*_{\Theta_k}, \tilde{\mathbf{w}}^*_{\Psi_k}) = (\tilde{\mathbf{v}}^*_{\Theta_k}, \tilde{\mathbf{v}}^*_{\Psi_k}) = (\tilde{\boldsymbol{\alpha}}_{\Theta_k}, \tilde{\boldsymbol{\alpha}}_{\Psi_k})$, which depend on the channel gains, but not on either $(a_{\Theta_k}, a_{\Psi_k})$ or $(b_{\Theta_k}, b_{\Psi_k})$. Also, the optimal solutions have the same form as the MRC solutions for combining the received signals in the sets Θ_k and Ψ_k. Thus, we can use two MRC receivers for combining the received signals in the sets Θ_k and Ψ_k, separately, as illustrated in Fig. 3.2. We note that Fig. 3.2 is slightly different from Fig. 2.2 on page 21 in that the second-step combining in the latter figure is an MRC receiver, but that in the former figure is not. The optimal linear combining weights in the second step in Fig. 3.2 will be presented in the next subsection.

Next, we minimize the BER expressions of the BL and the EL, as shown on the right hand side of (3.24) and (3.26), over $(a_{\Theta_k}, a_{\Psi_k})$ and $(b_{\Theta_k}, b_{\Psi_k})$, respectively

(see also (3.18) and (3.19) for the detailed BER expressions). In the following, we solve these problems separately.

3.3.3 The second combining step

A. Combining methods for the BL

i) Optimal solution: In Appendix B.2 on page 94, we show that the optimal weights in the second step are

$$a^*_{\Theta_k} = 1, \quad a^*_{\Psi_k} = \tan(\phi^*) \tag{3.28}$$

where ϕ^* is the solution of the following convex optimization problem:

$$\phi^* = \arg \min_{\phi \in (0,\pi/2)} \frac{1}{2} Q\left(A\cos\phi + B\sin\phi\right) + \frac{1}{2} Q\left(A\cos\phi + C\sin\phi\right) \tag{3.29}$$

where $A \geq 0$ and $C \geq B \geq 0$ are dependent on the channel gains, as defined in (B.7).

ii) Suboptimal solution – closed-form: In the following, we assume $a_\Theta = 1$ without loss of generality (see Appendix B.2), and find a suboptimal weight a_{Ψ_k}, which minimizes upper of the BER of the BL. From the BER expression of the BL in (B.8), and noting that $C \geq B \geq 0$, an upper bound for the BER of the BL is twice the dominant term. That is, we have

$$BER_{BL}(a_{\Psi_k}) \leq Q\left(\frac{A + Ba_{\Psi_k}}{\sqrt{1 + a^2_{\Psi_k}}}\right) \triangleq BER^{ub}_{BL}(a_{\Psi_k}) \tag{3.30}$$

where $BER^{ub}_{BL}(a_{\Psi_k})$ denotes the upper bound, as a function of a_{Ψ_k}. For high instantaneous SNR, the true BER value approaches the dominant term, i.e., a half

of the upper bound. Thus, minimizing the upper bound is also minimizing the true BER value in high SNR.

Now, minimizing the upper-bound BER, as shown in (3.30), is equivalent to maximizing the argument of the Q function, i.e.,

$$a^{\dagger}_{\Psi_k} \triangleq \arg\min_{a_{\Psi_k}\geq 0} BER^{ub}_{BL}(a_{\Psi_k}) = \arg\max_{a_{\Psi_k}\geq 0} \frac{A + Ba_{\Psi_k}}{\sqrt{1+a^2_{\Psi_k}}} \tag{3.31}$$

where the superscript † denotes a suboptimal value for the corresponding quantity. Similar to the solution of an MRC problem, we can show that

$$a^{\dagger}_{\Psi_k} = B/A = \frac{C^*_{\Psi_k}}{C^*_{\Theta_k}}(\sqrt{\rho}-\sqrt{\bar{\rho}}) = \frac{\|\boldsymbol{\alpha}_{\Psi_k}\|}{\|\boldsymbol{\alpha}_{\Theta_k}\|}(\sqrt{\rho}-\sqrt{\bar{\rho}}) \tag{3.32}$$

where we substituted A and B from (B.7), and $C^*_{\Theta_k}$ and $C^*_{\Psi_k}$ from (B.1). Substituting the suboptimal weight from (3.32) into (B.6), and noting that $a^{\dagger}_{\Theta_k} = 1$, after simplifying, the BER of the BL is given by

$$\begin{aligned} BER^{\dagger}_{BL} = {} & \frac{1}{2}Q\left(\sqrt{\frac{E_r(C^*_{\Theta_k})^2}{N_0} + \frac{E_r(C^*_{\Psi_k})^2(\sqrt{\rho}-\sqrt{\bar{\rho}})^2}{N_0}}\right) \\ & + \frac{1}{2}Q\left(\sqrt{\frac{E_r\left[(C^*_{\Theta_k})^2 + (C^*_{\Psi_k})^2(\rho-\bar{\rho})\right]^2}{\left[(C^*_{\Theta_k})^2 + (C^*_{\Psi_k})^2(\sqrt{\rho}-\sqrt{\bar{\rho}})^2\right]N_0}}\right) \end{aligned} \tag{3.33}$$

Finally, multiplying the weights in the two steps, we obtain the suboptimal weight vectors. From (3.25), and noting that $a^{\dagger}_{\Theta_k} = 1$, we have

$$\mathbf{w}^{\dagger}_{\Theta_k} = a^{\dagger}_{\Theta_k}\tilde{\mathbf{w}}^*_{\Theta_k} = \boldsymbol{\alpha}_{\Theta_k}/\|\boldsymbol{\alpha}_{\Theta_k}\|, \tag{3.34}$$

and from (3.25) and (3.32), we have

$$\begin{aligned} \mathbf{w}^{\dagger}_{\Psi_k} = a^{\dagger}_{\Psi_k}\tilde{\mathbf{w}}^*_{\Psi_k} &= \frac{\|\boldsymbol{\alpha}_{\Psi_k}\|}{\|\boldsymbol{\alpha}_{\Theta_k}\|}(\sqrt{\rho}-\sqrt{\bar{\rho}}) \times \boldsymbol{\alpha}_{\Psi_k}/\|\boldsymbol{\alpha}_{\Psi_k}\| \\ &= (\sqrt{\rho}-\sqrt{\bar{\rho}})\boldsymbol{\alpha}_{\Psi_k}/\|\boldsymbol{\alpha}_{\Theta_k}\| \end{aligned} \tag{3.35}$$

Note that we can scale all the weights by a positive value without changing the system performance. By multiplying both the weight vectors, as shown in (3.34) and (3.35), with $\|\boldsymbol{\alpha}_{\Theta_k}\|$, the suboptimal weights are finally given by

$$\mathbf{w}_{\Theta_k}^{\dagger} = \boldsymbol{\alpha}_{\Theta_k}, \quad \mathbf{w}_{\Psi_k}^{\dagger} = (\sqrt{\rho} - \sqrt{\bar{\rho}})\boldsymbol{\alpha}_{\Psi_k} \tag{3.36}$$

each of which only depends on its corresponding channel gain and the power allocation parameter ρ.

For comparison purposes, we define the effective output (instantaneous) SNR to be square of the argument of the Q-function of the dominant term of BER. From (3.33), we have

$$SNR_{BL,1}^{(eff)} = \frac{E_r(C_{\Theta_k}^*)^2}{N_0} + \frac{E_r(C_{\Psi_k}^*)^2(\sqrt{\rho} - \sqrt{\bar{\rho}})^2}{N_0} \tag{3.37}$$

We note that if both $C_{\Theta_k}^*$ and $C_{\Psi_k}^*$ are not equal to zero, our suboptimal method results in a strictly higher effective SNR than that of the simple combining technique in [32], which results in only the first term in (3.37). Also, the combining method in [31] uses $w_n = \alpha_{n,l}^{rd}$ for all n, i.e., $\mathbf{w}_{\Theta_k} = \boldsymbol{\alpha}_{\Theta_k}, \mathbf{w}_{\Psi_k} = \boldsymbol{\alpha}_{\Psi_k}$, as opposed to (3.36). Using $\mathbf{w}_{\Theta_k} = \boldsymbol{\alpha}_{\Theta_k}, \mathbf{w}_{\Psi_k} = \boldsymbol{\alpha}_{\Psi_k}$ in (3.12), we can find the corresponding BER expression for the BL. The effective SNR is given by

$$SNR_{BL,2}^{(eff)} = \frac{E_r\left[(C_{\Theta_k}^*)^2 + (C_{\Psi_k}^*)^2(\sqrt{\rho} - \sqrt{\bar{\rho}})\right]^2}{\left[(C_{\Theta_k}^*)^2 + (C_{\Psi_k}^*)^2\right]N_0} \tag{3.38}$$

which is shown in Appendix B.3 on page 96 to be strictly less than that in (3.37) for $\rho < 1$ (and both $C_{\Theta_k}^*, C_{\Psi_k}^* \neq 0$, which happens with probability one).

B. Combining methods for the EL

Similar to the BL case, from (3.19) and (3.26), we can show that the optimal weights in the second step for the EL are given by

$$b^*_{\Theta_k} = \tan\theta^*, \quad b^*_{\Psi_k} = 1 \tag{3.39}$$

where

$$\theta^* \;=\; \arg \min_{\theta\in(0,\pi/2)} BER^{(a)}_{EL}(\theta) \tag{3.40}$$

in which

$$BER^{(a)}_{EL}(\theta) \triangleq Q\left(D\cos\theta\right) + \frac{1}{2}Q\left(E\sin\theta + F\cos\theta\right) - \frac{1}{2}Q\left(E\sin\theta + G\cos\theta\right) \tag{3.41}$$

denotes the BER of the EL, as a function of θ, and

$$\begin{aligned} D &\triangleq \sqrt{\frac{E_r}{N_0}}C^*_{\Psi_k}\sqrt{\bar{\rho}}, & E &\triangleq 2\sqrt{\frac{E_r}{N_0}}C^*_{\Theta_k} \\ F &\triangleq \sqrt{\frac{E_r}{N_0}}C^*_{\Psi_k}(2\sqrt{\rho}-\sqrt{\bar{\rho}}), & G &\triangleq \sqrt{\frac{E_r}{N_0}}C^*_{\Psi_k}(2\sqrt{\rho}+\sqrt{\bar{\rho}}) \end{aligned} \tag{3.42}$$

We note, however, that the optimization problem in (3.40) is, in general, not convex. Therefore, a numerical search using, e.g., the Newton method [34], generally results in a local minimum.

Because of the difficulty in searching for a local (or global) minimum, we use a suboptimal combining method by letting $\theta^\dagger = 0$, so $b^\dagger_{\Theta_k} = 0$ to reduce the computational complexity. That is, we only use the combined signals, which include both the BL/EL for detecting the EL [32]. We show in Subsection 3.3.4 that

this suboptimal method gives results very close to the optimal one. By substituting $b_{\Theta_k} = b^{\dagger}_{\Theta_k} = 0, b_{\Psi_k} = b^{\dagger}_{\Psi_k} = 1$ into (3.19), the corresponding BER expression for the EL is given by

$$BER^{\dagger}_{EL} = Q\left(\sqrt{\frac{E_r}{N_0}} C^{*}_{\Psi_k}\sqrt{\bar{\rho}}\right) + \frac{1}{2}Q\left(\sqrt{\frac{E_r}{N_0}} C^{*}_{\Psi_k}(2\sqrt{\rho} - \sqrt{\bar{\rho}})\right) - \frac{1}{2}Q\left(\sqrt{\frac{E_r}{N_0}} C^{*}_{\Psi_k}(2\sqrt{\rho} + \sqrt{\bar{\rho}})\right) \tag{3.43}$$

For $b^{\dagger}_{\Theta_k} = 0, b^{\dagger}_{\Psi_k} = 1$, the suboptimal weights for the EL in both steps are given by (see (3.27) for the optimal weight vectors in the first step)

$$\mathbf{v}^{\dagger}_{\Theta_k} = \mathbf{0}, \quad \mathbf{v}^{\dagger}_{\Psi_k} = \boldsymbol{\alpha}_{\Psi_k} \tag{3.44}$$

where we have multiplied all the weights by $\|\boldsymbol{\alpha}_{\Psi_k}\|$.

Since the Q-function monotonically decreases, and $G \geq F \geq 0$, from (3.40), we have a lower bound for the BER of the EL as follows:

$$BER^{(a)}_{EL}(\theta) \;\; \geq \;\; Q\left(D\cos\theta\right) \geq Q\left(D\right) = Q\left(\sqrt{\frac{E_r}{N_0}} C^{*}_{\Psi_k}\sqrt{\bar{\rho}}\right) \tag{3.45}$$

for all $\theta \in (0, \pi/2)$. The lower bound will be used to compare with the suboptimal BER performance and will be shown to yield very close results.

Lastly, we note that for ease of implementation, we can design the optimal and suboptimal combining receivers by two steps as shown in Fig. 3.2. In the first step, we use two MRC receivers for the received signals which include only the BL and both the BL/EL separately. This step is optimal individually for both the BL and the EL. In the second step, we combine the two resulting signals to detect the BL and the EL, using either the optimal or the suboptimal weights.

3.3.4 Numerical BER performance comparison for both BL/EL

In the following, we compare the uncoded BER performances of the BL and the EL for the different combining methods above. For simplicity, we assume there are two relays. One is always sending the BL using QPSK, and the other is always sending both the BL/EL using hierarchical 16-QAM. We assume the relays experience independent flat Rayleigh fading. The channel state information is perfectly known at the receiver. For the BL, we plot the uncoded BER performances for the combining methods in [31, 32], and our optimal and suboptimal methods. For the EL, we plot our simple combining method, the locally suboptimal method, and the lower bound.

First, we consider the performance for the BL, as shown in Fig. 3.3 on page 65, for the power allocation parameter $\rho = 0.72$, a value which will be of interest below. We note that the combining method in [32] does not perform as well as the other methods since it only uses the QPSK received signal to detect the BL, and thus results in just the QPSK BER performance (with diversity order 1). Also, our suboptimal combining method of minimizing an upper-bound BER significantly outperforms the combining method used in [31]. We can observe approximately 1dB gain in the medium and high SNR region. Our suboptimal method performs almost as well as the optimal in the medium and high SNR region. For a higher value of ρ, say, $\rho = 0.8$ (i.e., conventional constellation), as shown in Fig. 3.4, our suboptimal combining method performs almost identical to the optimal one over

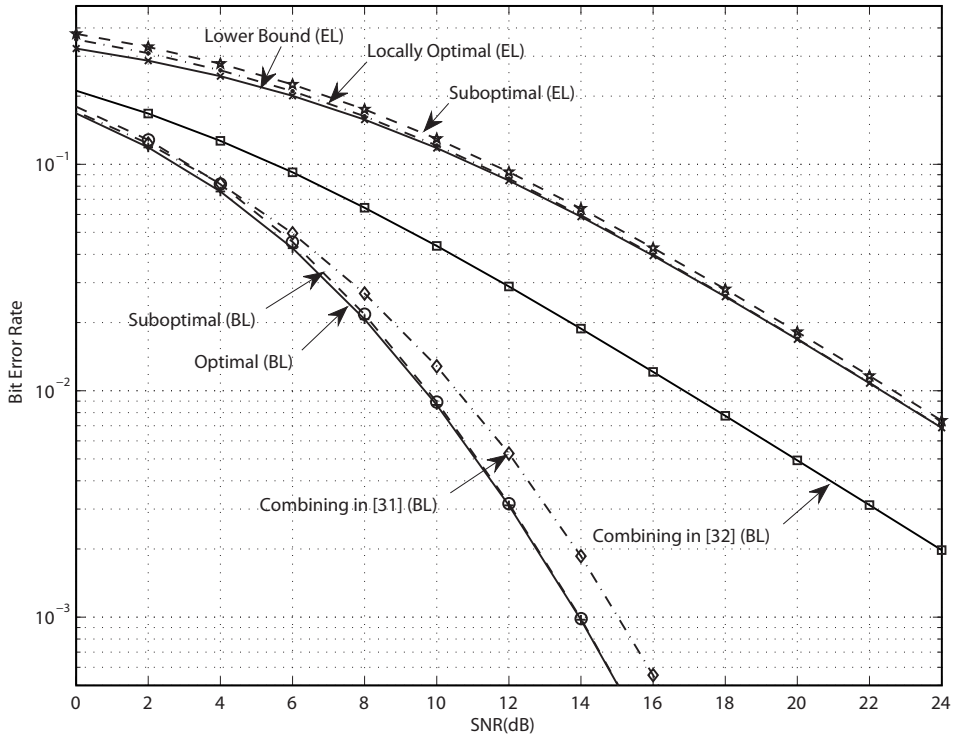

Figure 3.3: Comparison of uncoded BER performance for the BL and the EL with $\rho = 0.72$.

the range of SNR in the plot. The gain compared to the combining method in [31] reduces for a high value of ρ, but the proposed method is still much better than the method in [32], as can be seen in Fig. 3.4.

Next, we consider the performance for the EL. In Fig. 3.3, we observe that the suboptimal combining method performs very close to the locally optimal and the lower bound performances. For smaller ρ, the performance loss slightly increases. For higher values of ρ, say $\rho = 0.8$, the performance loss is almost negligible, as seen in Fig. 3.4. We note that in all cases, the locally optimal performance is almost identical to the lower bound for, say, the channel $SNR \geq$ 8dB, which suggests that the local optimum is very close, if not identical, to the

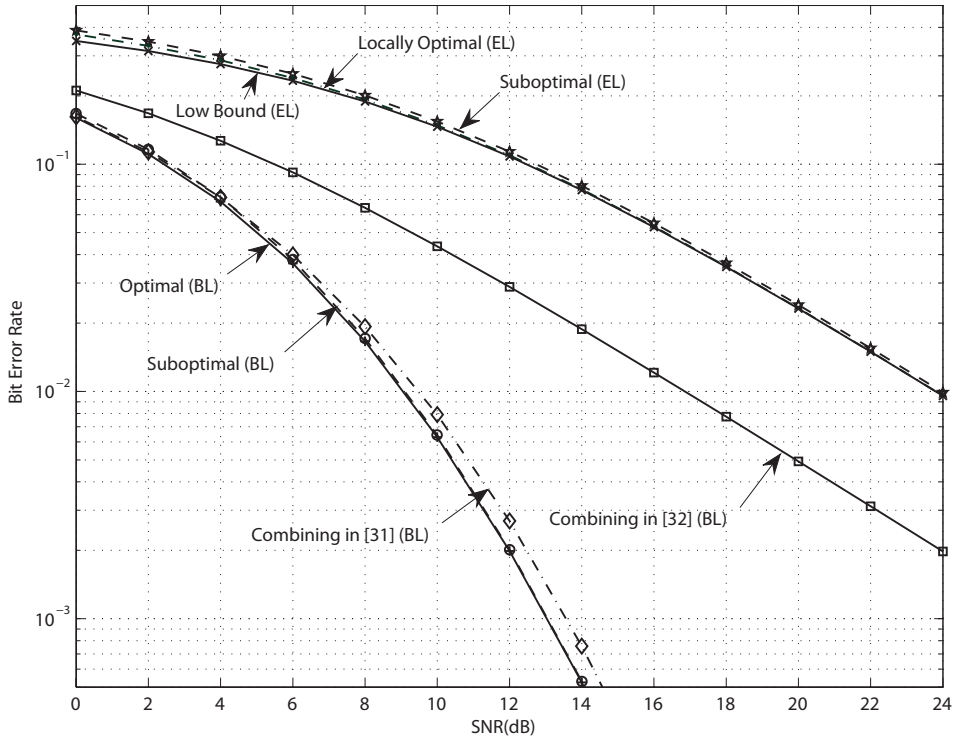

Figure 3.4: Comparison of uncoded BER performance for the BL and the EL with $\rho = 0.80$.

global optimum in this SNR region.

In summary, for the BL, our suboptimal combining method performs very close to the optimal. For the EL, the suboptimal combining method performs very well compared to the local optimal and the low-bound BER performance. Hence, in the numerical simulation in Section IV below, we will use the proposed suboptimal combining methods that have the closed-form weights, instead of numerically solving for the optimal (or local optimal) weights to reduce the computational complexity.

3.4 Application to video transmission: Simulation results

In this section, we apply the transmission protocol and our proposed suboptimal and closed-form combining methods at the destination for transmitting a video-encoded bitstream over the relay network.

3.4.1 Simulation setup

In the simulation, we assume there are four relays, and the direct link is so weak that it will be ignored unless otherwise stated. All the channels are assumed to be independent, and flat Rayleigh fading with normalized Doppler frequency $f_{dn} = 10^{-3}$ [45]. The average channel SNRs of all links from the source to the relays and from the relays to the destination are the same. We will first obtain the system performance in terms of the packet error rate (at the physical layer) for an i.i.d bitstream, and then the peak signal to noise ratio (PSNR) of a video-encoded bitstream for various average channel SNR values and power allocation parameters $\rho \in [0.6, 0.9]$. Our proposed suboptimal and closed-form combining methods at the destination will be used.

For the channel coding, we use a convolutional code of rate $r_{\text{fec}} = 1/2$ for the forward error correction (FEC) for all links. The convolutional code has constraint length 7 and generator polynomial (133,171) in octal. We use soft decoding for the Viterbi decoder; hence, soft-demodulated bits will be computed [47] from the

test statistics given in (3.8) with the suboptimal weights in (3.36) and (3.44) for the BL and the EL, respectively. The BL signal is considered as a noisy QPSK-modulated signal, thus the resulting soft-demodulated bits are equivalent to the soft bits calculation in [48].

We encode the Foreman and Soccer video sequences, which have medium and fast motion, respectively. Both video sequences have CIF resolution (352x288) and frame rate of 30fps. These test sequences are encoded with group of pictures (GoP) size=16 pictures, and use the full hierarchical B structure [38, 49], where the I-frame occurs once per GoP. For the hierarchical B structure, the frames in decreasing order of importance are given as follows: $I_{0/16}, B_8, B_4, B_{12}$, $B_2, B_6, B_{10}, B_{14}, B_1, B_3, \ldots, B_{15}$. For convenience at the physical layer, we choose a slice to have a fixed size of 376 bytes (or less). Each NAL unit contains one slice of size 383 bytes (or less), including the header. For each GoP of 16 frames, we assign the more important frames to the BL and the others to the EL (at the frame level) such that the difference in the number of NAL units between the two layers, from the first GoP up to the current encoding GoP, is smallest. For example, we suppose the total number of NAL units of the BL and the EL up to the last encoded GoP are 100 and 102, respectively. The number of NAL units of frames in the current GoP are $3, 3, 3, 2, 2, 2, 1, 1, \ldots, 1$ (the frames are in the decreasing order of importance), with 25 NAL units in total. If we assign the first 6 frames to the BL and the last 10 frames to the EL, the total numbers of NAL units of the BL and the EL will be 115 and 112, respectively. If we assign the first 5 frames to

the BL and the remaining to the EL, then the total numbers of NAL units of the BL and the EL will be 113 and 114, respectively. Our method will select the latter, because it makes the difference in the number of NAL units between the two layers smallest. Using this method, the numbers of NAL units of the BL and the EL for the first 10 GoPs of the Foreman sequence are 412 and 408, respectively. Those corresponding numbers for the Soccer sequence are 649 and 646. Zero-padding will be used to make the two layers have exactly the same number of NAL units.

At the physical layer, we use a frame length of $2\text{x}400/r_{\text{fec}} = 1600$ bytes, which is assumed to be sufficient to transmit a pair of NAL units and the physical frame header. Note that each pair of NAL units consists of one from the BL and one from the EL, where the BL NAL unit is mapped into the MSBs and the EL NAL unit is mapped into the LSBs of the hierarchical 16-QAM symbols. In this simulation, we use a pair of block bit interleavers of size 80x80 bits each (i.e., 800 bytes)[3] for the BL and the EL separately to partially decorrelate the channel fading correlation.

We repeatedly send the first 10 GoPs (i.e., $N_{\text{frm}} = 160$ frames) over the relay network for 100 times. The received bitstreams are then decoded and the average PSNR is computed for various channel SNRs and power allocation parameters ρ.

For the m-th decoded video sequence for $m = 1, 2, \ldots 100$, the PSNR is

[3]A block bit interleaver is assumed to write the input bitstream in the rows and read the bitstream out from the columns.

computed as follows:

$$PSNR_m = 10 \log_{10} \frac{255^2}{\overline{MSE}_m} \tag{3.46}$$

where

$$\overline{MSE}_m = \frac{1}{N_{\text{frm}}} \sum_{k=1}^{N_{\text{frm}}} MSE_{m,k} \tag{3.47}$$

where $MSE_{m,k}$ denotes the mean square error between the k-th original frame and the corresponding received frame of the m-th sequence. The final average PSNR is averaged over 100 realizations $\{PSNR_m\}$. We use the motion-copy error concealment mode for the H.264/AVC decoder [38]; however, if a whole frame is lost, it will be copied from the previous one.

The simulation is also repeated for the single-layer scheme with the classical 16-QAM modulation, where we recall that all the bits in the bitstream are considered as having equal priority.

3.4.2 Packet error rate for an i.i.d. bitstream

In Fig. 3.5, we plot the packet error rate (PER) for both the single-layer and double-layer scheme, where an i.i.d. bitstream was sent. The abscissa is the power allocation parameter, ρ, for the double-layer scheme. The PERs of the BL and the EL packets are plotted separately. As the single-layer scheme uses the classical 16-QAM with no distinction among the input bits, the single-layer scheme only depends on channel SNR, and not ρ. It is, however, plotted as a single point for each channel SNR for comparison.

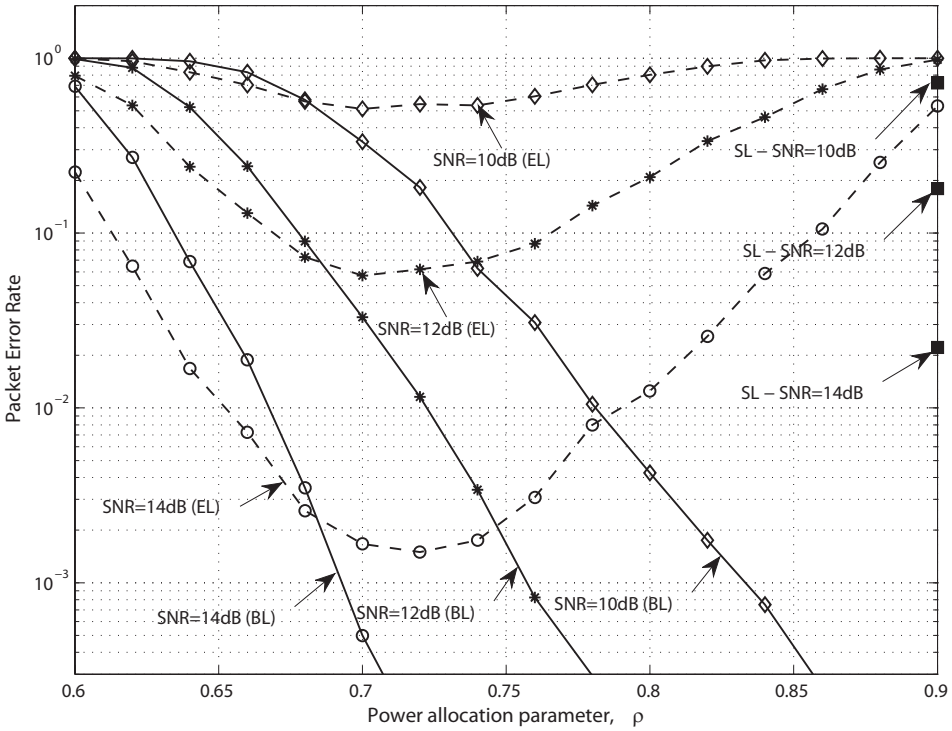

Figure 3.5: Packet error rate of the double-layer and single-layer scheme.

For each channel SNR, we observe that the PER of the BL monotonically decreases as the power allocation parameter ρ increases (see Fig. 3.5). This is because for a higher ρ, the BL is allocated more power, while the EL is allocated less power, i.e., higher BL signal power and less interference caused by the EL. For the EL performance, the plot shows that the PERs of the EL are not a monotonic function of ρ. This can be explained as follows: For $\rho \geq 0.72$, the BL is successfully decoded most of the time, and so the EL performance mainly depends on the power allocated to it; thus, the PER of the EL monotonically increases as $\bar{\rho} = 1 - \rho$ decreases. In contrast, for $\rho \leq 0.70$, as ρ decreases, the relays are not able to reliably detect the BL (because of the decreased SINR of the BL), and thus they

frequently keep silent. The destination does not receive enough signals from the relays; hence, both PER of the BL and the PER of the EL become worse.

It is also interesting to note that for many values of ρ (e.g., $\rho \in [0.70, 0.76]$), both the BL and the EL PER performances of the double-layer scheme are better than the PER performance of the single-layer scheme. This is because a relay may fail to decode a packet if the single-layer scheme is used due to low channel SNR, but it would still be able to decode the BL portion if the double-layer scheme is used, and forward it to the destination, which enhances the overall system performance.

3.4.3 PSNR performance for layered video sequences: Four relays without the direct link

A. Decodable bitstreams

Firstly, we note that there are a few received bitstreams at low channel SNR and small values of ρ, which are invalid bitstreams in the sense that the H.264/AVC decoder does not produce any output picture. We refer to these invalid bitstreams as undecodable. If no packet is successfully received, the null bitstream is also considered as undecodable. In Figs. 3.6 and 3.7 (on page 73), we plot the percentage of decodable bitstreams over all 100 received bitstreams, which corresponds to 100 channel realizations, for the Foreman and the Soccer sequences, respectively. We found that there were some undecodable bitstreams only at low channel $SNR \leq 11$dB and small power allocation parameter $\rho \leq 0.62$.

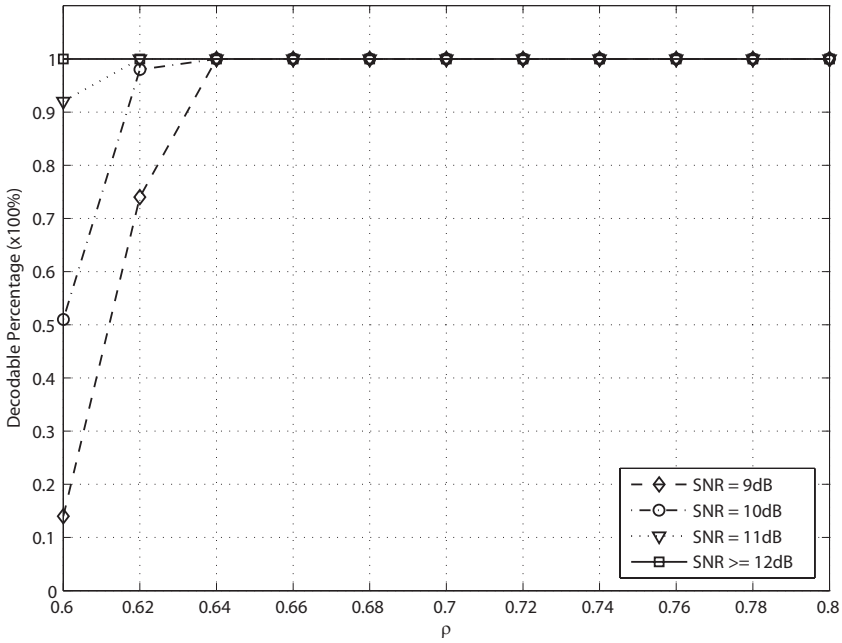

Figure 3.6: Percentage of successfully decoded bitstreams for the Foreman sequence.

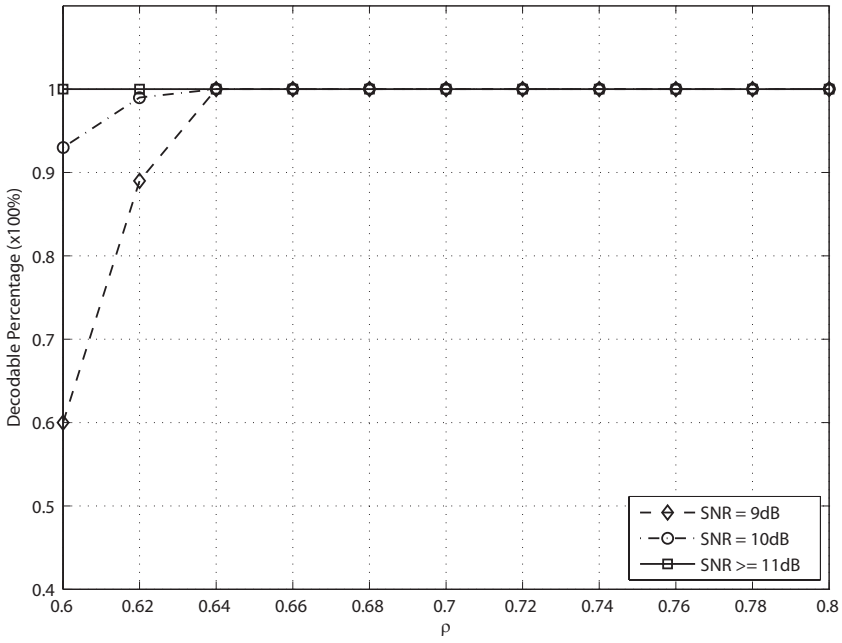

Figure 3.7: Percentage of successfully decoded bitstreams for the Soccer sequence.

For an undecodable bitstream, we compute the PSNR relative to the mean value of each frame. We plot the average PSNR values, averaging over all the received bitstreams, including the undecodable bitstreams. We also plot the average PSNR values, averaging over only the decodable bitstreams. We found that these curves are visually undistinguishable (the plot is not shown here). Thus, in the following, we only present the PSNR computed only from the decodable bitstreams.

B. PSNR performance versus the power allocation parameter

In Figs. 3.8 and 3.9, we plot the average PSNR versus the power allocation values ρ, parameterized by channel SNR for the Foreman sequence and the Soccer sequence, respectively.

For the Foreman sequence, as shown in Fig. 3.8, we observed that either too high or too low values of the power allocation parameter ρ does not result in good PSNR performance. The reasons are similar to the i.i.d. data with PER performance. That is, too high or too low a value of ρ allows either the BL or the EL (or nothing) to be successfully received, but usually not both. We observe that at the medium and high SNR region (say $SNR \geq 11$dB), the best power allocation parameter is around $\rho \approx 0.74$. In the low SNR region, a high value of ρ is preferred to better protect the BL. In the very high SNR region, the PSNR is saturated and many values of ρ can approach the maximum PSNR value.

The general observations mentioned above for the Foreman sequence also hold for the Soccer sequence (see Fig. 3.9). For example, the best power alloca-

tion parameter is around $\rho \approx 0.74$ for the medium and high SNR regions. The differences between the Foreman and the Soccer sequences will be discussed later.

C. PSNR performance versus channel SNR

In Fig. 3.10, we plot the average PSNR versus channel SNR for various power allocation values ρ for the Foreman sequence. We observe that when we allocate too little power to the BL, say $\rho \leq 0.64$, the PSNR performance of the double-layer scheme is worse than that of the single-layer scheme over the range of the plotted SNRs, which is because the BL is rarely successfully decoded. When we increase $\rho = 0.68 \rightarrow 0.76$, the PSNR performance improves and outperforms the single-layer scheme, because in this range, the BL can be decoded successfully with higher probability, and so can the EL. If we continue to increase $\rho = 0.80 \rightarrow 0.88$, the BL is more reliably received, but the EL reliability decreases, since less power is allocated to it. Thus, the PSNR performance decreases. For a high value of ρ in the high channel SNR region, e.g., $\rho = 0.88$ and $SNR \geq 13$dB, the performance of the double-layer scheme is worse than the single-layer scheme. In the low SNR region, a high value of ρ is preferred to better protect the BL, even though the EL cannot be received correctly.

For the Soccer sequence, as plotted in Fig. 3.11, similar observations can be made. Note, however, that the performance of the Soccer sequence is worse than that of the Foreman sequence. For example, at a channel $SNR = 12$dB, the best PSNR of the Soccer sequence is about 27.7dB, while that of the Foreman

sequence is about 30.1dB. The main reason is the high motion nature of the Soccer sequence. The motion-copy error concealment mode for a high motion video sequence does not perform as well as for a lower motion video sequence. Also, when the instantaneous channel SNR is low, whole frame loss can occur, and in this case we substitute for it with the previous frame. Such copy-frame does not result in a good PSNR for the high-motion Soccer sequence, whereas copy-frame is not too bad for the medium-motion Foreman sequence.

For both sequences, we observe that the 'best' double-layer scheme, which is when the system has the capability to adapt ρ to the average channel SNR, is significantly better than the single-layer scheme over all the SNR region plotted (see both Figs. 3.10 and 3.11). Particularly, about 2-2.5dB gain in channel SNR or 5-7dB gain in the PSNR can be observed. We note that in the very high SNR region (say $SNR \geq 16$dB), the PSNR for the double-layer scheme is saturated, and the single-layer scheme performs as well as the double-layer scheme.

Finally, we note that if we fix $\rho \in [0.72, 0.76]$, i.e., the system does not adapt ρ to channel SNR, the PSNR performance of the double-layer scheme still significantly outperforms the single-layer scheme over all the range of the SNRs considered (except for a very high SNR value such as 17dB).

3.4.4 PSNR performance for layered video sequences: Two relays with the direct link

The objects of this subsection is to consider the performances of the relay network with the direct link for double-layer scheme and single-layer scheme. Unlike the previous numerical results, in this subsection, we consider a relaying network of two relays with a direct link. We again assume all the relay links from the source to the relays and from the relays to the destination have equal average channel SNR. The two relays are located at about halfway from the source to the destination. The log-distance path loss model with the path loss exponent of 3.5 is assumed (see, e.g., [50]). Thus, the average channel SNR of the direct link is less than those of the relay links by $10 \log_{10} 2^{3.5} = 10.54$dB.

In Figs. 3.12 and 3.13, we plot the PSNR performances versus the average channel SNR. We observe a large improvement of the double-layer scheme, compared to the single-layer scheme. The double-layer scheme achieves the best performance at the power allocation parameter $\rho \approx 0.72$, which has about 2-2.5dB gain in SNR, or 5-7dB gain in PSNR, compared to the single-layer scheme.

3.5 Conclusions

In this chapter, we consider decode-and-forward relay wireless networks using both hierarchical 16-QAM and QPSK. The source broadcasts a message with two layers to all the relays and the destination. Depending on the number of successfully decoded layers, a relay can use either hierarchical 16-QAM or QPSK to transmit both layers or one layer, respectively, to the destination. By considering a hierarchical 16-QAM symbol as the superposition of two QPSK symbols, we proposed a relaying protocol and novel combining methods for the received signals at the destination. We derived the optimal linear-combining solutions in terms of minimizing the uncoded BER, where the optimal solution for the BL can be obtained by convex optimization programming. We also presented suboptimal combining methods for both the BL and the EL, which have closed-form solutions and perform very close to the optimal. Both our proposed optimal and suboptimal methods significantly outperform other combining methods in the literature.

We applied the proposed double-layer scheme with our suboptimal combining method to transmit layered video bitstreams through the relaying wireless networks. Simulation results showed that the double-layer scheme using hierarchical 16-QAM largely outperforms the classical single-layer scheme using conventional 16-QAM. For example, either about 2-2.5dB gain in channel SNR or 5-7dB gain in the PSNR was observed.

3.6 Acknowledgements

Chapter III of this dissertation is, in full, a reprint of the material as it appears in Tu V. Nguyen, Pamela C. Cosman, and Lauence B. Milstein, "Layered Video Transmission over Decode-and-Forward Wireless Relay Networks using Hierarchical Modulation," submitted to *IEEE Transactions on Image Processing,* 2013, and in Tu V. Nguyen and Laurence B. Milstein, "Layered Transmission over Decode-and-Forward Wireless Relay Networks using Superposition Coding," *submitted to IEEE Transactions on Communications*, 2013. I was the primary author of all these publications. The co-authors Professor Cosman and Professor Milstein directed and supervised the research which forms the basis for Chapters III.

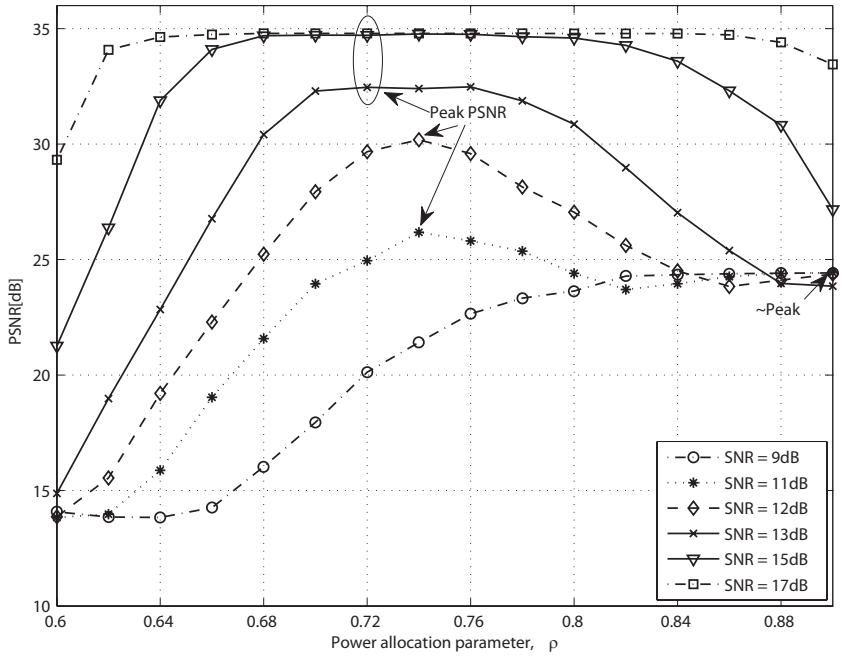

Figure 3.8: Average PSNR versus ρ for the Foreman sequence.

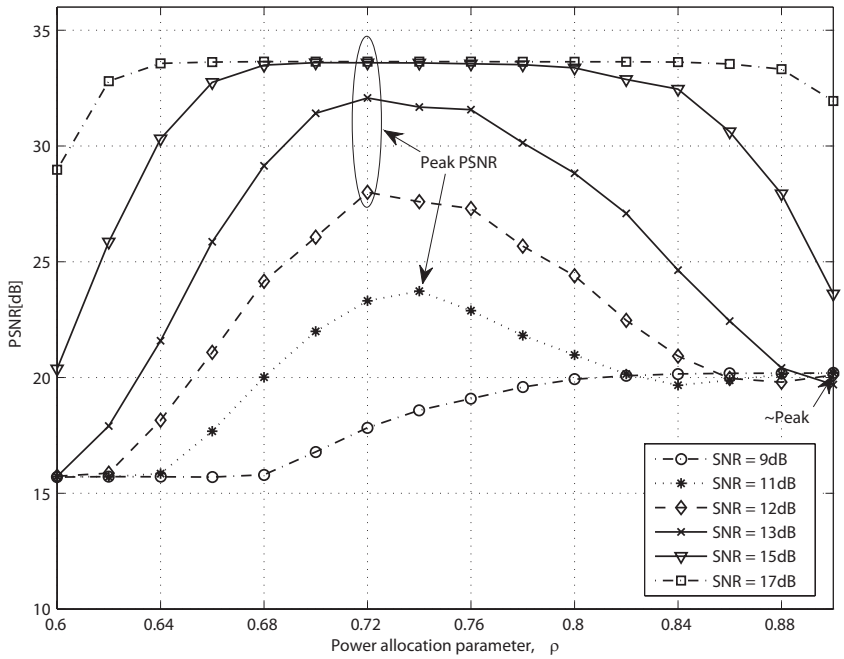

Figure 3.9: Average PSNR versus ρ for the Soccer sequence.

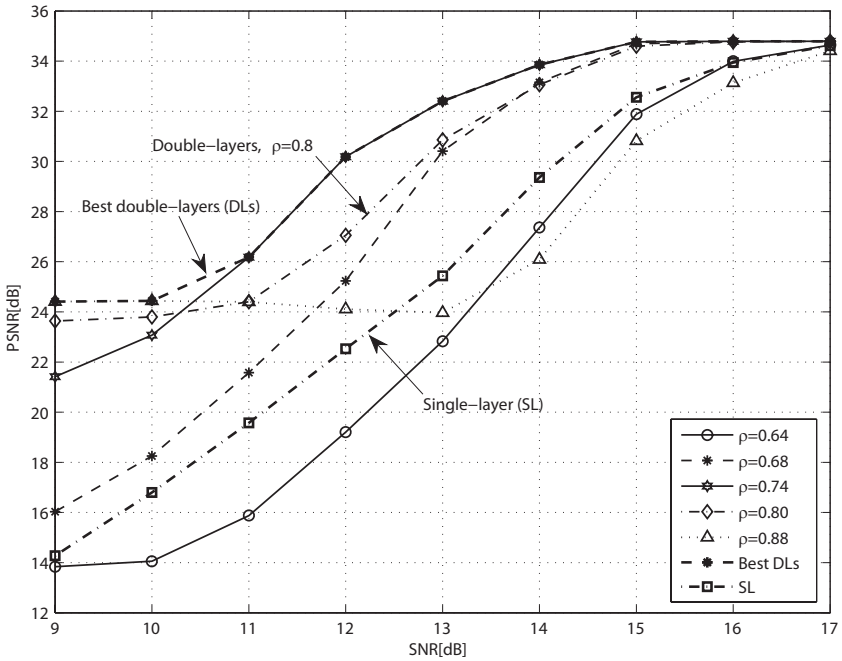

Figure 3.10: Average PSNR versus channel SNR for the Foreman sequence.

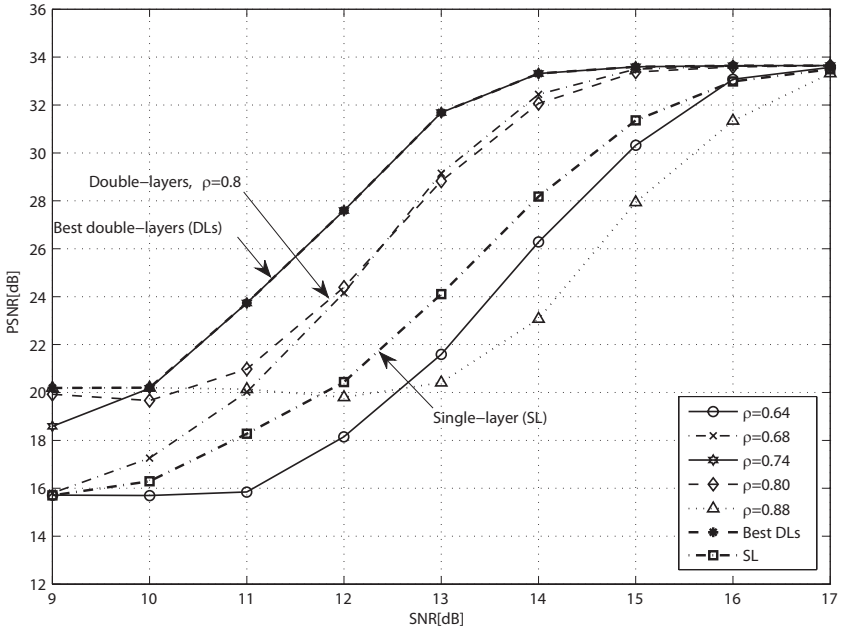

Figure 3.11: Average PSNR versus channel SNR for the Soccer sequence.

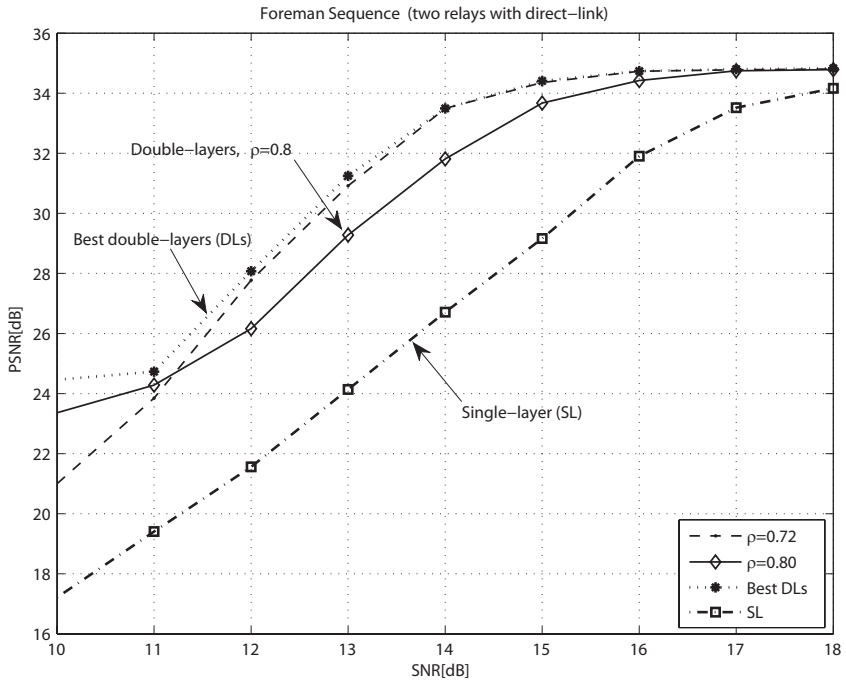

Figure 3.12: Average PSNR versus channel SNR of system with two relays and the direct link for the Foreman sequence.

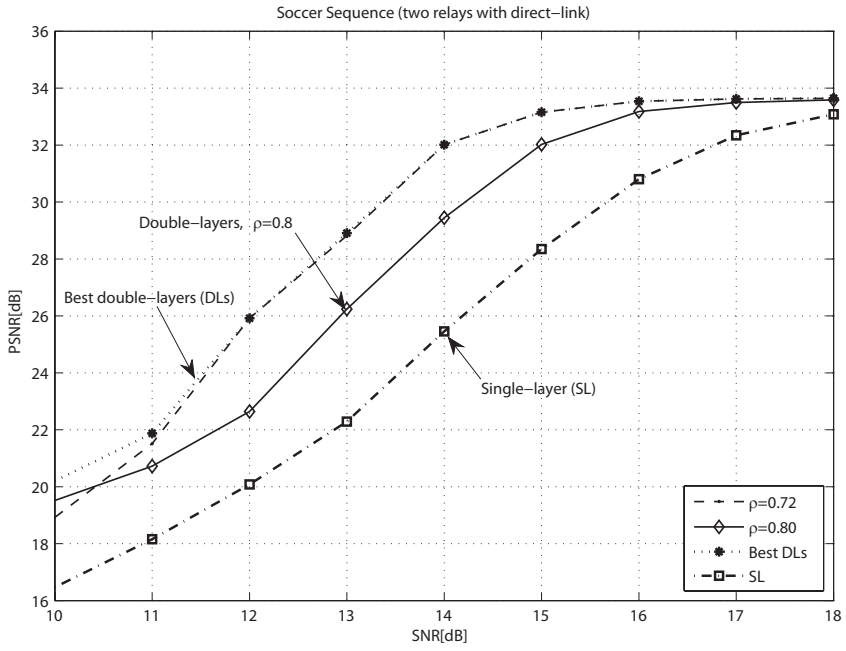

Figure 3.13: Average PSNR versus channel SNR of system with two relays and the direct link for the Soccer sequence.

Chapter 4

Conclusions and Future Work

4.1 Conclusions

In this dissertation, we considered a relay network with a single source, a single destination, and multiple relays. The relays are half-duplex and use the decode-and-forward protocol.

In Chapter II, a successively refinable Gaussian source partitioned into two layers is transmitted using superposition coding. In the first time slot, the source broadcasts two layers to all the relays and the destination. The relays decode the message separately. Depending on the channel state, a relay can successfully decode two layers, successfully decode one layer, or decode nothing. To reduce the latency and simplify the system design, we do not assume any feedback channels, and we do not consider channel state information at the transmitter of any terminal. Also, the relays are not able to communicate with one another. Rather, in the second time slot, we assume a relay re-encodes and forwards all the success-

fully decoded layers to the destination. If both layers are successfully decoded, superposition coding is used for multiplexing; otherwise, superposition coding is not used. The destination thus receives multiple signals, each of which can include either one layer or two layers. We derived the optimal linear-combining receiver at the destination, where both the optimal weight vector and the combined SINR have closed forms. Using the optimal combining method at the destination, we derived the average throughput and the expected distortion. Since these quantities were not expressed in closed form, we derived a closed-form lower bound to the average throughput and a closed-form upper bound to the expected distortion. We optimized the system parameters, such as the power and rate allocations for superposition coding, based on the closed-form bounds. Given these suboptimal system parameters, we obtained the average throughput and the expected distortion numerically. Numerical results showed that the proposed two-layer scheme using superposition coding with the optimal linear combining method can gain up to 1-1.5 dB in channel SNR for the average throughput, or 1.5-2dB in channel SNR for the expected distortion, compared to the conventional one-layer scheme.

In Chapter III, a layered video-encoded bitstream is transmitted over the wireless relay networks. The source broadcasts a message with two layers to all the relays and the destination using hierarchical 16-QAM. Depending on the number of successfully decoded layers, a relay can use either hierarchical 16-QAM or QPSK to transmit both layers or the base layer, respectively, to the destination. By considering a hierarchical 16-QAM symbol as the superposition of two QPSK symbols,

we proposed a relaying protocol and derived the optimal linear-combining receiver for the received signals at the destination. The optimal linear combining solution, which minimizes the uncoded BER, can be obtained by a two-step combining method. In the first step, we optimize over the weight vector directions, which have closed-form solutions. In the second step, we optimize over the lengths of the weight vectors, which were obtained by the convex optimization programming for the BL, while a local optimum was achieved for the EL. We also presented suboptimal combining methods in the second step for both the BL and the EL, which have closed-form solutions and performed very close to the optimal. Both our proposed optimal and suboptimal methods significantly outperformed other combining methods in the literature. We applied the proposed double-layer scheme with the suboptimal combining method for transmitting layered video-encoded bitstreams through the wireless relay networks. Simulation results showed that the double-layer scheme using hierarchical 16-QAM significantly outperformed the classical single-layer scheme using conventional 16-QAM. For example, either about 2-2.5dB gain in channel SNR or 5-7dB gain in the PSNR was observed.

4.2 Future work

Based on the results in this dissertation, possible future work to enhance the performance of video transmission over a wireless network are follows:

- Increasing the number of source layers to three or more, and using higher

order hierarchical modulation such as 64 or 256 QAM. Multiplex hierarchical modulation methods in [19] can also be used to provide multiple levels of unequal error protection.

- Considering additional UEP techniques such as using rate-compatible punctured convolutional/turbo coding in conjunction with hierarchical modulation. We note that for any given layer, all transmitters should use the same code rate (but the rates can vary layer by layer) so that the optimal combining method can be straightforwardly extended.

- Adaptively controlling the source encoding rate to match the number of output encoded bits to number of channel bits, which can be reliably transmitted through the network to maximize the end-to-end video transmission quality.

- Assuming there are many relays available, where the short-term average channel SNRs for the relay links can be slowly changing over time due to mobility. For example, by considering a relay selection method, we choose the best subset of relays, whose average channel SNRs are maximized, for relay cooperation.

- Considering multiple antennas and space-time coding deployed at each terminal to achieve spatial diversity and/or multiplexing gain.

Appendix A

Combining Techniques for Superposition Coding Scheme

A.1 Globally optimal linear combining at the destination

In this appendix, we derive the optimal linear combining solution for the received signals at the destination, each of which includes either only the BL or the BL/EL. We will solve this in two step as follows.

Step 1: *Factorization*

In the first step, we separate the maximization problem into two sub-problems. We note that for any vector $\mathbf{w}_{\Theta_k}$ and $\mathbf{w}_{\Psi_k^+}$, we can write

$$\mathbf{w}_{\Theta_k} = a_{\Theta_k}\tilde{\mathbf{w}}_{\Theta_k}, \quad \mathbf{w}_{\Psi_k^+} = a_{\Psi_k^+}\tilde{\mathbf{w}}_{\Psi_k^+} \tag{A.1}$$

for $\|\tilde{\mathbf{w}}_{\Theta_k}\| = \|\tilde{\mathbf{w}}_{\Psi_k^+}\| = 1$, and a_{Θ_k} and $a_{\Psi_k^+}$ are a scalar. We note that $|a_{\Theta_k}|$ and $|a_{\Psi_k^+}|$ equal the norms of $\mathbf{w}_{\Theta_k}$ and $\mathbf{w}_{\Psi_k^+}$, respectively. From (2.13) on page (18),

we have

$$C_{\Theta_k}(\mathbf{w}_{\Theta_k}) = a_{\Theta_k}\tilde{\mathbf{w}}_{\Theta_k}^T\boldsymbol{\alpha}_{\Theta_k} \triangleq a_{\Theta_k}\tilde{C}_{\Theta_k}(\tilde{\mathbf{w}}_{\Theta_k}),$$

$$C_{\Psi_k^+}(\mathbf{w}_{\Psi_k^+}) = a_{\Psi_k^+}\tilde{\mathbf{w}}_{\Psi_k^+}^T\boldsymbol{\alpha}_{\Psi_k^+} \triangleq a_{\Psi_k^+}\tilde{C}_{\Psi_k^+}(\tilde{\mathbf{w}}_{\Psi_k^+}), \tag{A.2}$$

where we denote $\tilde{C}_{\Phi}(\tilde{\mathbf{w}}_{\Phi}) \triangleq \tilde{\mathbf{w}}_{\Phi}^T\boldsymbol{\alpha}_{\Phi}$ and drop the dependence on $\tilde{\mathbf{w}}_{\Phi}$ whenever there is no confusion. Thus, we can rewrite the SINR of the BL, as shown in (2.16), as follows

$$SINR_{BL}(a_{\Theta_k}, a_{\Psi_k^+}, \tilde{\mathbf{w}}_{\Theta_k}, \tilde{\mathbf{w}}_{\Psi_k^+}) = \frac{P_r\left(a_{\Theta_k}\tilde{C}_{\Theta_k} + \sqrt{\rho}a_{\Psi_k^+}\tilde{C}_{\Psi_k^+}\right)^2}{\bar{\rho}P_r a_{\Psi_k^+}^2\tilde{C}_{\Psi_k^+}^2 + (a_{\Theta_k}^2 + a_{\Psi_k^+}^2)\sigma_0^2} \tag{A.3}$$

The optimization problem in (2.17) is equivalent to

$$SINR_{BL}^* = \underset{\substack{a_{\Theta_k}, a_{\Psi_k^+} \\ \|\tilde{\mathbf{w}}_{\Theta_k}\|=\|\tilde{\mathbf{w}}_{\Psi_k^+}\|=1}}{\text{maximize}} \; SINR_{BL}(a_{\Theta_k}, a_{\Psi_k^+}, \tilde{\mathbf{w}}_{\Theta_k}, \tilde{\mathbf{w}}_{\Psi_k^+}) \tag{A.4}$$

Since the only constraints in (A.4) are $\|\tilde{\mathbf{w}}_{\Theta_k}\| = \|\tilde{\mathbf{w}}_{\Psi_k^+}\| = 1$, we can first optimize over $a_{\Theta_k}, a_{\Psi_k^+}$ and then over $\tilde{\mathbf{w}}_{\Theta_k}, \tilde{\mathbf{w}}_{\Psi_k^+}$ as follows:

$$SINR_{BL}^* = \underset{\|\tilde{\mathbf{w}}_{\Theta_k}\|=\|\tilde{\mathbf{w}}_{\Psi_k^+}\|=1}{\text{maximize}} \; \underset{a_{\Theta_k}, a_{\Psi_k^+}}{\text{maximize}} \; SINR_{BL}(a_{\Theta_k}, a_{\Psi_k^+}, \tilde{\mathbf{w}}_{\Theta_k}, \tilde{\mathbf{w}}_{\Psi_k^+}) \tag{A.5}$$

Note that we can rewrite (A.3) as follows:

$$SINR_{BL}(a_{\Theta_k}, a_{\Psi_k^+}, \tilde{\mathbf{w}}_{\Theta_k}, \tilde{\mathbf{w}}_{\Psi_k^+}) = \frac{P_r\left(a_{\Theta_k}\cdot\tilde{C}_{\Theta_k} + a_{\Psi_k^+}\cdot\sqrt{\rho}\tilde{C}_{\Psi_k^+}\right)^2}{a_{\Theta_k}^2\sigma_0^2 + a_{\Psi_k^+}^2\left(\bar{\rho}P_r\tilde{C}_{\Psi_k^+}^2 + \sigma_0^2\right)} \tag{A.6}$$

which can be considered the combined SINR of two signals with the channel gains $\tilde{C}_{\Theta_k}$ and $\sqrt{\rho}\tilde{C}_{\Psi_k^+}$ and the noise powers σ_0^2 and $\left(\bar{\rho}P_r\tilde{C}_{\Psi_k^+}^2 + \sigma_0^2\right)$, respectively. Similar to the solution for an MRC receiver, we have the optimal values of $a_{\Theta_k}, a_{\Psi_k^+}$ given by

$$a_{\Theta_k} = \frac{\tilde{C}_{\Theta_k}}{\sigma_0^2}, \quad a_{\Psi_k^+} = \frac{\sqrt{\rho}\tilde{C}_{\Psi_k^+}}{\bar{\rho}P_r\tilde{C}_{\Psi_k^+}^2 + \sigma_0^2} \tag{A.7}$$

and the combined SINR for the BL is given by

$$SINR_{BL}(\tilde{\mathbf{w}}_{\Theta_k}, \tilde{\mathbf{w}}_{\Psi_k^+}) = \frac{P_r \tilde{C}^2_{\Theta_k}}{\sigma_0^2} + \frac{\rho P_r \tilde{C}^2_{\Psi_k^+}}{\bar{\rho} P_r \tilde{C}^2_{\Psi_k^+} + \sigma_0^2} \tag{A.8}$$

which now only depends on the $\tilde{\mathbf{w}}_{\Theta_k}, \tilde{\mathbf{w}}_{\Psi_k^+}$. In the next step, we need to maximize over $\tilde{\mathbf{w}}_{\Theta_k}, \tilde{\mathbf{w}}_{\Psi_k^+}$. Since the first and second term in (A.8) only depends on $\tilde{\mathbf{w}}_{\Theta_k}$ and $\tilde{\mathbf{w}}_{\Psi_k^+}$, respectively, we have

$$\underset{\|\tilde{\mathbf{w}}_{\Theta_k}\|=\|\tilde{\mathbf{w}}_{\Psi_k^+}\|=1}{\text{maximize}} SINR_{BL}(\tilde{\mathbf{w}}_{\Theta_k}, \tilde{\mathbf{w}}_{\Psi_k^+}) = \underset{\|\tilde{\mathbf{w}}_{\Theta_k}\|=1}{\text{maximize}} \frac{P_r \tilde{C}^2_{\Theta_k}}{\sigma_0^2} + \underset{\|\tilde{\mathbf{w}}_{\Psi_k^+}\|=1}{\text{maximize}} \frac{\rho P_r \tilde{C}^2_{\Psi_k^+}}{\bar{\rho} P_r \tilde{C}^2_{\Psi_k^+} + \sigma_0^2} \tag{A.9}$$

That is, our maximization problem can be separated into two maximization problems with the optimal combining weights a_{Θ_k} and $a_{\Psi_k^+}$ given in (A.7). In the following, we consider the solutions to these maximization problems separately.

Step 2: *Maximizations*

In this step, we need to find $\tilde{\mathbf{w}}_{\Theta_k}$ and $\tilde{\mathbf{w}}_{\Psi_k^+}$ for the sub-optimizations as shown in (A.9).

- *The first maximization problem in (A.9):* That is,

$$SINR^*_{BL,1} \triangleq \underset{\|\tilde{\mathbf{w}}_{\Theta_k}\|=1}{\text{maximize}} \frac{P_r \tilde{C}^2_{\Theta_k}}{\sigma_0^2} = \underset{\|\tilde{\mathbf{w}}_{\Theta_k}\|=1}{\text{maximize}} \frac{P_r (\tilde{\mathbf{w}}^T_{\Theta_k} \boldsymbol{\alpha}_{\Theta_k})^2}{\sigma_0^2} \tag{A.10}$$

  Similar to the MRC solution, the optimal solution is given by

$$\tilde{\mathbf{w}}_{\Theta_k} = \boldsymbol{\alpha}_{\Theta_k} / \|\boldsymbol{\alpha}_{\Theta_k}\| \tag{A.11}$$

  and the resulting maximum combined SINR is given by

$$SINR^*_{BL,1} = \frac{P_r \|\boldsymbol{\alpha}_{\Theta_k}\|^2}{\sigma_0^2} \tag{A.12}$$

- *The second maximization problem in (A.9):* That is,

$$SINR^*_{BL,2} = \underset{\|\tilde{\mathbf{w}}_{\Psi_k^+}\|=1}{\text{maximize}} \frac{\rho P_r \tilde{C}^2_{\Psi_k^+}}{\bar{\rho} P_r \tilde{C}^2_{\Psi_k^+} + \sigma_0^2} \tag{A.13}$$

which is *not* a classical MRC problem. However, due to the special structure of the objective function, we can show that

$$\arg \max_{\|\tilde{\mathbf{w}}_{\Psi_k^+}\|=1} \frac{\rho P_r \tilde{C}^2_{\Psi_k^+}}{\bar{\rho} P_r \tilde{C}^2_{\Psi_k^+} + \sigma_0^2} = \arg \max_{\|\tilde{\mathbf{w}}_{\Psi_k^+}\|=1} \frac{P_r \tilde{C}^2_{\Psi_k^+}}{\sigma_0^2} \tag{A.14}$$

Similar to the MRC solution, the optimal solution is given by

$$\tilde{\mathbf{w}}_{\Psi_k^+} = \boldsymbol{\alpha}_{\Psi_k^+} / \|\boldsymbol{\alpha}_{\Psi_k^+}\| \tag{A.15}$$

Also, the resulting maximum SINR is given by

$$SINR^*_{BL,2} = \frac{\rho P_r \|\boldsymbol{\alpha}_{\Psi_k^+}\|^2}{\bar{\rho} P_r \|\boldsymbol{\alpha}_{\Psi_k^+}\|^2 + \sigma_0^2} \tag{A.16}$$

From (A.12) and (A.16), we have the optimum SINR for the BL is given by

$$SINR^*_{BL} = SINR^*_{BL,1} + SINR^*_{BL,2} = \frac{P_r \|\boldsymbol{\alpha}_{\Theta_k}\|^2}{\sigma_0^2} + \frac{\rho P_r \|\boldsymbol{\alpha}_{\Psi_k^+}\|^2}{\bar{\rho} P_r \|\boldsymbol{\alpha}_{\Psi_k^+}\|^2 + \sigma_0^2} \tag{A.17}$$

For the optimum weights, substituting (A.11) and (A.15) in (A.7), we have the optimum weights in the second step are given by

$$a_{\Theta_k} = \frac{\|\boldsymbol{\alpha}_{\Theta_k}\|}{\sigma_0^2}, \quad a_{\Psi_k^+} = \frac{\sqrt{\rho}\|\boldsymbol{\alpha}_{\Psi_k^+}\|}{\bar{\rho} P_r \|\boldsymbol{\alpha}_{\Psi_k^+}\|^2 + \sigma_0^2} \tag{A.18}$$

where we note that $\tilde{C}_{\Theta_k} = \|\boldsymbol{\alpha}_{\Theta_k}\|$ and $\tilde{C}_{\Psi_k^+} = \|\boldsymbol{\alpha}_{\Psi_k^+}\|$. Finally, using (A.11), (A.15), and (A.18) in (A.1), the effective optimum weights in both steps are given by

$$\mathbf{w}_{\Theta_k} = a_{\Theta_k} \tilde{\mathbf{w}}_{\Theta_k} = \frac{\boldsymbol{\alpha}_{\Theta_k}}{\sigma_0^2} \tag{A.19}$$

$$\mathbf{w}_{\Psi_k^+} = a_{\Psi_k^+} \tilde{\mathbf{w}}_{\Psi_k^+} = \frac{\sqrt{\rho}\boldsymbol{\alpha}_{\Psi_k^+}}{\bar{\rho} P_r \|\boldsymbol{\alpha}_{\Psi_k^+}\|^2 + \sigma_0^2} \tag{A.20}$$

A.2 The CDF of the optimum combined SINR of the BL

In this appendix, we consider the cumulative distribution function (CDF) of the optimum MRC-combined SINR of the BL, as given in (2.25) for the case of i.i.d. Rayleigh fading. Define

$$U_{y_k} \triangleq \frac{P_r\|\boldsymbol{\alpha}_{\Theta_k}\|^2}{\sigma_0^2}, \quad V_{z_k} \triangleq \frac{\rho P_r\|\boldsymbol{\alpha}_{\Psi_k^+}\|^2}{\sigma_0^2+\bar{\rho}P_r\|\boldsymbol{\alpha}_{\Psi_k^+}\|^2} \tag{A.21}$$

Then, we have

$$SINR_{d,bl}(\Theta_k,\Psi_k^+) \;=\; U_{y_k}+V_{z_k} \tag{A.22}$$

where, as defined before, y_k and z_k are the number of elements of the sets Θ_k and Ψ_k^+, respectively. The CDF of U_{y_k} is given as follows:

$$F_{U_{y_k}}(u) \triangleq \Pr(U_{y_k}\le u) = \gamma_{inc}\big(u/\Gamma_d, y_k\big) \tag{A.23}$$

where $\Gamma_d \triangleq P_r\Omega_0/\sigma_0^2$ and Ω_0 is the second moment of the fading. Similar to the calculation in (2.29), we have

$$\begin{aligned} F_{V_{z_k}}(v) &\triangleq \Pr(V_{z_k}\le v) = \Pr\left(\frac{\rho P_r\|\boldsymbol{\alpha}_{\Psi_k^+}\|^2}{\sigma_0^2+\bar{\rho}P_r\|\boldsymbol{\alpha}_{\Psi_k^+}\|^2}\le v\right) \\ &= \begin{cases} \gamma_{inc}\Big(\frac{v}{\Gamma_d(\rho-\bar{\rho}v)}, z_k\Big), & \text{if } \rho-\bar{\rho}v>0 \\ 1 & \text{if } \rho-\bar{\rho}v\le 0 \end{cases} \end{aligned} \tag{A.24}$$

We note that the random variables U_{y_k} and V_{z_k} are independent. Thus, the

CDF of the sum is given by

$$\begin{aligned} F_{SINR_{d,bl}}(z) &= \int_0^z f_{U_{y_k}}(u) F_{V_{z_k}}(z-u)du \\ &= \int_0^z \frac{(u/\Gamma_d)^{y_k-1} e^{-u/\Gamma_d}}{(y_k!)\Gamma_d} F_{V_{z_k}}(z-u)du \end{aligned} \tag{A.25}$$

where $f_{U_{y_k}}(u) \triangleq \frac{d}{du} F_{U_{y_k}}(u)$, and $F_{V_{z_k}}(.)$ is given in (A.24).

Appendix B

Combining Techniques for the Hierarchical Modulation Scheme

B.1 The first combining step: Optimal for the BL/EL

First, we note that, similar to the MRC solution, from the definitions in (3.9) on page 53, we can show that

$$\begin{aligned} C_{\Theta_k}(\tilde{\mathbf{u}}_{\Theta_k}) &\leq C_{\Theta_k}(\tilde{\boldsymbol{\alpha}}_{\Theta_k}) = \|\boldsymbol{\alpha}_{\Theta_k}\| \triangleq C^*_{\Theta_k}, \quad \text{for all } \|\tilde{\mathbf{u}}_{\Theta_k}\| = 1, \\ C_{\Psi_k}(\tilde{\mathbf{u}}_{\Psi_k}) &\leq C_{\Psi_k}(\tilde{\boldsymbol{\alpha}}_{\Psi_k}) = \|\boldsymbol{\alpha}_{\Psi_k}\| \triangleq C^*_{\Psi_k}, \quad \text{for all } \|\tilde{\mathbf{u}}_{\Psi_k}\| = 1 \end{aligned} \tag{B.1}$$

where the optimum normalized weight vectors $\tilde{\boldsymbol{\alpha}}_{\Theta_k}, \tilde{\boldsymbol{\alpha}}_{\Psi_k}$ are given in (3.25).

The BER expressions for the BL and the EL in (3.18) and (3.19) have the following forms, respectively,

$$f(x,y) \triangleq \frac{1}{2}Q(ax+by) + \frac{1}{2}Q(ax+cy) \tag{B.2}$$

$$g(x,y) \triangleq Q(dx) + \frac{1}{2}Q(2ax+by) - \frac{1}{2}Q(2ax+cy) \tag{B.3}$$

where $a, b, c, d \geq 0$, $c \geq b$, and x, y correspondingly represent $C_{\Theta_k}(\tilde{\mathbf{w}}_{\Theta_k})$ and $C_{\Psi_k}(\tilde{\mathbf{w}}_{\Psi_k})$. Similar to [19], we can show that both $f(x, y)$ and $g(x, y)$ are non-increasing in (x, y) for $x, y \geq 0$. Therefore, from (B.1), and noting that $C_{\Theta_k}(\tilde{\mathbf{w}}_{\Theta_k}), C_{\Psi_k}(\tilde{\mathbf{w}}_{\Psi_k}) \geq 0$ for $\tilde{\mathbf{w}}_{\Theta_k}, \tilde{\mathbf{w}}_{\Psi_k} \succeq 0$, we have

$$BER_{BL}(a_{\Theta_k}, a_{\Psi_k}, \tilde{\mathbf{w}}_{\Theta_k}, \tilde{\mathbf{w}}_{\Psi_k}) \;\geq\; BER_{BL}(a_{\Theta_k}, a_{\Psi_k}, \tilde{\boldsymbol{\alpha}}_{\Theta_k}, \tilde{\boldsymbol{\alpha}}_{\Psi_k}) \tag{B.4}$$

for all $\tilde{\mathbf{w}}_{\Theta_k}, \tilde{\mathbf{w}}_{\Psi_k} \succeq 0$ and $\|\tilde{\mathbf{w}}_{\Theta_k}\| = \|\tilde{\mathbf{w}}_{\Psi_k}\| = 1$, and similarly

$$BER_{EL}(b_{\Theta_k}, b_{\Psi_k}, \tilde{\mathbf{v}}_{\Theta_k}, \tilde{\mathbf{v}}_{\Psi_k}) \;\geq\; BER_{EL}(b_{\Theta_k}, b_{\Psi_k}, \tilde{\boldsymbol{\alpha}}_{\Theta_k}, \tilde{\boldsymbol{\alpha}}_{\Psi_k}) \tag{B.5}$$

for all $\tilde{\mathbf{v}}_{\Theta_k}, \tilde{\mathbf{v}}_{\Psi_k} \succeq 0$ and $\|\tilde{\mathbf{v}}_{\Theta_k}\| = \|\tilde{\mathbf{v}}_{\Psi_k}\| = 1$. That is, we have (3.24) and (3.26) respectively.

B.2 The second combining step: Optimal for the BL

From (3.18) on page 56, we denote

$$\begin{aligned} BER_{BL}(a_{\Theta_k}, a_{\Psi_k}) &\triangleq BER_{BL}(a_{\Theta_k}, a_{\Psi_k}, \tilde{\mathbf{w}}^*_{\Theta_k}, \tilde{\mathbf{w}}^*_{\Psi_k}) \\ &= \frac{1}{2} Q\left(\frac{a_{\Theta_k}\sqrt{E_r} C^*_{\Theta_k} + a_{\Psi_k}\sqrt{E_r} C^*_{\Psi_k}\left(\sqrt{\rho} - \sqrt{\bar{\rho}}\right)\right]}{\sqrt{(a^2_{\Theta_k} + a^2_{\Psi_k}) N_0}} \right) \\ &\quad + \frac{1}{2} Q\left(\frac{a_{\Theta_k}\sqrt{E_r} C^*_{\Theta_k} + a_{\Psi_k}\sqrt{E_r} C^*_{\Psi_k}\left(\sqrt{\rho} + \sqrt{\bar{\rho}}\right)\right]}{\sqrt{(a^2_{\Theta_k} + a^2_{\Psi_k}) N_0}} \right) \end{aligned} \tag{B.6}$$

where $\tilde{\mathbf{w}}^*_{\Theta_k}, \tilde{\mathbf{w}}^*_{\Psi_k}$ are the optimal weight vectors in the first step. We note that if $(a_{\Theta_k}, a_{\Psi_k})$ minimizes $BER_{BL}(a_{\Theta_k}, a_{\Psi_k})$, so does $(K_c a_{\Theta_k}, K_c a_{\Psi_k})$, for some constant

$K_c > 0$. Therefore, without loss of generality, we can assume $a_{\Theta_k} = 1$, and we only need to optimize over a_{Ψ_k}. For further notational simplicity, we define

$$A \triangleq \frac{\sqrt{E_r}C^*_{\Theta_k}}{\sqrt{N_0}}, \quad B \triangleq \frac{\sqrt{E_r}C^*_{\Psi_k}}{\sqrt{N_0}}(\sqrt{\rho} - \sqrt{\bar{\rho}}), \quad C \triangleq \frac{\sqrt{E_r}C^*_{\Psi_k}}{\sqrt{N_0}}(\sqrt{\rho} + \sqrt{\bar{\rho}}) \quad \text{(B.7)}$$

where $A \geq 0$ and $C \geq B \geq 0$. Then, the BER for the BL, as a function of a_{Θ_k} is given by

$$\begin{aligned} BER_{BL}(a_{\Psi_k}) &\triangleq BER_{BL}(1, a_{\Psi_k}) \\ &= \frac{1}{2}Q\left(\frac{A + Ba_{\Psi_k}}{\sqrt{1 + a^2_{\Psi_k}}}\right) + \frac{1}{2}Q\left(\frac{A + Ca_{\Psi_k}}{\sqrt{1 + a^2_{\Psi_k}}}\right) \end{aligned} \quad \text{(B.8)}$$

The optimization can be written as follows:

$$\min_{a_{\Psi_k} > 0} BER_{BL}(a_{\Psi_k}) \quad \text{(B.9)}$$

The function $\frac{A+Ba_{\Psi_k}}{\sqrt{1+a^2_{\Psi_k}}}$ is generally neither convex nor concave in $a_{\Psi_k} > 0$. Thus, in general, (B.9) is not a convex optimization problem. However, for $a_{\Psi_k} > 0$, define

$$\phi = \tan^{-1}(a_{\Psi_k}), \quad \phi \in (0, \pi/2) \quad \text{(B.10)}$$

Substituting $a_{\Psi_k} = \tan(\phi)$ in (B.9), we have

$$\begin{aligned} BER^{(a)}_{BL}(\phi) &\triangleq BER_{BL}(\tan(\phi)) \\ &= \frac{1}{2}Q\left(A\cos\phi + B\sin\phi\right) + \frac{1}{2}Q\left(A\cos\phi + C\sin\phi\right) \end{aligned} \quad \text{(B.11)}$$

The function $(A\cos\phi + B\sin\phi)$ is concave for all $A, B \geq 0$ in $\phi \in (0, \pi/2)$. The function $Q(x)$ is convex and monotonically decreases for $x \geq 0$. Thus, $Q\left(A\cos\phi + B\sin\phi\right)$ is convex for all $A, B \geq 0$ [34], and so is the $BER^{(a)}_{BL}(\phi)$. Therefore, we can efficiently use convex optimization programming [34] to solve for ϕ^*, which minimizes $BER^{(a)}_{BL}(\phi)$, as shown in (3.29).

B.3 Effective output SNR comparison

In the following, we will show that

$$SNR_{BL,1}^{(eff)} \geq SNR_{BL,2}^{(eff)} \tag{B.12}$$

which are defined in (3.37) and (3.38) on page 61, respectively. Applying Cauchy-Schwarz inequality, i.e., $(x_1^2 + x_2^2)(y_1^2 + y_2^2) \geq (x_1 y_1 + x_2 y_2)^2$, for

$$\begin{aligned} x_1 &= C_{\Theta_k}^*, \quad x_2 = C_{\Psi_k}^*(\sqrt{\rho} - \sqrt{\bar{\rho}}) \\ y_1 &= C_{\Theta_k}^*, \quad y_2 = C_{\Psi_k}^* \end{aligned} \tag{B.13}$$

we have

$$\begin{aligned} &\left[(C_{\Theta_k}^*)^2 + (C_{\Psi_k}^*)^2(\sqrt{\rho} - \sqrt{\bar{\rho}})^2\right] \cdot \left[(C_{\Theta_k}^*)^2 + (C_{\Psi_k}^*)^2\right] \\ &\qquad \geq \left[C_{\Theta_k}^* \cdot C_{\Theta_k}^* + C_{\Psi_k}^* \cdot C_{\Psi_k}^*(\sqrt{\rho} - \sqrt{\bar{\rho}})\right]^2 \end{aligned} \tag{B.14}$$

with the equality happen if and only if $y_1 = Kx_1$ and $y_2 = Kx_2$, for a constant K, i.e.,

$$C_{\Theta_k}^* = KC_{\Theta_k}^*, \quad C_{\Psi_k}^* = KC_{\Psi_k}^*(\sqrt{\rho} - \sqrt{\bar{\rho}}) \tag{B.15}$$

which happens if and only if $\rho = 1$ (or $C_{\Theta_k}^* = 0$ or $C_{\Psi_k}^* = 0$, which happen with zero probability, thus, we will be ignored).

Equation (B.14) implies that

$$\left[(C_{\Theta_k}^*)^2 + (C_{\Psi_k}^*)^2(\sqrt{\rho} - \sqrt{\bar{\rho}})^2\right] \geq \frac{\left[(C_{\Theta_k}^*)^2 + (C_{\Psi_k}^*)^2(\sqrt{\rho} - \sqrt{\bar{\rho}})\right]^2}{(C_{\Theta_k}^*)^2 + (C_{\Psi_k}^*)^2} \tag{B.16}$$

which is equivalent to (B.12), that is

$$\frac{E_r(C^*_{\Theta_k})^2}{N_0} + \frac{E_r(C^*_{\Psi_k})^2(\sqrt{\rho}-\sqrt{\bar{\rho}})^2}{N_0} \geq \frac{E_r\left[(C^*_{\Theta_k})^2 + (C^*_{\Psi_k})^2(\sqrt{\rho}-\sqrt{\bar{\rho}})\right]^2}{\left[(C^*_{\Theta_k})^2 + (C^*_{\Psi_k})^2\right]N_0} \quad \text{(B.17)}$$

where the equality holds if and only if $\rho = 1$.

Bibliography

[1] S.M. Alamouti, "A simple transmit diversity technique for wireless communications," IEEE Journal on Selected Areas in Communications, vol. 16, no. 10, pp. 1451-1458, Oct. 1998.

[2] V. Tarokh, H. Jafarkhani, and A. R. Calderbank, "Space-time block coding for wireless communications: Performance results," IEEE Journal on Selected Areas in Communications, vol. 17, no. 3, p. 451460, Mar. 1990.

[3] L. Zheng and D.N.C. Tse, "Diversity and multiplexing: a fundamental tradeoff in multiple-antenna channels," IEEE Transactions on Information Theory, vol.49, no.5, pp. 1073-1096, May 2003.

[4] T.M. Cover and A.A. El Gamal, "Capacity theorems for the relay channel," IEEE Transactions on Information Theory, Sep. 1979.

[5] A. Sendonaris, E. Erkip, and B. Aazhang, "User cooperation diversity–Part I: System description," IEEE Transactions on Communications, vol. 51, no. 11, pp. 1927-1938, Nov. 2003.

[6] J. N. Laneman and G. W. Womell, "Distributed space-time coded protocols for exploiting cooperative diversity in wireless networks," IEEE Transactions on Information Theory, vol. 49, no. 10, pp. 2415-2425, Oct. 2003.

[7] J. N. Laneman, D. N. C. Tse, and G. W. Wornell, "Cooperative diversity in wireless networks: Efficient protocols and outage behavior," IEEE Transactions on Information Theory vol. 50, no. 12, pp. 3062-3080, Dec. 2004.

[8] Y. Zhao, R. Adve, and T. J. Lim, "Improving amplify-and-forward relay networks: optimal power allocation versus selection," IEEE Transactions on Wireless Communications, vol. 6, no. 8, pp. 3114-3123, Aug. 2007.

[9] S. S. Ikki and M. H. Ahmed, "On the performance of cooperative diversity networks with the nth best-relay selection scheme," IEEE Transactions on Communications, vol. 58, no. 11, pp. 3062-3069, Nov. 2010.

[10] A. Nosratinia, T.E. Hunter, and A. Hedayat, "Cooperative communication in wireless networks," IEEE Communications Magazine, vol.42, no.10, pp. 74-80, Oct. 2004.

[11] H. Muhaidat, and M. Uysal, "Cooperative Diversity with Multiple-Antenna Nodes in Fading Relay Channels," IEEE Transactions on Wireless Communications, vol.7, no.8, pp.3036-3046, Aug. 2008.

[12] Y. Tian and A. Yener, "The Gaussian Interference Relay Channel: Improved Achievable Rates and Sum Rate Upperbounds Using a Potent Relay," IEEE Transactions on Information Theory, vol.57, no.5, pp.2865-2879, May 2011.

[13] A. Bletsas, H. Shin, M. Z. Win, and A. Lippman, "A simple cooperative diversity method based on network path selection," IEEE Journal on Selected Areas in Communications, vol. 24, no. 3, pp. 659-672 Mar. 2006.

[14] T. M. Cover, J. A. Thomas, *Elements of Information Theory,* Second Edition, Wiley, July 2006.

[15] P. Popovski and E. Carvalho "Improving the Rates in Wireless Relay Systems through Superposition Coding," IEEE Transactions on Wireless Communications, vol. 7, no. 12, pp. 4831-4836, Dec. 2008.

[16] J. Hagenauer,"Rate-compatible punctured convolutional codes (RCPC codes) and their applications," IEEE Transactions on Communications, Vol. 36(4), pp. 389-400, Apr. 1988.

[17] L. H. C. Lee, "New rate-compatible punctured convolutional codes for Viterbi decoding," IEEE Transactions on Communications, Vol. 42(12), pp. 3073-3079, Dec. 1994.

[18] A. R. Calderbank and N. Seshadri, "Multilevel codes for unequal error protection," IEEE Transactions on Information Theory, vol. 39, no. 4, pp. 1234-1248, Jul. 1993.

[19] S.H. Chang, M. Rim, P.C. Cosman, and L.B. Milstein, "Optimized Unequal Error Protection Using Multiplexed the hierarchical Modulation," IEEE Transactions on Information Theory, vol.58, no.9, pp.5816-5840, Sep. 2012.

[20] ETSI, EN 300 744, V1.5.1, *Digital Video Broadcasting (DVB): framing structure, channel coding and modulation for digital terrestrial television*, Nov. 2004.

[21] M.R. Chari, F. Ling, A. Mantravadi, R. Krishnamoorthi, R. Vijayan, G.K. Walker, and R. Chandhok, "FLO physical layer: An Overview," IEEE Transactions on Broadcasting, vol. 53, no. 1, pt. 2, pp. 145-160, Mar. 2007.

[22] D. Song and C.W. Chen, "Scalable H.264/AVC video transmission over MIMO wireless systems with adaptive channel selection based on partial channel information," IEEE Transactions on Circuits and Systems for Video Technology, vol. 17, no. 9, pp. 1218-1226, Sep. 2007.

[23] M. F. Sabir, R.W. Heath, and A. C. Bovik, "An unequal error protection scheme for multiple input multiple output systems," in Thirty-Sixth Asilomar Conference on Signals, Systems and Computers, Pacific Grove, California, USA, pp. 575-579, Nov. 2002.

[24] Y. Qian, L. Ping, and M. Ronghong, "Unequal error protection scheme for multiple-input and multiple-output wireless systems," in IEEE 64th Vehicular Technology Conference, Montreal, Canada, Sep. 2006.

[25] G.H. Yang, D. Shen, and V.O.K. Li, "Unequal error protection for MIMO systems with a hybrid structure," in IEEE International Symposium on Circuits and Systems, ISCAS 2006, Island of Kos, Greece, May 2006, pp. 682-685.

[26] O. Alay, T. Korakis, W. Yao, and S. Panwar, "Layered wireless video multicast using directional relays," ICIP 15th IEEE International Conference on Image Processing, vol., no., pp.2020-2023, Oct. 2008.

[27] O. Alay, T. Korakis, W. Yao, and S. Panwar, "Layered Wireless Video Multicast Using Relays," IEEE Transactions on Circuits and Systems for Video Technology, vol.20, no.8, pp.1095-1109, Aug. 2010.

[28] D. Gunduz and E. Erkip, "Source and Channel Coding for Cooperative Relaying," IEEE Transactions on Information Theory, vol. 53, no. 10, pp. 3454-3475, Oct. 2007.

[29] Z. He, J. Cai, and C.W. Chen, "Joint source channel rate-distortion analysis for adaptive mode selection and rate control in wireless video coding," IEEE Transactions on Circuits and Systems for Video Technology, vol.12, no.6, pp.511,523, Jun. 2002.

[30] H. Kim, R. Annavajjala, P.C. Cosman, and L.B. Milstein, "Source-channel rate optimization for progressive image transmission over block fading relay channels," IEEE Transactions on Communications, vol.58, no.6, pp.1631-1642, Jun. 2010.

[31] H.X. Nguyen, H.H. Nguyen, and T. Le-Ngoc, "Signal Transmission With Unequal Error Protection in Wireless Relay Networks," IEEE Transactions on Vehicular Technology, vol.59, no.5, pp.2166-2178, Jun. 2010.

[32] H. Kim, P.C. Cosman, and L.B. Milstein, "Superposition coding based cooperative communication with relay selection," Conference Record of the Forty

Fourth Asilomar Conference on Signals, Systems and Computers, vol., no., pp.892-896, Nov. 2010.

[33] Hobin Kim, "Cross-layer optimization for the transmission of multimedia," Ph.D. Dissertation, ECE Department, University of California at San Diego, La Jolla, CA, 2011.

[34] S. Boyd and L. Vandenberghe, *Convex Optimization,* Cambridge University Press, 2004.

[35] *Advanced Video Coding for Generic Audiovisual Services*, ITU-T Recommendation H.264&ISO/IEC 14496-10 AVC, v3: 2005.

[36] T. Wiegand, G.J. Sullivan, G. Bjontegaard, and A. Luthra, "Overview of the H.264/AVC video coding standard," IEEE Transactions on Circuits and Systems for Video Technology., vol.13, no.7, pp.560-576, Jul. 2003.

[37] T. Stutz, A. Uhl, "A Survey of H.264 AVC/SVC Encryption," IEEE Transactions on Circuits and Systems for Video Technology, vol.22, no.3, pp.325-339, Mar. 2012.

[38] JVT, "H.264/AVC reference software," [Online]. Available: http://iphome.hhi.de/suehring/tml/.

[39] D. G. Brennan, "Linear diversity combing techniques," IRE Proceedings, vol.47, pp. 1075-1101, Jun. 1959.

[40] X. Dong and N.C. Beaulieu, "Optimal maximal ratio combining with correlated diversity branches," IEEE Communications Letters, vol.6, no.1, pp.22-24, Jan. 2002.

[41] C. Siriteanu and S.D. Blostein, "Maximal-Ratio Eigen-Combining for Smarter Antenna Arrays," IEEE Transactions on Wireless Communications, vol.6, no.3, pp.917-925, Mar. 2007.

[42] B. Holter and G.E. Oien, "The optimal weights of maximum ratio combiner using an eigenfilter approach," IEEE Nordic Signal Processing Symposium, Hurtigruten, Norway, 2002.

[43] J.G. Proakis, *Digital Communications*, Third Edition, New York: McGraw-Hill, 1995.

[44] M. Abramowitz and I.A. Stegun, *Handbook of Mathematical Functions: with Formulas, Graphs, and Mathematical Tables.* Dover, New York, 1990.

[45] Y.R. Zheng and C. Xiao, "Simulation models with correct statistical properties for Rayleigh fading channels," IEEE Transactions on Communications, vol.51, no.6, pp.920-928, Jun. 2003.

[46] P. K. Vitthaladevuni and M.S. Alouini, "A recursive algorithm for the exact BER computation of generalized the hierarchical QAM constellations," IEEE Transactions on Information Theory, vol.49, pp.297-307, Jan. 2003.

[47] T. Brink, J. Speidel, and Y. Ran-Hong, "Iterative demapping and decoding for multilevel modulation," IEEE Global Telecommunications Conference, vol.1, no., pp.579-584, 1998.

[48] F. Tosato and P. Bisaglia, "Simplified soft-output demapper for binary interleaved COFDM with application to HIPERLAN/2," IEEE International Conference on Communications, vol.2, no., pp.664-668, May 2002.

[49] H. Schwarz, D. Marpe, and T. Wiegand, "Overview of the scalable video coding extension of H.264/AVC," IEEE Transactions on Circuits and Systems for Video Technology, vol.17, no.9, pp.1103-1120, Sep. 2007.

[50] S.Y. Seidel and T.S. Rappaport, "914 MHz path loss prediction models for indoor wireless communications in multi floored buildings," IEEE Transactions on Antennas and Propagation, vol.40, no.2, pp.207-217, Feb. 1992.

[51] T.V. Nguyen and L.B. Milstein, "Optimal Linear-Combining Receiver for Layered Transmission for Decode-and-Forward Relays using Superposition Coding," submitted to IEEE Asilomar Conference on Signals, Systems and Computers, 2013.

[52] T.V. Nguyen and L.B. Milstein, "Layered Transmission over Decode-and-Forward Wireless Relays Networks using Superposition Coding," submitted to IEEE Transactions on Communications, 2013.

[53] T.V. Nguyen, P.C. Cosman, and L.B. Milstein, "Optimized Receiver Design for Layered Transmission for Decode-and-Forward Relays using Hierarchical Modulation," submitted to IEEE Asilomar Conference on Signals, Systems and Computers, 2013.

[54] T.V. Nguyen, P.C. Cosman, and L.B. Milstein, "Layered Video Transmission over Decode-and-Forward Wireless Relay Networks using Hierarchical Modulation," submitted to IEEE Transactions on Image Processing, 2013.

[55] T.V. Nguyen, E. Masry, and L.B. Milstein, "Channel Model and Performance Analysis of QAM Multiple Antenna Systems at 60-GHz in the Presence of Human Activity," IEEE Global Telecommunications Conference (GLOBECOM 2011), vol., no., pp.1-6, Dec. 2011.